

國立臺灣師範大學地球科學研究所

碩士論文

比較建模與觀測落日時的天文折射現象

**Comparison of Modeled and Observed
Astronomical Refraction of the Setting Sun**

研究生：吳育倫

Yu-Lun Wu

指導教授：傅學海 博士

Hsieh-Hai Fu

中華民國一零一年一月

Abstract

In this work, we try to calculate the astronomical refraction of the setting sun. The light path from a source outside the earth's atmosphere is a curve due to the astronomical refraction, and this curve depends on the observed location and the angle between celestial body and the horizon, especially when the celestial body is near the horizon. The astronomical refraction is influenced by the density and temperature of the vertical atmosphere structure. The CWB rawinsonde observed data is used to construct the vertical density structure of the atmosphere. The sunset images taken on the September 17, 2011, October 17, 2011 and October 28, 2011 at Tamshui, and these images are used as comparison of model and observed astronomical refraction of the setting sun. The difference of the model and the observed setting sun in minimum is $-0.70''$ when the un-refracted incident angle is at 0.749674° above the real horizon, in maximum is $123.72''$ when the un-refracted incident angle is at 1.387341° above the real horizon.

Key Words: Astronomical Refraction, Sunset, Refraction, Atmosphere, Rawinsonde, Observe

摘要

在本研究中，我們嘗試計算得出落日時的天文折射現象。在光線通過大氣層的過程中，它會因為受到大氣層折射的影響而使光線的路徑逐漸彎曲，這即為天文折射現象。天文折射現象的彎曲程度受到天體的仰角所影響，在天頂時最小而在地平面時最大。天文折射現象是受到空氣的密度所影響，其與空氣的溫度和壓力息息相關，為了得到大氣的垂直密度結構，我們使用中央氣象局的雷文送(無線電探空儀)傳回的大氣垂直資料。我們用來比對的落日照片是在 2011 年 9 月 17 日，2011 年 10 月 17 日與 2011 年 10 月 28 日在淡水海邊所拍攝。將拍攝的落日與建模計算的落日仰角進行比對，兩者間的差異最小時是在天體仰角高度為 0.749674° 時，差異量為 $-0.70''$ ；兩者間差異量最大時是在天體仰角高度為 1.387341° 時，差異量為 $123.72''$ 。

關鍵字：天文折射、落日、折射、大氣層、雷文送、觀測

致 謝

首先我要感謝我的指導教授傅學海老師，在我的修課及研究過程中給我許多意見與方向，激發我的思考，以及許多的指導與鼓勵，讓我能夠完成這篇論文，三年來感謝老師的諄諄教誨，給了我許多研究上的幫助。

感謝口試委員管一政老師與林沛練老師，在百忙之中仍能抽空前來並給予指導與建議，讓我明白論文仍然不足需修該之處。

感謝研究所的同學與學長姐及學弟妹們，經常一起熬夜拼進度與觀測的憲隆與翔宇，以及總是默默幫我們擋下許多瑣事的晟庭學長，還有經常來幫忙的鴻選、宗賢、心潔、姿穎、逸翔等人，還有既會抓我去打球又會幫我畫地圖的育群學弟，室友易儒、伯東與建勳，有你們在左右相伴，給予我在做論文這段期間許多的幫助。

感謝峻鳴、牧笛、林怡、偉珊、為瀚這些瘦咖咖的成員還有濟榕、雅祺，在我苦悶的研究生涯中可以一起出野外爬山親近自然放鬆身心，讓我可以重獲戰力。孟遠、仕豪、百穗、榮倫、嫩妘、儷芙這些老朋友也總是給予支持和鼓勵。以及實習學校的同事和師長們的勉勵，在你們的勉勵下我才能有今日。

要感謝的人實在太多，總是會有族繁不及備載的親友師長們，最後要感謝仲元與我的家人們，時常體諒我晝夜顛倒的生活，感謝你們大家的支持與鼓勵，在你們的支持下我才能義無反顧的繼續努力，謝謝你們！

Contents

1	Introduction01
2	Observation04
3	Data Process13
3-1	Calibrate the altitude angle of the real sun (the unfracted sun) by the photo time13
3-2	The Central Weather Bureau (CWB) rawinsonde data17
3-3	The refraction index of the moist air18
3-4	The refraction between each layer of the atmosphere24
3-5	The light path during the atmosphere27
4	Result and Discussion29
5	Conclusion44
6	Reference46
7	Appendix49
7-A	The CWB rawinsonde data49
7-B	The IDL source code60
7-C	The observation without measured the real horizon.77

List of Figures

Fig 2-1.	The maximum distance of horizontal direction of the solar image (in pixel).04
Fig 2-2.	The sea level in our image.07
Fig 2.3.	The scene while photo the setting sun09
Fig 2.4.	The difference of the water surface in the connected tubes looks from different height.10
Fig 2.5.	The real horizon and the apparent sea level.11
Fig 2.6.	The location of the observation on the map.12
Fig. 3-1.	To calculate the angle θ_c from transit time to image time.14
Fig. 3-2.	To calculate the angle θ_c to the altitude angle θ_x16
Fig 3-3.	The refraction between the boundaries of different layers.24
Fig 3-4.	The light path of the astronomical refraction.27
Fig 4-1.1.	The modeled sun and the observed sun on the image which was taken on September 17, 2011 morning.30
Fig 4-1.2.	The height to pressure and the height to temperature figures which observed by CWB rawinsonde on 00:00 UT September 17, 2011.31

List of Figures

Fig 4-2.1.	The modeled sun and the observed sun on the image which was taken on September 17, 2011 evening.32
Fig 4-2.2.	The height to pressure and the height to temperature figures which observed by CWB rawinsonde on 12:00 UT September 17, 2011.33
Fig 4-3.1.	The modeled sun and the observed sun on the image which was taken on October 17, 2011 evening.34
Fig 4-3.2.	The height to pressure and the height to temperature figures which observed by CWB rawinsonde on 12:00 UT October 17, 2011.35
Fig 4-4.1.	The modeled sun and the observed sun on the image which was taken on October 28, 2011 evening.36
Fig 4-4.2.	The height to pressure and the height to temperature figures which observed by CWB rawinsonde on 12:00 UT October 28, 2011.37

List of Tables

Table.2-1. The equipment with the observe date.06
Table2-2. The Latitude, Longitude and the altitude with the observe date.08
Table 4-1. The result of the observation on September 17, 2011 morning.38
Table 4-2. The result of the observation on September 17, 2011 evening.39
Table 4-3. The result of the observation on October 17, 2011 evening.40
Table 4-4. The result of the observation on October 17, 2011 evening.41

Introduction

The difference of the position and shape of the observed setting sun and the model are compared, and the model of the setting sun is built in terms of the vertical atmosphere structure reconstructed from the Central Weather Bureau (CWB) rawinsonde data. The astronomical refraction model is established under the real weather condition, and the terrestrial refraction is gotten from the observation of the real horizontal level.

The astronomical refraction could be improved in the field of archaeoastronomy, which often use some ancient monuments to align with the rising and setting of the celestial bodies (Schaefer, 1990), and it is also being improved in the field of astrometry. When stars separated 30" at K band at a zenith angle 45° , the astronomical refraction could cause the relative astrometry accuracy up to 12,000 μas , it's 120 times of desired accuracy (Joseph, 1998). Both of astronomical and terrestrial refraction causes the refraction correction angle to vary slightly for different frequencies. This refractive condition explains the observance of the "green spot" at sunset when the horizon is exceptionally clear. Although the refraction model presented here emphasizes visible refraction phenomena, a modified version can also be applied to the radio frequency for corrections on Global Position System (GPS) signals (Michael, 1996).

The astronomical refraction had been known long before. About two thousand years ago, the astronomer Claudius Ptolemy of Alexandria, founds that the rising and setting point of celestial objects were deflected toward the North. Ptolemy indicated that this deflection was caused by

reflection, and he also mentioned that the amount of refraction would decrease with increase altitude angle, and reaching to zero at the zenith (Smith, 1996). The Italian astronomer Gian Domenico Cassini according the Snell's law, assumed the earth's atmosphere were composed by the same density of gas, construct the "concentric spherical shell model" and the "plane parallel layer model". Cassini using the amount of refraction to estimate the height of earth's atmosphere as 6.82 km, the refractive index is 1.000284 while the radius of earth is 6377.36 km (Mahan, 1962).

Sugawa suggest that the astronomical refraction has a seasonal variation, the minimum is occurred in the summer while the zenith angle is 85° , the refraction angle is about $08' 34''.09$, the maximum is occurred in the winter while the zenith angle is about $09'40''.68$. (Sugawa, 1955)

The atmosphere of US standard model is used widely. In the 1962, Garfunkel used a piecewise linear representation of the atmosphere (Garfunkel, 1967), and Hao-jian Yan developed his scheme for a standard atmosphere (Yan, 1996), based on the model of US standard atmosphere. Thomas and Joseph were also used the US standard atmosphere into the astronomical refraction to simulate the solar rim of the real sun image (Thomas and Joseph, 1996).

During the period of 1988 to 1989, Bradleye Schaefer observed the sunset in difference location on earth to estimate the astronomical refraction, the astronomical refraction is from 0.234° to 1.678° , and the mean is 0.64° (Schaefer, 1990) .

Russell D. Sampson who use the camera to record the solar image

and use the rawinsonde to contribute the vertical atmosphere structure and used into similar the astronomical refraction of the setting sun (Sampson, 2003), and tried to compared them on different seasons (Sampson, 2005) and at different longitude (Sampson, 2008) of the astronomical refraction of the setting sun.

The relation between the refractive index and the air composition was modeled by experiments, which considered the temperature, pressure, relative humidity and the density of the CO₂. This model is tested the air temperature from -40°C to +100°C, and the pressure from 80 to 120 kPa and the relative humidity from 0 to 100%, and it should apply the wavelength from 300 nm to 1690 nm (Ciddor, 1996).

In this work, a DSLR camera with Canon 400mm f/5.6 L lens to observed the setting/rising sun, and used the air refraction index model which established by Pholip E. Ciddor in 1996, and use the CWB rawinsonde data to structure the real vertical structure atmosphere to simulate and compared the astronomical refraction model with the observed setting sun.

Observations

We use the Canon EOS Camera with lens to observe the setting sun, the observed log as shown on Table.2-1.

The image scale will be influenced by the CCD size and the focal length. The focal length is changed a little while the image is focused on a nearby object moving to a long-distant object, such as the Sun. To solve this problem, the maximum distance of horizontal direction of the solar image (in pixel) on image as the observed sun's diameter (shown on the following figure), and calculated with the known sun diameter (in arcsec) which searched from JPL Horizon System as the image scale.



Fig 2-1. The maximum length of horizontal direction of the solar image (in pixel).

The observed time is used the time recorded inside camera, adjusted by NTP (Network Time Protocol) program published by National Time and Frequency Standard Laboratory. The GPS time is also used to compare with the NTP time, and there is no difference between these two time-meters. Because of the camera's time unit is only recorded to second, our accuracy of the time is 1 second which caused the altitude angle accuracy of the sun would be $\pm 7.5''$.

Table.2-1 The equipment with the observe date. The observed date with * means this observation is sunrise, and others are sunset

Observe date	Camera	Lens	Image Scale (arcsec/pixel)
May 8, 2009	Canon EOS 30D	Phoenix 80HD f=480mm, F/5.6	2.723
June 1, 2010*	Canon EOS 50D	Canon EF 400mm F/5.6 L	2.468
August 21, 2010	Canon EOS 50D	Canon EF 400mm F/5.6 L	2.456
September 3, 2010	Canon EOS 50D	Canon EF 400mm F/5.6 L	2.461
September 8, 2010	Canon EOS 50D	Canon EF 400mm F/5.6 L	2.445
September 25, 2010	Canon EOS 50D	Canon EF 400mm F/5.6 L	2.460
October 12, 2010	Canon EOS 7D	Canon EF 400mm F/5.6 L	2.246
September 17, 2011*	Canon EOS 7D	Canon EF 400mm F/5.6 L	2.232
September 17, 2011	Canon EOS 7D	Canon EF 400mm F/5.6 L	2.244
October 17, 2011	Canon EOS 7D	Canon EF 400mm F/5.6 L	2.244
October 28, 2011	Canon EOS 7D	Canon EF 400mm F/5.6 L	2.233

The time of sunrise and sunset will be directly influent in the observed location, and a GPS logger is used to show the data of location. The GPS logger, Holux M241 which uses MTK MT3318 GPS chipset, the accuracy of this GPS logger in location is less than 3 meters and the accuracy in altitude is less than 5 meters. The data of location gotten from GPS is accepted, because the altitude error less than 0.1 arcsec, and the image scale is larger than 2.2 arcsec/pixel. The altitude error is considered while use the visual horizon to define as the real horizon, it would cause 170" on altitude angle. The GPS data in 2011 are more reliable because the value of mean is used that the GPS data recorded continuously more than 30 minutes, while the location gotten from GPS is lower because the first value appeared was used before 2011.

The images are rotated a small angle, 0.1° to 0.9° , according to the sea level of the image itself. But the sea level in our image is really wave line other than a straight line, so that the mean sea level is used.



Fig 2-2. The sea level in our image is not a straight line so that the mean sea level (the dashed line) is used.

Table2-2. The Latitude, Longitude and the altitude with the observe date.

Observe Date	Latitude	Longitude	Height (m)
May 8, 2009	E 121°24'26.4"	N 25°11'08.3"	11
June 1, 2010*	E 121°59'09.2"	N 25°01'17.1"	15
August 21, 2010	E 121°24'26.4"	N 25°11'08.5"	11
September 3, 2010	E 121°24'26.4"	N 25°11'08.3"	9
September 8, 2010	E 121°24'26.3"	N 25°11'08.3"	12
September 25, 2010	E 121°24'26.4"	N 25°11'08.3"	11
October 12, 2010	E 121°24'26.4"	N 25°11'08.3"	13
September 17, 2011*	E 121°59'35.5"	N 25°00'01.6"	6
September 17, 2011	E 121°24'35.5"	N 25°11'01.6"	5
October 17, 2011	E 121°24'35.5"	N 25°11'01.6"	5
October 28, 2011	E 121°24'26.2"	N 25°11'06.4"	5

A much better method for finding the real horizon in the image field is used in each run of 2011. The sea level is not the real horizon because of the terrestrial refraction and the location height. If the altitude is higher than zero, the sea level of more distant will be seen, and it will be lower than real horizon. Furthermore, the apparent sea level will be higher than real sea level due to the terrestrial refraction. The terrestrial refraction makes the real sea level downer than the apparent sea level, and it would between 28.80" to 448.20" (Sampon, 2003).

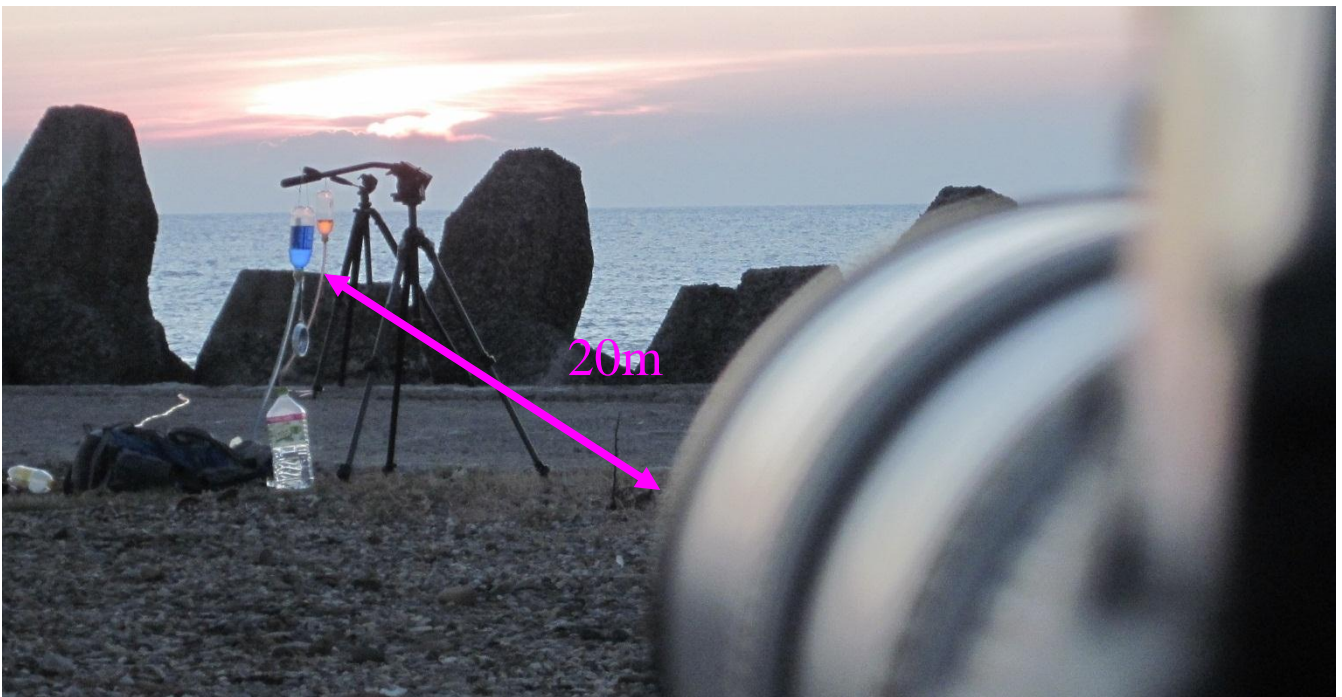


Fig 2.3. The scene while photo the setting sun. The distance between camera to the nearby bottle is 20 meters, and the distance between the blue and red bottle is 8 meters. The camera was set at the same height of the water surface in the bottles.

A connected tube is used to find the real horizon, and two bottles filling the water are connected with a long tube, 8-meter interval. The distance between of camera and the first bottle of connecting tube is 20 meters. The height of camera is adjusted to fit the same level of the surface of two bottles; that means the line along the center of camera image and the water surface of two bottles as the real horizon level. In order to distinguish these two bottles, the water is dyeing in color ink, closer is blue and the other is red. The deviation between water surfaces of two bottles is less than 1 mm.

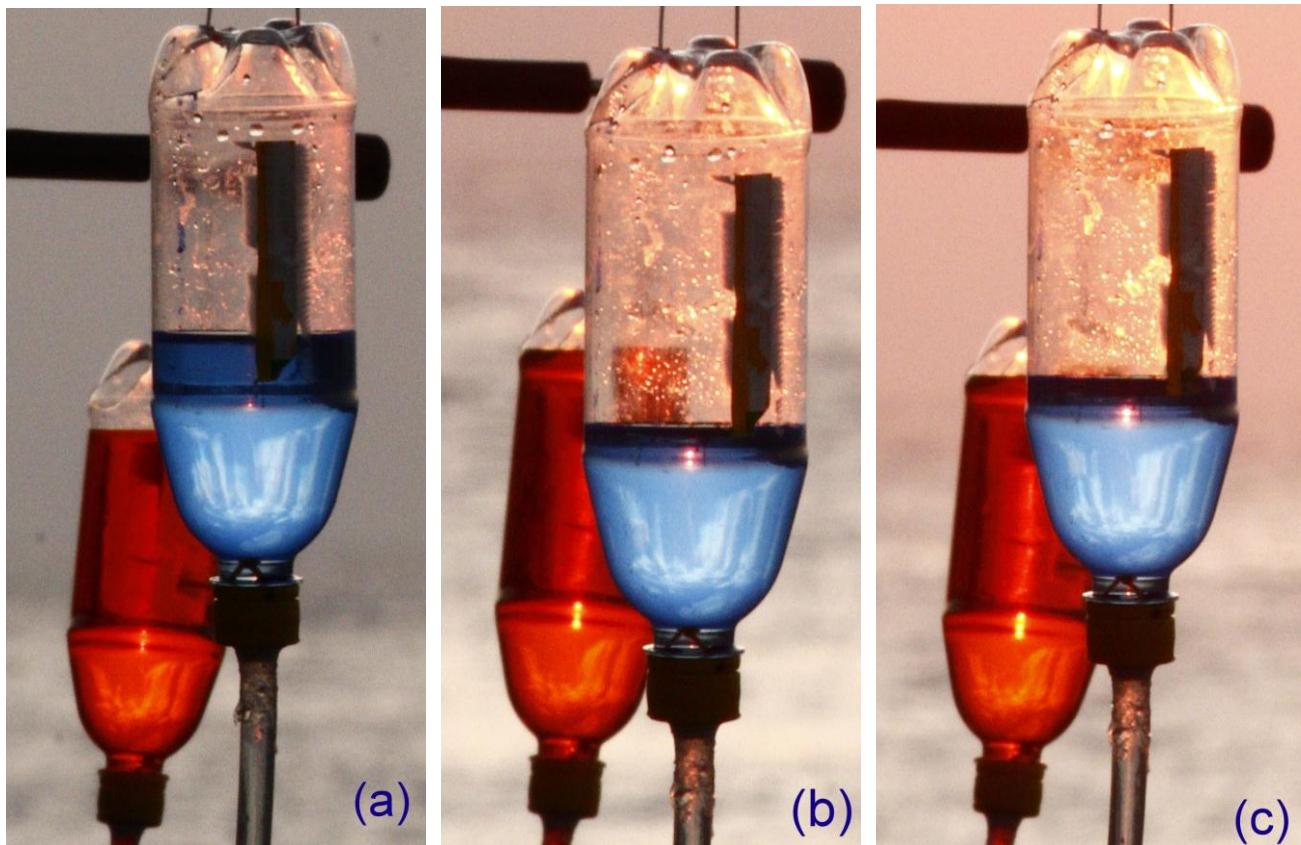


Fig 2.4. The difference of the water surface in the connected tubes looks from different height, and the near bottle is dyeing in blue and the far bottle is dyeing in red. (a) While the camera is lower than the water level, the water in the near bottle would look higher than the far bottle. (b) While the camera is higher than the water level, the water in the near bottle would look lower than the far bottle. (c) While the camera is at the same height of the water level, the water in the near and far bottles would be at the same height.

Because of the focus, when we are focus on the sun or the sea level, even we let the aperture as F32.0 the closer bottles are still fuzzy. This makes error about 11.16" when we trying to determine the real horizon, but we couldn't make the focus on the bottles because this will make the image scale changed.

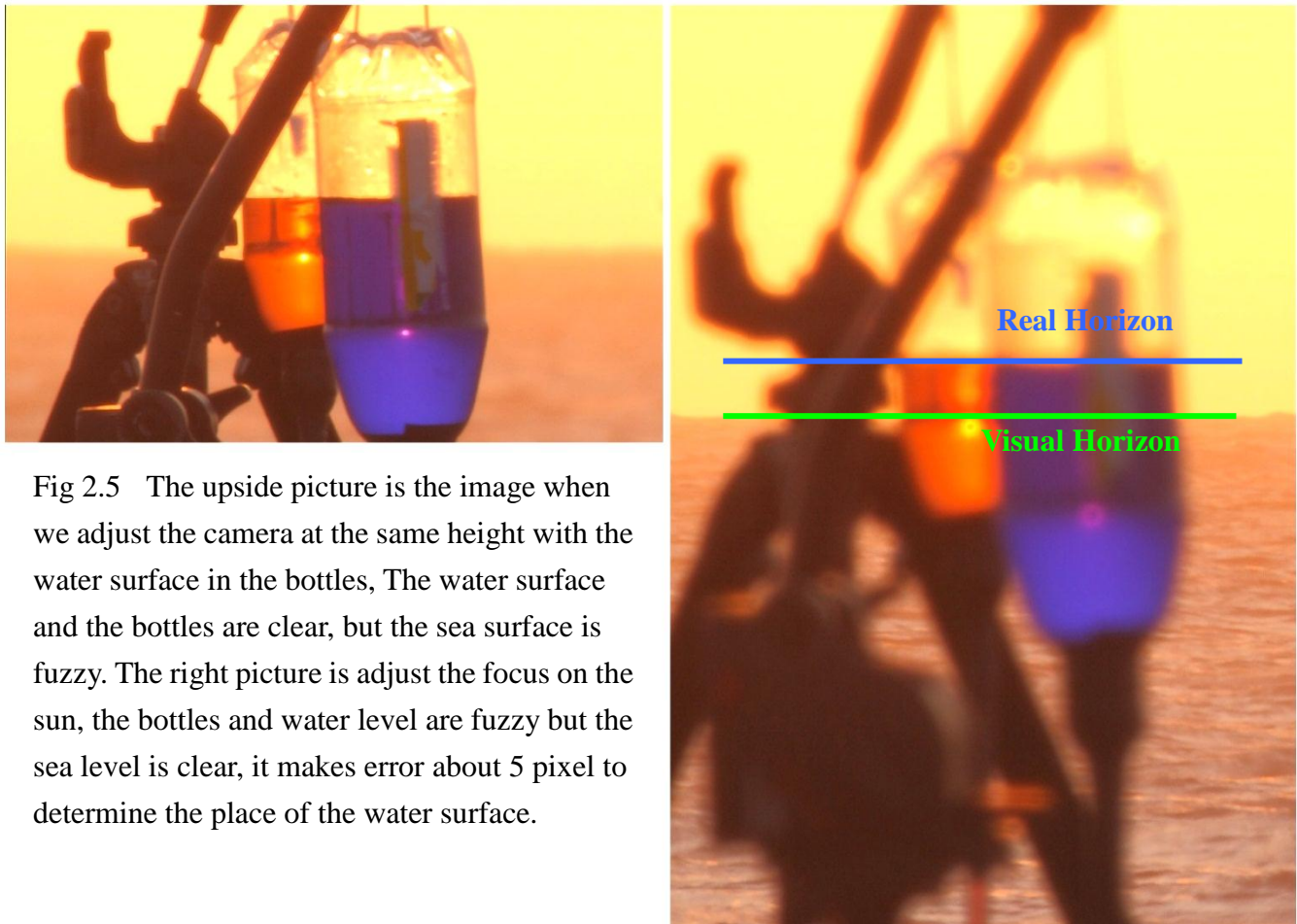


Fig 2.5 The upside picture is the image when we adjust the camera at the same height with the water surface in the bottles, The water surface and the bottles are clear, but the sea surface is fuzzy. The right picture is adjust the focus on the sun, the bottles and water level are fuzzy but the sea level is clear, it makes error about 5 pixel to determine the place of the water surface.

We also use the rawinsonde data to construct the vertical structure of the atmosphere, the rawinsonde was launched by the Central Weather

Bureau (CWB) Banciao weather station where is $121^{\circ} 26' 1.57''$ E, $24^{\circ} 59' 57.5''$ N in GRS67 ($121^{\circ} 26.3' 111''$ E, $24^{\circ} 59' 51.02''$ N in WGS84). The distance between the location rawinsonde launched to the location where we observed the setting sun is 17 km and to the location where we observed the rising sun is 61 km. The rawinsonde launched at 00 hour UT and 12 hour UT every day, it presence 2 to 3 hours delay of the time we observed the setting or rising sun.

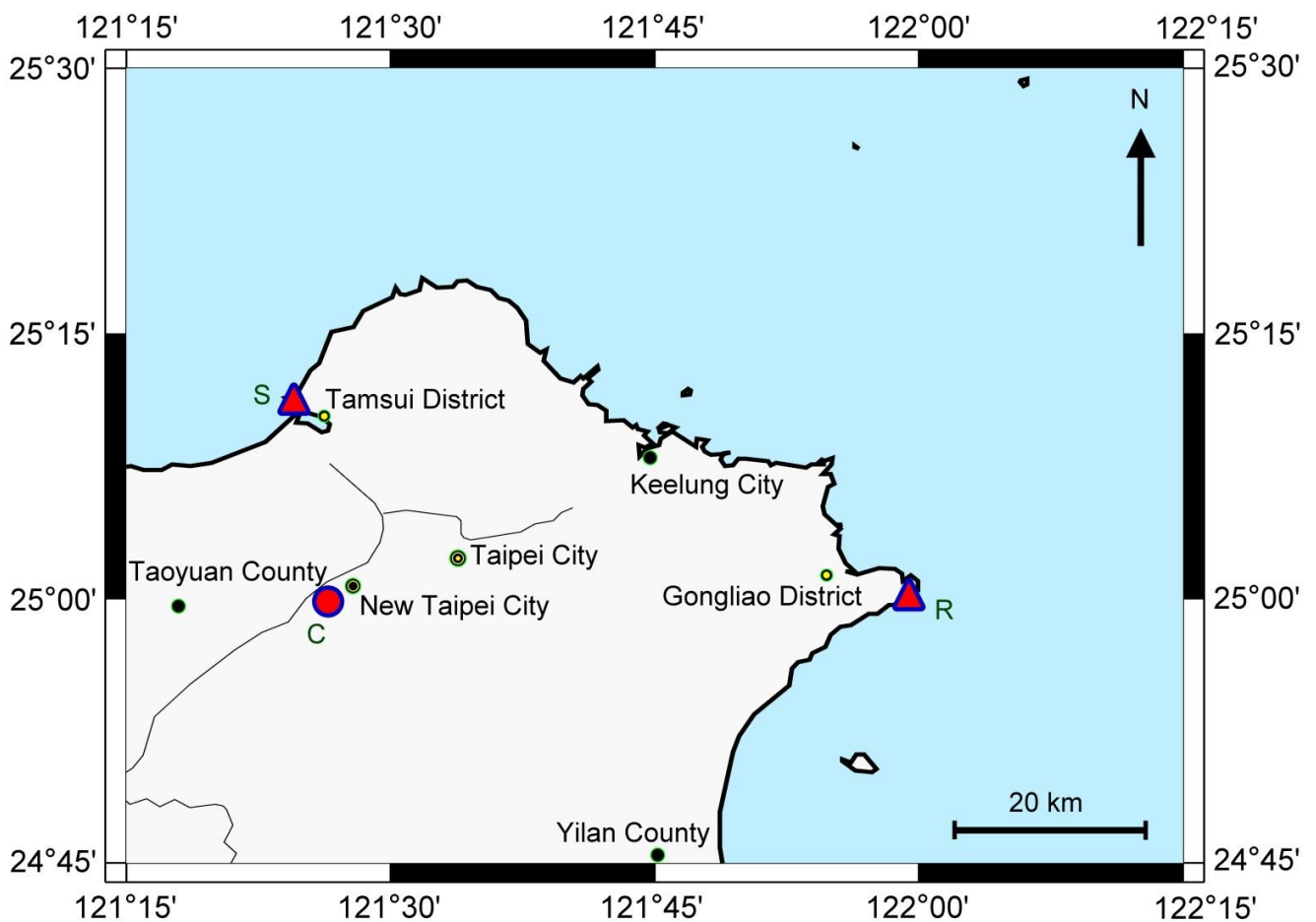


Fig 2.6. This map shows the northern Taiwan coast and where the location we observed. The red triangle with the letter S marked is the location we observed the setting sun, where is nearby the Tamsui district, New Taipei city. The red triangle with the letter R marked is the location we observed the rising sun, where is nearby the Gongliao district, New Taipei city. The red circle with the letter C marked is the location where the Central Weather Bureau (CWB) launched the rawinsonde.

Data Process

3-1 Calibrate the altitude angle of the real sun (the unfracted sun) by the photo time

The camera time had been set to the real local time, it would record the time in the EXIF information when we take the setting or the rising sun, so we can use the photo time to calibrate the altitude angle of the real sun (the un-refracted sun).

The transit time is from the Astronomical Almanac, which longitude is recorded at the 120° E. We calculated the transit time to the longitude of observe location by

$$\text{Transit time}' = \frac{(\text{Lon} - 120^\circ)}{15} + \text{Transit time}$$

Where the Transit time' is the transit time at the observe location, unit in hour, the Lon is the longitude of observe location, the Transit time is the transit time at the longitude 120° E, unit is in hour too.

The S_t means the sun position at the transit time, the transit time is T_t and the coordinates of the sun at transit time is α_t, δ_t . The S means the sun position at the image time, the image time is T and the coordinates of the sun at image time is α, δ . The coordinates of the sun at the transit time and the image time are come from the USNO website.

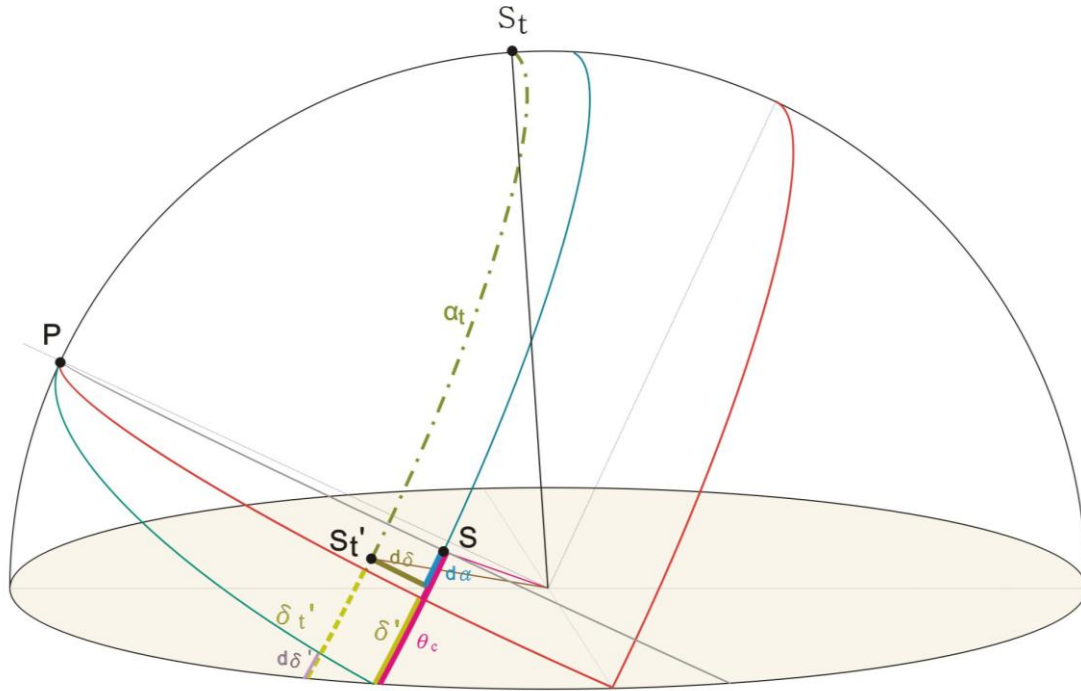


Fig 3-1. To calculate the angle θ_c from the transit time to the image time, the red line is the celestial equator and the right ascension line which zenith angle is 90° . S_t is the sun at the transit time, S is the sun at the image time, St' is the sun at the transit time coordinates rotate to the image time. The $d\alpha$, $d\delta$ are the difference of the coordinates between the transit time to the image time.

The time units are transformed into hour. The time between the transit time to the image time is dT , which is $dT=T-T_t$, during this time the celestial body had rotated an angle α_t where

$$\alpha_t = dT \times 15^\circ.$$

When a celestial object rotate from the transit time to the horizon, it needs rotate more than 90° when the declination is greater than 0° , and needs to rotate less than 90° when the declination is less than 0° , so that when the celestial body is maintain at the same coordinate from the transit time to the set time, it needs rotate $90^\circ + \delta'$, where δ' is an angle related with the declination, which δ' is

$$\delta' = \sin^{-1} \left[\frac{\tan \delta}{\tan(90^\circ - \varphi)} \right], \quad 3-1.1$$

Where δ is the declination, φ is the longitude of the observe location.

Therefore, when the sun is at the transit time coordinate α_t, δ_t , it needs rotate $90^\circ + \delta_t'$, where δ_t' comes from the formula 3-1.1.

But the sun is not stay at the same position, during the image time, the sun had moved to the coordinate α, δ . The RA is inverse the rotate direction of the diurnal motion, which moved an angle $d\alpha$ which is $d\alpha = \alpha - \alpha_t$. The declination had also moved an angle $d\delta$ which is $d\delta = \delta - \delta_t$. The angle $d\delta$ would cause an little angle $d\delta'$ on the RA direction to calculate the rotate angle by diurnal motion from the sun transit to set, where $d\delta' = \delta' - \delta_t'$, and also equal to

$$d\delta' = \left\{ \sin^{-1} \left[\frac{\tan \delta}{\tan(90^\circ - \varphi)} \right] \right\} - \left\{ \sin^{-1} \left[\frac{\tan \delta_t}{\tan(90^\circ - \varphi)} \right] \right\}$$

When at the transit time, the sun needs to rotate an angle $90^\circ + \delta_t'$ to reach the horizon. When at the image time, it needs to rotate an angle θ_c to reach the horizon. Consider the coordinates of the sun at the transit time and the image time is not the same, the angle θ_c is

$$\theta_c = 90^\circ + \delta_t' + d\delta' - d\alpha - \alpha_t$$

Finally need to transport the celestial coordinates into the horizontal coordinates, the Z is the zenith, the sun at image time is S, the declination of the sun at the miage time is δ . The angle $\alpha = \sin^{-1}[(\sin\varphi)/(\cos\delta)]$, $\delta_L = \sin^{-1}[(\sin\delta)/(\cos\varphi)]$, $\theta = \sin^{-1}(\sin\alpha \sin\delta_L)$, $\beta = \cos^{-1}[\cos\varphi \cos(\theta_c - \theta)]$, $L_x = \sin^{-1}[\sin\varphi/\sin\beta]$, $N = L_x + \delta - 90^\circ$, the altitude angle of the sun at the image time $\theta_x = \sin^{-1}[\sin\beta/\sin N]$.

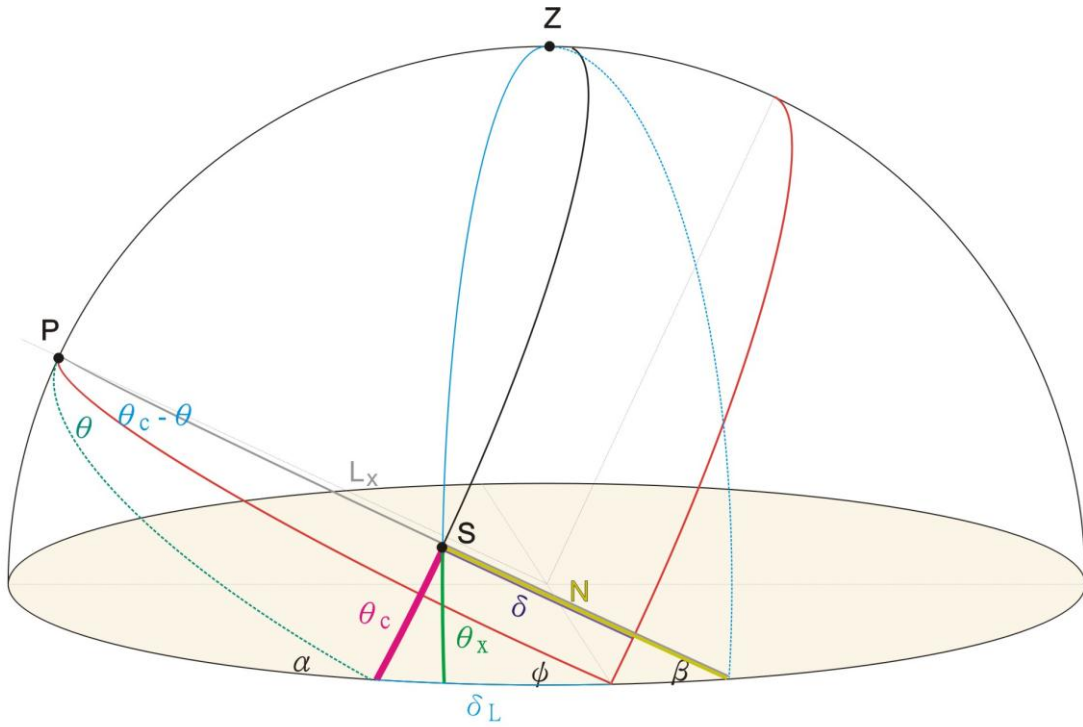


Fig 3-2. To calculate the angle θ_c from the celestial coordinates to the altitude θ_x on the horizontal coordinate.

3-2 The Central Weather Bureau (CWB) rawinsonde data

The Central Weather Bureau (CWB) rawinsonde data had been auto calibrated into hundred different layers from 11 meters height to about 34000 meters height, in order to precise simulate the light path in each layer of the air, we use linear interpolation of each layer into 200 layers. Therefore the vertical structure of the atmosphere has been separate into 24000 to 28000 layers.

The observation of rawinsonde carried out at 12:00 UT September 17, 2011 is only up to 17422 meters height, it may cause error about 30".

3-3 The refraction index of the moist air

The refractivity of the air is decided by the density of the air, and the density of the air is decided by the pressure, temperature, and relative humidity of the air, especially by the pressure and temperature. We used the refractivity model made by Ciddor in 1996, which contained with pressure, temperature, relative humidity and the CO_2 density to construct the refractivity.

The refractivity of the air n in this model which followed by:

$$n = \left[\left(\frac{\rho_a}{\rho_{a_{xs}}} \right) (n_{a_{xs}} - 1) + \left(\frac{\rho_w}{\rho_{ws}} \right) (n_{ws} - 1) \right] + 1 \quad (A)$$

where the ρ_a is the density of the dry air while the pressure and the temperature is under the observation situation which is in the formula (c1), the $\rho_{a_{xs}}$ is the density of the dry air which is under the standard states which is in the formula (c2), the $n_{a_{xs}}$ means the refractivity of the dry air while under the standard states and which is in the formula (a), the ρ_w is the density of the pure water vapor while the temperature and pressure is under the observe situation and which is in the formula (c3), the ρ_{ws} is the density of the pure water vapor while under the standard states and which is in the formula (c4), the n_{ws} is the refractivity of the pure water vapor while under the standard states but the relative humidity is 100% and it is in the formula (b), the standard states is defined as the temperature t is $15^\circ C$, the pressure P is 101325 pa, the relative humidity is 0% and the density of the CO_2 is at 450 ppm.

The n_{axs} means the refractivity of the dry air which is under the standard states, which comes from:

$$n_{axs} = \{(n_{as} - 1)[1 + 0.534 \times 10^{-6}(\chi_c - 450)]\} + 1, \quad (a)$$

.....

where the χ_c is the density of CO_2 which is under the observe situation, and n_{as} is the refractivity of the dry air which is under the standard states but not contained with the CO_2 , which is:

$$n_{as} = \left(\frac{k_1}{k_0 - \sigma^2} + \frac{k_3}{k_2 - \sigma^2} \right) \times 10^{-8} + 1,$$

where the σ is the reciprocal of the vacuum wavelength in inverse micrometers, the k_0, k_1, k_2, k_3 are the constants involved in the standard phase and group refractivity of dry air where $k_0 = 238.0185 \mu m^{-2}$, $k_1 = 5792105 \mu m^{-2}$, $k_2 = 57.362 \mu m^{-2}$ and $k_3 = 167917 \mu m^{-2}$, the σ in our program is set as $1/550 \text{ nm}^{-1}$, and the density of CO_2 χ_c is set as 450 ppm.

The n_{ws} means the refractivity of the pure water vapor while under the standard states, it comes from:

$$n_{ws} = [cf(w_0 + w_1\sigma^2 + w_2\sigma^4 + w_3\sigma^6)] \times 10^{-8} + 1, \quad (b)$$

.....

where the σ is the reciprocal of the vacuum wavelength in inverse micrometers, the $w_0, w_1, w_2,$ and w_3 are the constants involved in the standard phase and group refractivity of water vapor with value, $w_0 = 295.235 \mu m^{-2}$, $w_1 = 2.6422 \mu m^{-2}$, $w_2 = -0.032380 \mu m^{-4}$ and $w_3 = 0.004028 \mu m^{-2}$, the $cf = 1.022$ is the correction factor finds by fitting the

calculations to the measurements, and the σ in our program is also set as $1/550 \text{ nm}^{-1}$.

The ρ means the density of the air, which comes from:

$$\rho = \left(\frac{PM_a}{ZRT} \right) \left[1 - X_w \left(1 - \frac{M_w}{M_a} \right) \right], \quad \text{(c)}$$

Where P is the pressure in pa, T is the temperature in K, R is the gas constant which value is $R = 8.314510 \text{ J mol}^{-2} \text{ K}^{-1}$, M_w is the molecular weight of the water vapor which is $M_w = 0.018015 \text{ kg/mol}$, M_a is the molecular weight of the dry air which contained with χ_c ppm of CO_2 , and $M_a = 10^{-3} [28.9635 + 12.011 \times 10^{-6} (X_c - 400)] \text{ kg/mol}$, due to the CWB rawinsonde doesn't detected the density of CO_2 , all the observed value χ_c were set as the value 450 ppm., and the χ_w is the mole fraction of the water vapor which is in the moist air, which is:

$$X_w = \frac{f h \text{ svp}}{P}, \quad \text{(c-a)}$$

where the h is the relative humidity in %, the P is the pressure in pa, the $f = \alpha + \beta P + \gamma^2$ is the enhancement factor of water vapor in air, $\alpha = 1.0662$, $\beta = 3.14 \times 10^{-8} \text{ pa}$, $\gamma = 5.6 \times 10^{-7} \text{ } ^\circ\text{C}^{-2}$ and $t = T - 273.15 \text{ } ^\circ\text{C}$, T is the temperature in K, the svp is the saturation vapor pressure of water vapor in air, which is $\text{svp} = \exp(AT^2 + BT + C + D/T) \text{ pa}$, and $A = 1.2378847 \times 10^{-5} \text{ K}^{-2}$, $B = -1.9121316 \times 10^{-2} \text{ K}^{-1}$, $C = 33.93711047$, $D = -6.3431645 \times 10^3 \text{ K}$.

The Z is the compressibility of the moist air, which is defined by:

$$Z = 1 - \left(\frac{P}{T}\right) \left[a_0 + a_1 t + a_2 t^2 + (b_0 + b_1 t) X_w + (c_0 + c_1 t) X_w^2 \right] + \left(\frac{P}{T}\right)^2 (d + e X_w^2), \dots \text{(c-b)}$$

Where the χ_w is the mole fraction of the water vapor which is in the moist air and is in the formula (c-a), the P is the pressure in pa, T is the temperature in K, t is the temperature in °C, $a_0 = 1.58123 \times 10^{-6} \text{ KPa}^{-1}$, $a_1 = -2.9331 \times 10^{-8} \text{ Pa}^{-1}$, $a_2 = 1.1043 \times 10^{-10} \text{ K}^{-1} \text{ Pa}^{-1}$, $b_0 = 5.707 \times 10^{-6} \text{ K Pa}^{-1}$, $b_1 = -2.051 \times 10^{-8} \text{ Pa}^{-1}$, $c_0 = 1.9898 \times 10^{-4} \text{ K Pa}^{-1}$, $c_1 = -2.376 \times 10^{-6} \text{ Pa}^{-1}$, $d = 1.83 \times 10^{-11} \text{ K}^2 \text{ Pa}^{-2}$ and $e = -0.765 \times 10^{-8} \text{ K}^2 \text{ Pa}^{-2}$.

While Z is meaning the compressibility of the dry air, the temperature T is 288.15K, the pressure P is 1013.25 pa, the mole fraction of the water vapor which is in the moist air χ_w is 0. Put all of these values into the formula (c-b), and then get the compressibility of the dry air Z_a . While Z is meaning the compressibility of the pure water vapor, the temperature T is 293.15K, the pressure P is 1333 pa, the mole fraction of the water vapor which is in the moist air χ_w is 1. Put all of these values into the formula (c-b), and then get the compressibility of the pure water vapor Z_w .

The ρ_a in the formula (A) is the density of the dry air while the pressure and the temperature is under the observation situation. It is under the situation that the temperature T and the pressure P is the temperature and pressure in each layer of the air we recorded during observed by the rawinsonde, and the relative humidity h is 0%, the density of CO_2 χ_c is set

as 450 ppm., and the compressibility of the moist air Z is equal to the compressibility of the dry air Z_a . Put all of these values into the formula (c), and then get the density of the dry air ρ_a , it is the formula (c1).

The $\rho_{a,ss}$ in the formula (A) is the density of the dry air while the pressure and the temperature is under the standard states. It is under the situation that the temperature T is $15\text{ }^\circ\text{C}$, the pressure P is 101325 pa, the relative humidity h is 0%, the density of CO_2 χ_c is set as 450 ppm., and the compressibility of the moist air Z is equal to the compressibility of the dry air Z_a . Put all of these values into the formula (c), and then get the density of the dry air $\rho_{a,ss}$, it is the formula (c2).

The ρ_w in the formula (A) is the density of the pure water vapor while the pressure and the temperature is under the observation situation. It is under the situation that the temperature T and the pressure P is the temperature and pressure in each layer of the air we recorded during observed by the rawinsonde, and the relative humidity h in each layer is observed by the rawinsonde, the density of CO_2 χ_c is set as 450 ppm., and the compressibility of the moist air Z is equal to the compressibility of the pure water vapor Z_w . Put all of these values into the formula (c), and then get the density of the dry air ρ_w , it is the formula (c3).

The $\rho_{w,ss}$ in the formula (A) is the density of the pure water vapor which is under the standard states. It is under the situation that the temperature T is $15\text{ }^\circ\text{C}$, the pressure P is 101325 pa, and the relative

humidity h is 100 %, the density of CO_2 χ_c is set as 450 ppm., and the compressibility of the moist air Z is equal to the compressibility of the pure water vapor Z_w . Put all of these values into the formula (c), and then get the density of the dry air ρ_{ws} , it is the formula (c4).

Finally combined the density of the dry air while the pressure and the temperature is under the observation situation ρ_a , the density of the dry air while the pressure and the temperature is under the standard states ρ_{axs} , the density of the pure water vapor while the pressure and the temperature is under the observation situation ρ_w , the density of the pure water vapor which is under the standard states ρ_{ws} , the refraction index of the dry air which is under the standard states n_{axs} , and the refraction index of the pure water vapor while under the standard states n_{ws} into the formula (A), got the refractivity in the each layer of air n .

We use the Central Weather Bureau (CWB) rawinsonde data which record the pressure, temperature and relative humidity respond to the height and use these data to establish different refraction index of each layer of atmosphere.

3-4 The refraction between each layer of the atmosphere

While a light path incomes from outside of the atmosphere, it would has a incidence angle in the top of the atmosphere, and the light path would followed the snell's law on the surface of two different layer of atmosphere, which is shows on the figure.

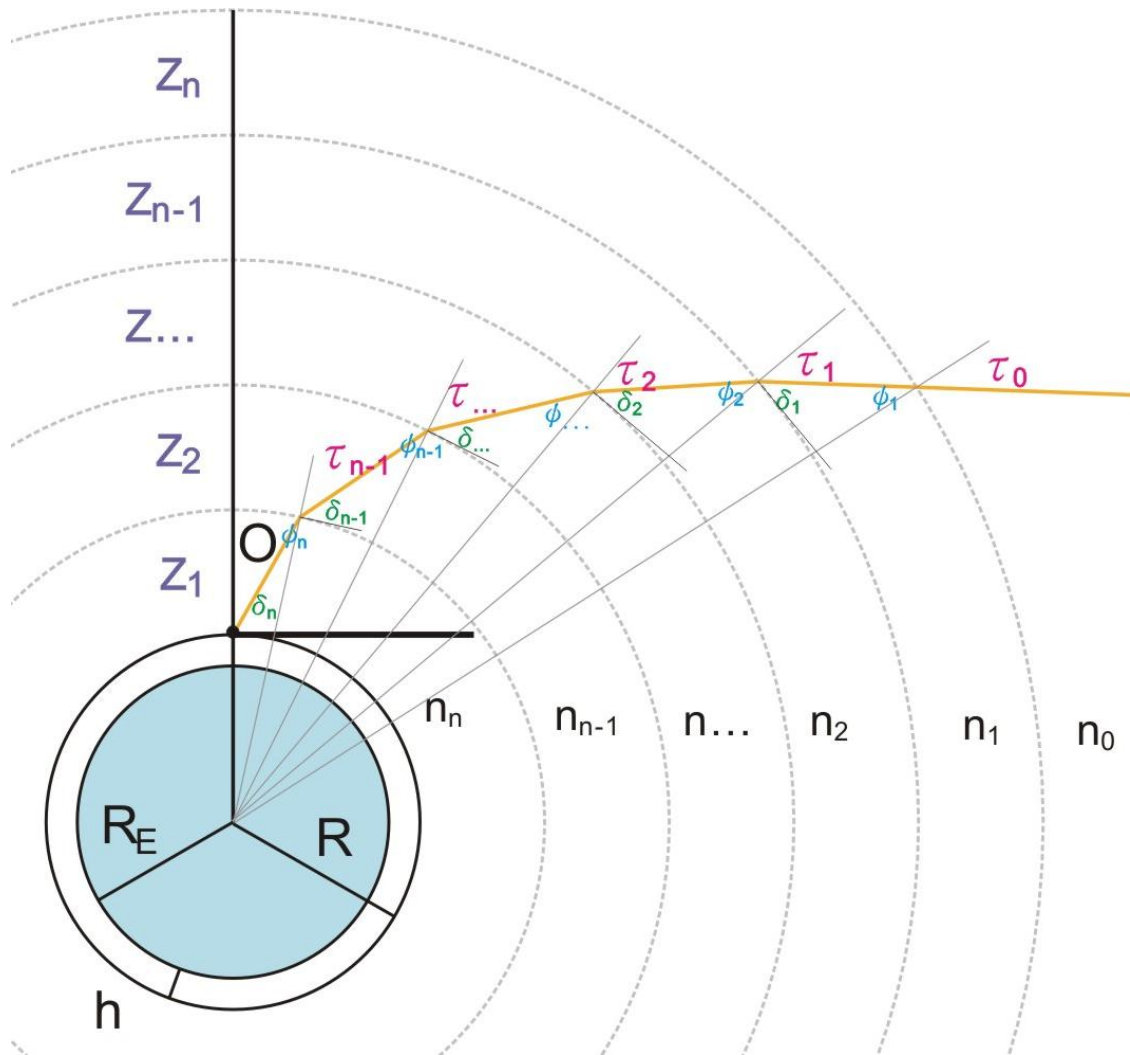


Fig 3-3. The refraction between the boundary of different layers.

The radius of the earth R_E is 6374248 meters, which is from the ellipsoid defined by WGS84, use the latitude of the observe location to calculate the radius to the center of the ellipsoid as R_E . The height of the observe location h is also considered, so the radius of the observe location to the center of the earth R is R_E+h , we assumed the earth is a sphere

because in our model the difference from sphere to ellipsoid is quite small to ignore. The $Z_1, Z_2, \dots, Z_{n-1}, Z_n$ are the different thickness of the vertical atmosphere layers described in the chapter 3-2, the different refraction index are described chapter 3-3, and the refraction index outside the atmosphere is set as $n_0 = 1$.

The process of the light path is followed the snell's law, refractive at the boundary of the different layer of the atmosphere. The light path would be curved continuously till light-ray reach the ground. On the first boundary between the first layer of atmosphere to the space, the incidence angle is τ_0 and the refraction angle is $\varphi_1 = \sin^{-1} \left(\frac{n_0 \tau_0}{n_1} \right)$. In the first layer of the atmosphere, we could calibrate the incidence angle τ_1 of the second boundary between the first and second layer of the atmosphere. The Complementary angle of the incidence δ_1 is $\delta_1 = \cos^{-1} \left\{ \frac{[R_E + (Z_1 + Z_2 + \dots + Z_{n-1} + Z_n)] \times \sin \varphi_1}{R_E + (Z_1 + Z_2 + \dots + Z_{n-1})} \right\}$ and the incidence angle of the second τ_1 is $\tau_1 = 90^\circ - \delta_1$.

Summary all above, we get the relation the angles repending to the light path during each layer of atmosphere:

$$\text{In the first layer: } \delta_1 = \cos^{-1} \left\{ \frac{[R_E + (Z_1 + Z_2 + \dots + Z_{n-1} + Z_n)] \times \sin \left(\frac{n_0 \tau_0}{n_1} \right)}{R_E + (Z_1 + Z_2 + \dots + Z_{n-2} + Z_{n-1})} \right\},$$

$$\tau_1 = 90^\circ - \delta_1, \quad \varepsilon_1 = 90^\circ - \varphi_1 - \delta_1$$

$$\text{In the second layer: } \delta_2 = \cos^{-1} \left\{ \frac{[R_E + (Z_1 + Z_2 + \dots + Z_{n-2} + Z_{n-1})] \times \sin \left(\frac{n_1 \tau_1}{n_2} \right)}{R_E + (Z_1 + Z_2 + \dots + Z_{n-2} + Z_{n-2})} \right\},$$

$$\tau_2 = 90^\circ - \delta_2, \quad \varepsilon_2 = 90^\circ - \varphi_2 - \delta_2$$

$$\text{In the last second layer: } \delta_{n-1} = \cos^{-1} \left\{ \frac{[R_E + (Z_1 + Z_2)] \times \sin \left(\frac{n_{n-2} \tau_{n-2}}{n_{n-1}} \right)}{R_E + Z_1} \right\},$$

$$\tau_{n-1} = 90^\circ - \delta_{n-1} \quad ,$$

$$\varepsilon_{n-1} = 90^\circ - \varphi_{n-1} - \delta_{n-1}$$

In the last layer:

$$\delta_n = \cos^{-1} \left\{ \frac{[R_B + Z_1] \times \sin\left(\frac{n_{n-1} \tau_{n-1}}{n_n}\right)}{R_B} \right\} \dots\dots\dots (3-4)$$

$$\varepsilon_n = 90^\circ - \varphi_n - \delta_n,$$

where the δ_n in the last layer is the altitude angle of the refracted sun in the astronomical refraction model.

3-5 The light path during the atmosphere

We use the results calculated in 3-1 to calibrate the altitude angle of the unfracted sun (the real sun), but due to the refraction of the atmosphere, the light path is followed the real sun path which wouldn't reach the observe place on the ground. If the light path reach the ground in front of the observe location, the incidence angle should add a little angle, $\tau_0' = \tau_0 + \theta + r_x$, to correct the light path.

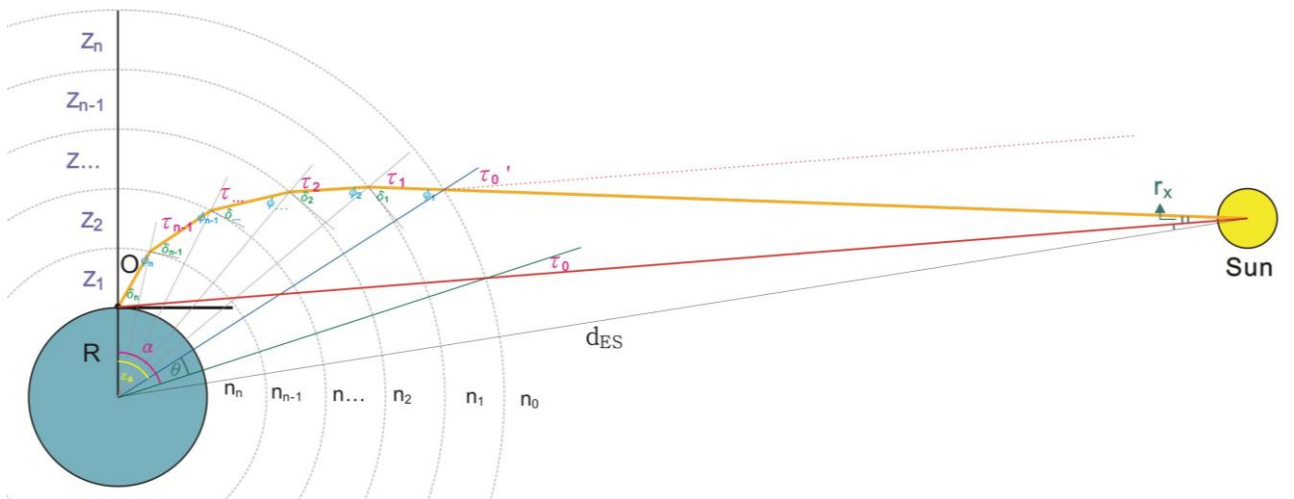


Fig. 3-4. The red line is the light path from the real sun, but due to the refraction of the atmosphere, the light path should a little higher than the red line, then the light path would be refracted then reach the ground where is the observer's location.

The angle τ_0 is the original incidence angle on the top of the atmosphere, which could calculate from the real sun's altitude angle θ_z which had calculated in chapter 3-1.

$$\text{The } \tau_0 \text{ is } \tau_0 = \sin^{-1} \left[\frac{R \cos \theta_z}{R + (Z_1 + Z_2 + \dots + Z_n)} \right]$$

Then we could calculate the central angle α , which is $\alpha = 90^\circ - \theta_z - \tau_0$.

We use the τ_0 as the incidence angle into chapter 3-4 to calculate the

light path, and when the light path reach the ground, the refracted sun's altitude δ_n will be calculated, and all of the central angle ϵ_α by summing up the central angles during the process of the light path refracted in different layer of the atmosphere, $\epsilon_\alpha = \epsilon_1 + \epsilon_2 + \dots + \epsilon_n$.

When the light path is followed the real sun's light path (the red line in fig 3-5.1), the light path couldn't reach the Observer's position, it should followed the orange line path which had add a little angle to let the light path reaches the observer's location.

We add a little central angle θ to let the light path reach the observer's location, due to the sun still not a real unlimited far object, the incidence angle should be changed to τ_0' while we add a little central angle θ , and $\tau_0' = \tau_0 + \theta + r_x$.

The angle r_x is comes from:

$$r_x = \tan^{-1} \left\{ \frac{[R_E + (Z_1 + Z_2 + \dots + Z_n)] \times \sin^{-1} \left[\tau_0 + \theta - \sin^{-1} \left(\frac{R_E \cos \theta_Z}{d_{ES}} \right) \right]}{d_{ES} - [R_E + (Z_1 + Z_2 + \dots + Z_n)] \times \cos \left[\tau_0 + \theta - \sin^{-1} \left(\frac{R_E \cos \theta_Z}{d_{ES}} \right) \right]} \right\} - \sin^{-1} \left(\frac{R_E \cos \theta_Z}{d_{ES}} \right),$$

Where the d_{ES} is the distance between the earth and the sun at the photo time calaulated from the USNO.

The central angle θ is restricted it conform to the equation,

$$\alpha - (\epsilon_\alpha - \theta) \leq 0.018''.$$

That means when the light path reach the ground, it is less than 0.556 meter around the observer's real location.

Result and Discussion

At three dusk and at one dawn, the observations of the setting sun and rising sun with the measured real horizon, the images of setting/rising sun are compared with the model. However, there are six dusk and one dawn, only the images of setting/rising sun (without the measured real horizon) are also analyzed in the Appendix E.

For the observations of setting or rising sun without the real horizon, the sea level in the image is used as the real horizon, and it will derive the real horizon upper the sea level about 258.35" when the observer's is at 5 meters height. The setting or rising sun without the measured real horizon ignored the terrestrial refraction which occurred the error of the real horizon is about 300".

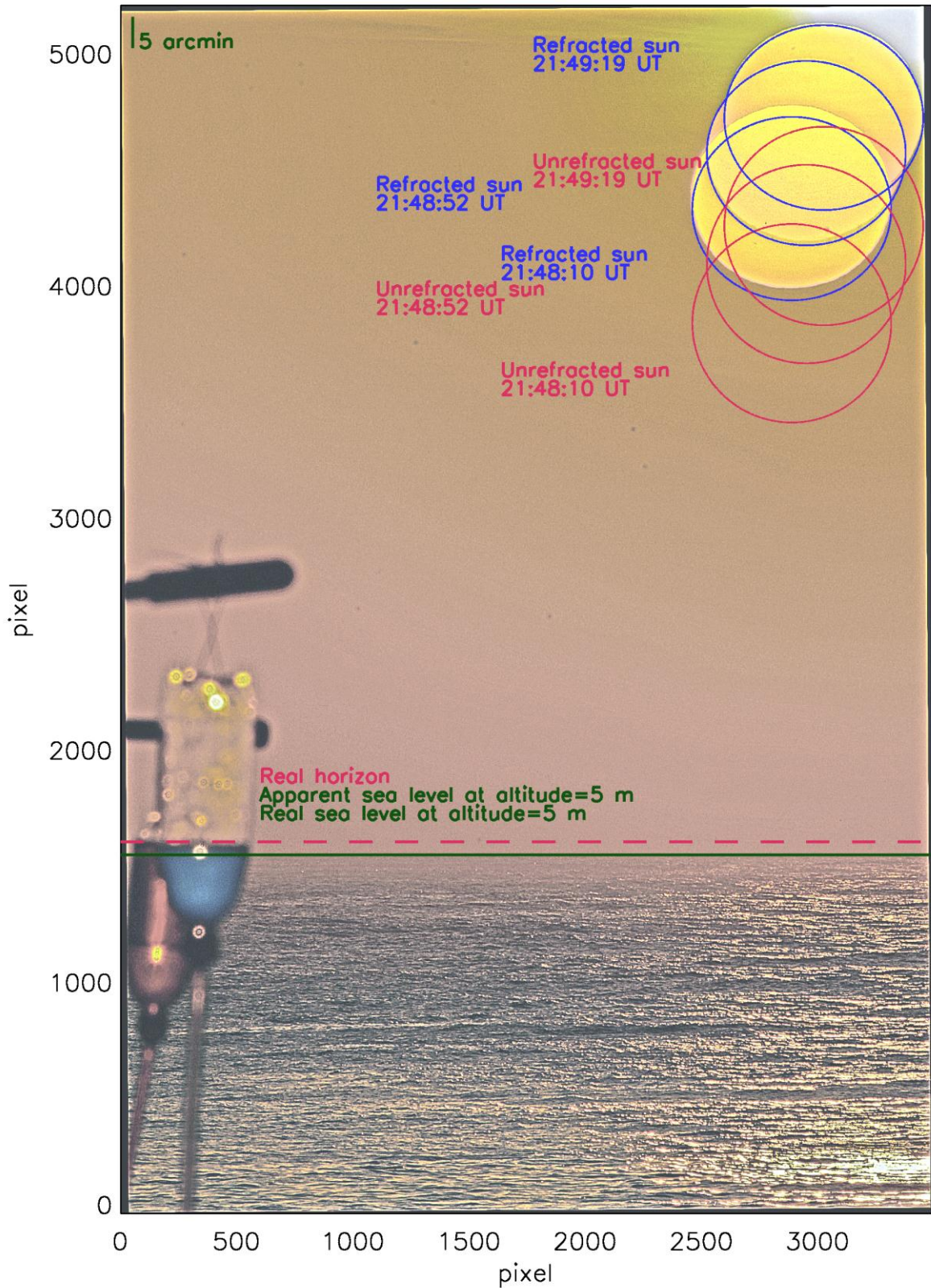


Fig 4-1.1. The refracted sun (blue) and the unrefracted sun (pink), compared with the observed sun during the sunrise in September 17, 2011 with measured the real horizon. The pink dashed line is the real horizon from the observation, the green line is the apparent sea level at altitude=5 m and the green dashed line is the real sea level without the terrestrial refraction at altitude=5 m.

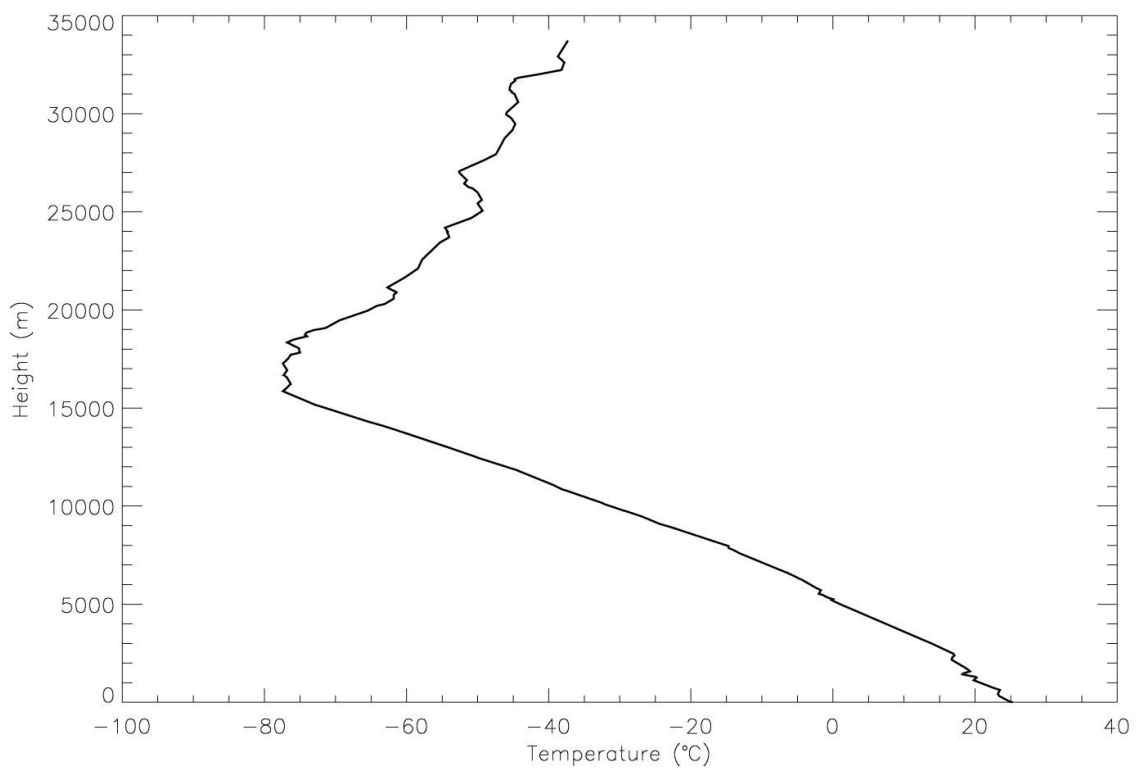
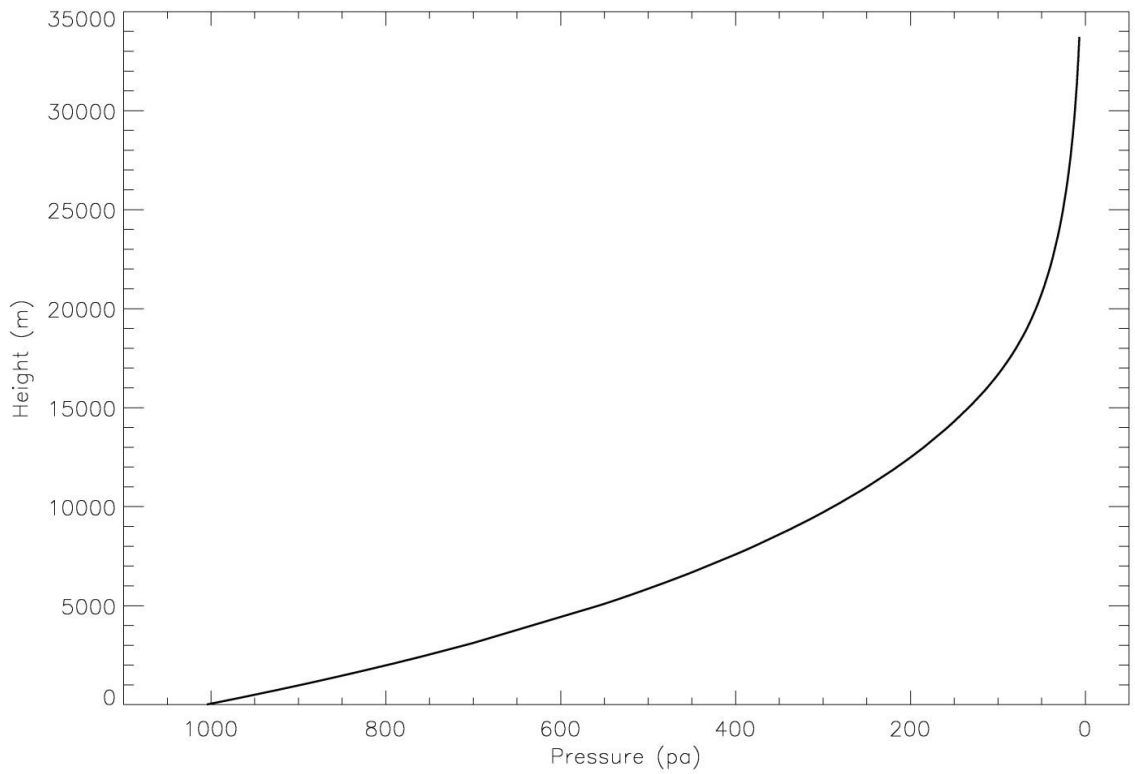


Fig 4-1.2. The height to pressure fig (up) and the height to temperature fig (down) during observe at September 17, 2011 morning, the data is from the CWB rawinsonde which launched at 00:00 UT September 17, 2011.

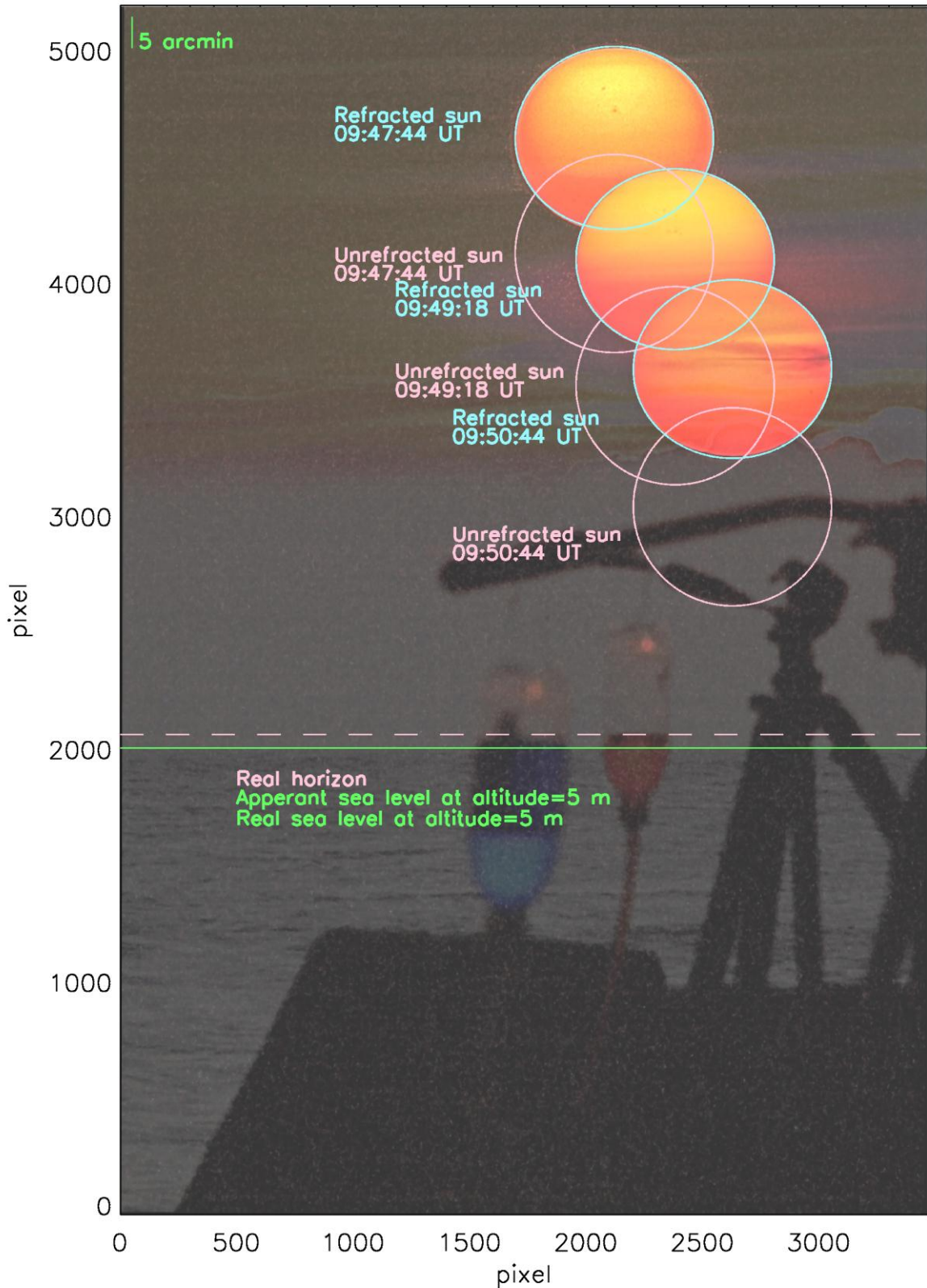


Fig 4-2.1. The refracted sun (blue) and the unrefracted sun (pink), compared with the observed sun during the sunset in September 17, 2011 with measured the real horizon. The pink dashed line is the real horizon from the observation, the green line is the apperant sea level at altitude=5 m and the green dashed line is the real sea level without the terrestrial refraction at altitude=5 m.

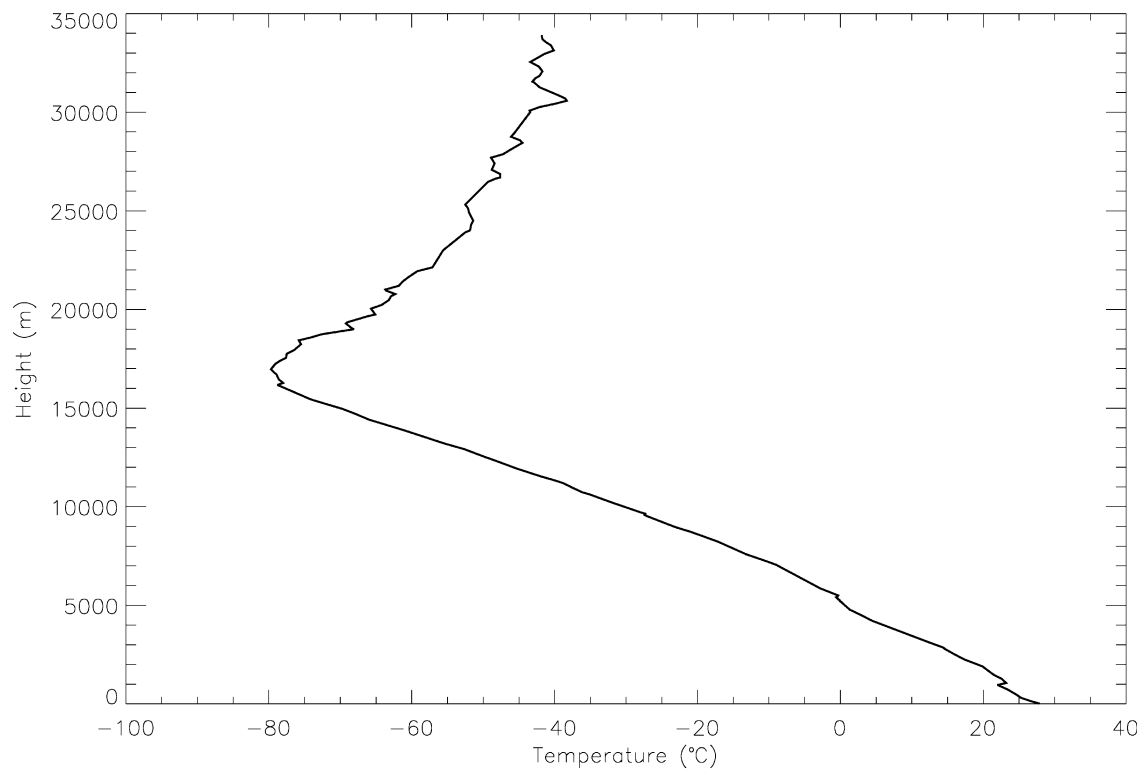
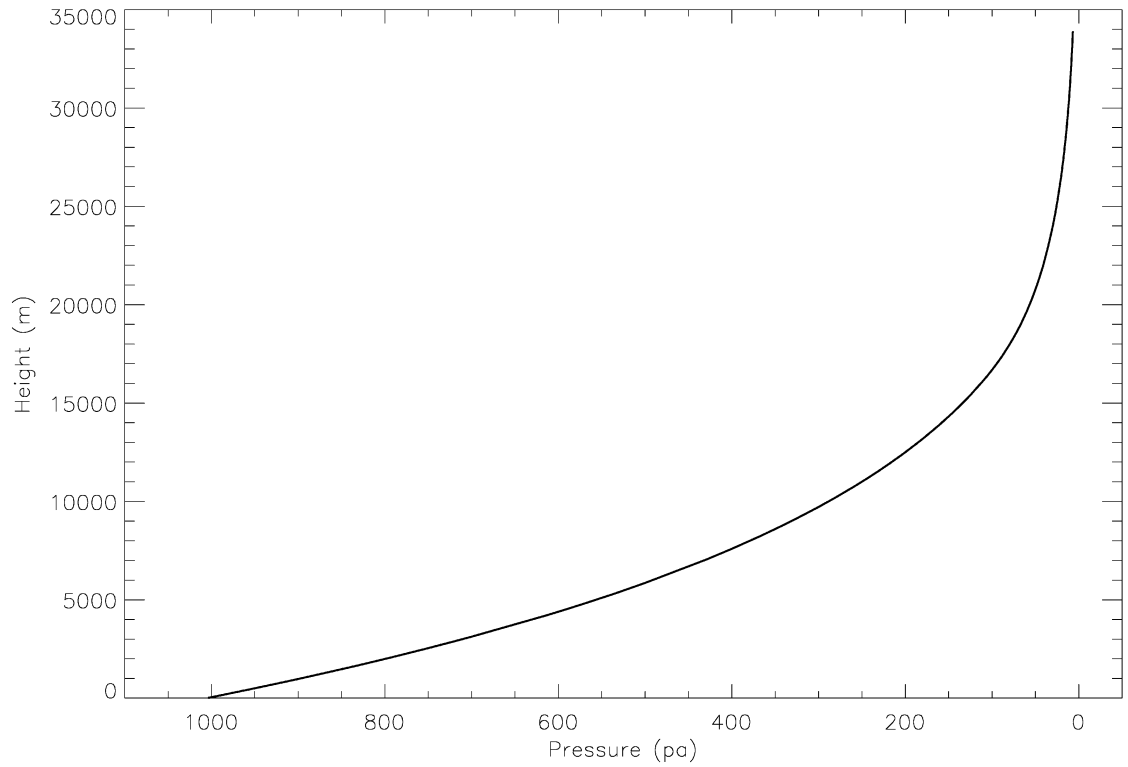


Fig 4-2.2. The height to pressure fig (up) and the height to temperature fig (down) during observe at September 17, 2011 night, the data is from the CWB rawinsonde which launched at 12:00 UT September 17, 2011.

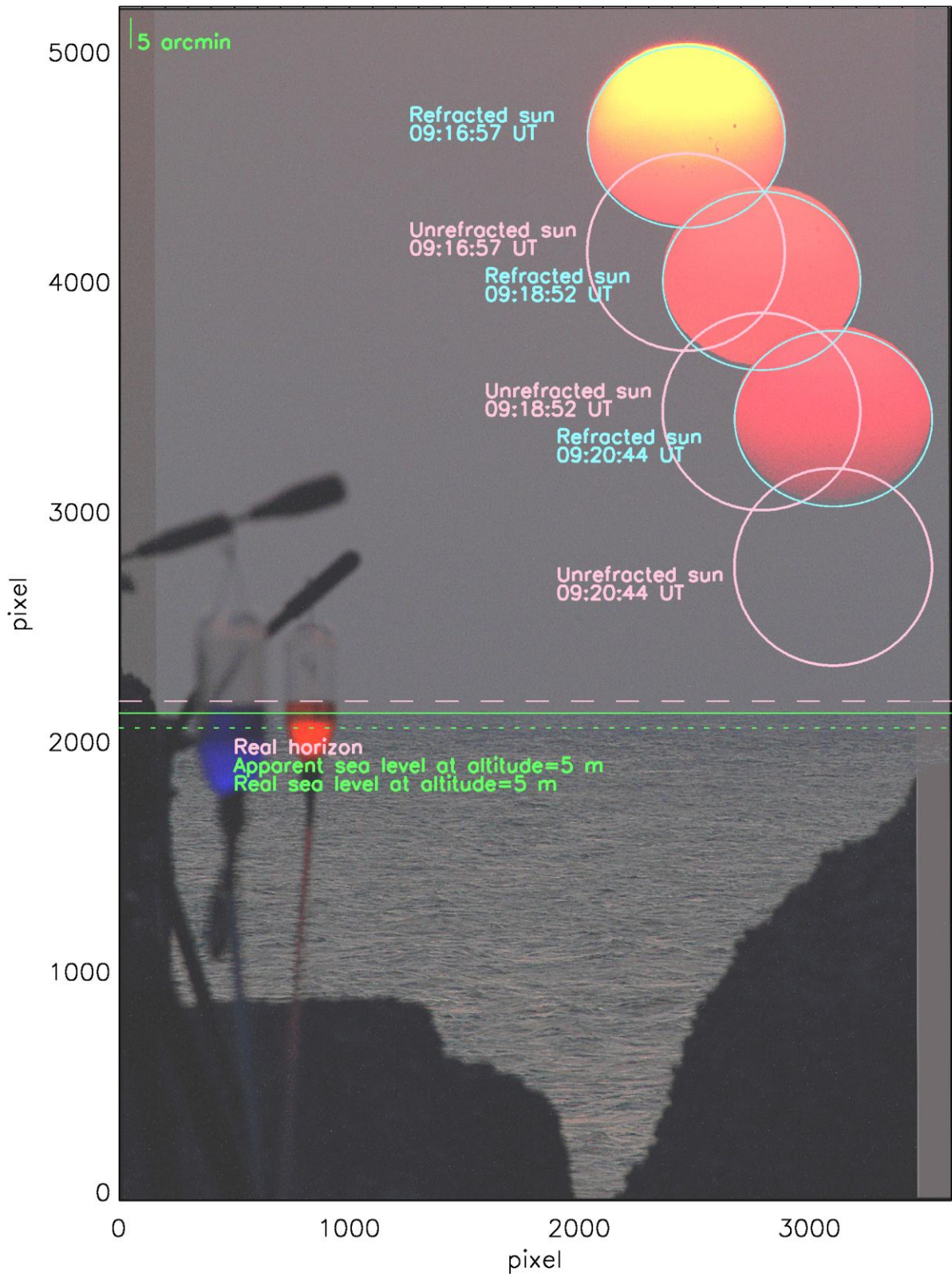


Fig 4-3.1. The refracted sun (blue) and the unrefracted sun (pink), compared with the observed sun during the sunset in October 17, 2011 with measured the real horizon. The pink dashed line is the real horizon from the observation, the green line is the apparent sea level at altitude=5 m and the green dashed line is the real sea level without the terrestrial refraction at altitude=5 m.

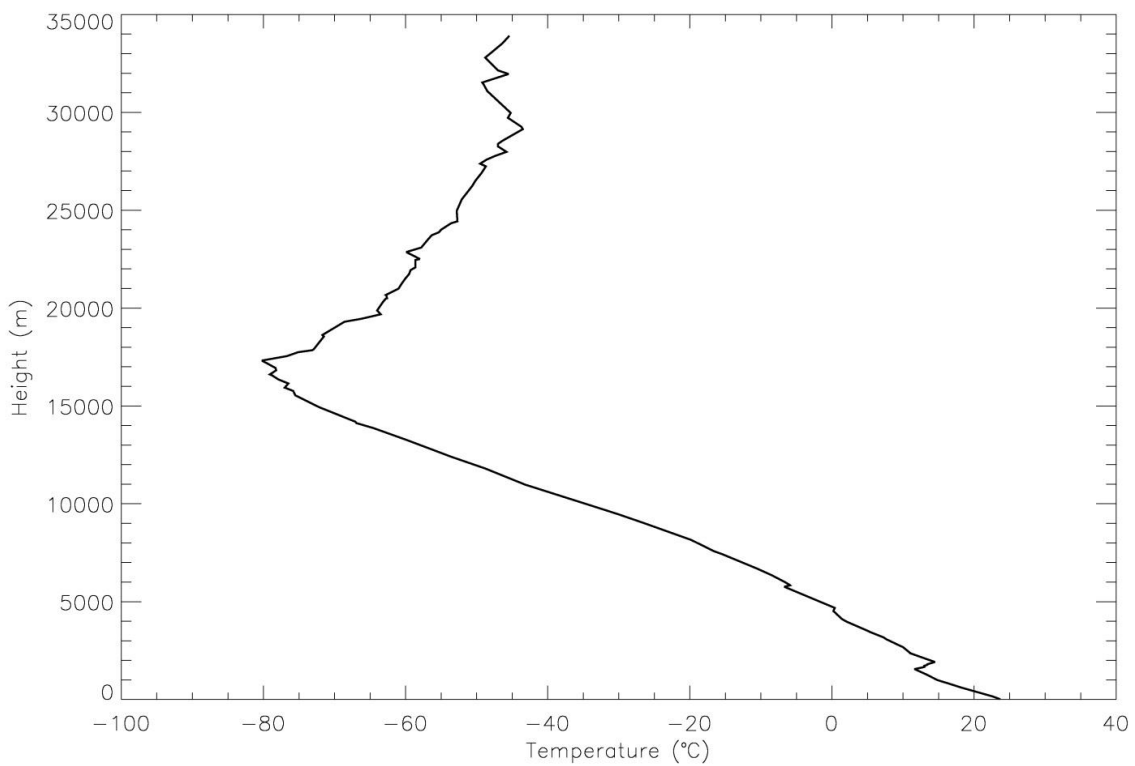
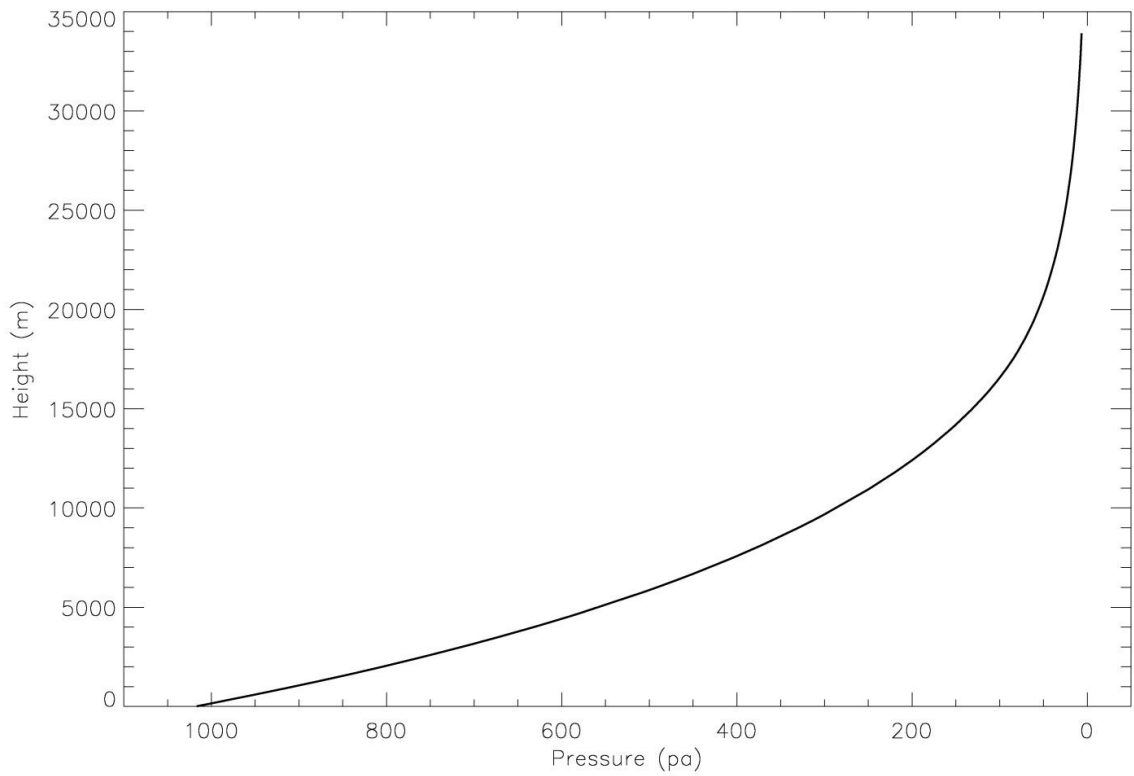


Fig 4-3.2. The height to pressure fig (up) and the height to temperature fig (down) during observe at October 17, 2011 night, the data is from the CWB rawinsonde which launched at 12:00 UT October 17, 2011.

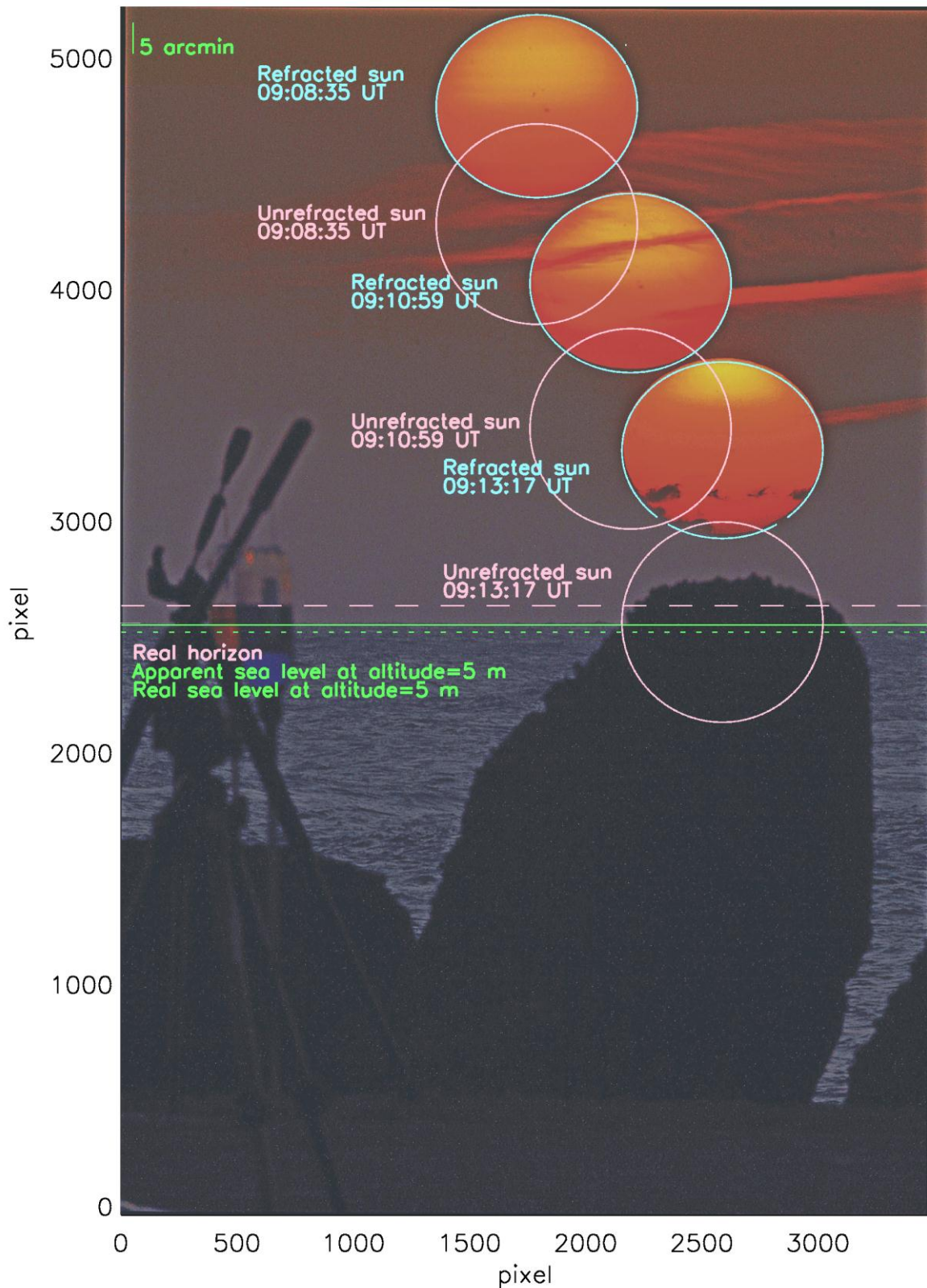


Fig 4-4.1. The refracted sun (blue) and the unrefracted sun (pink), compared with the observed sun during the sunset in October 28, 2011 with measured the real horizon. The pink dashed line is the real horizon from the observation, the green line is the apparent sea level at altitude=5 m and the green dashed line is the real sea level without the terrestrial refraction at altitude=5 m.

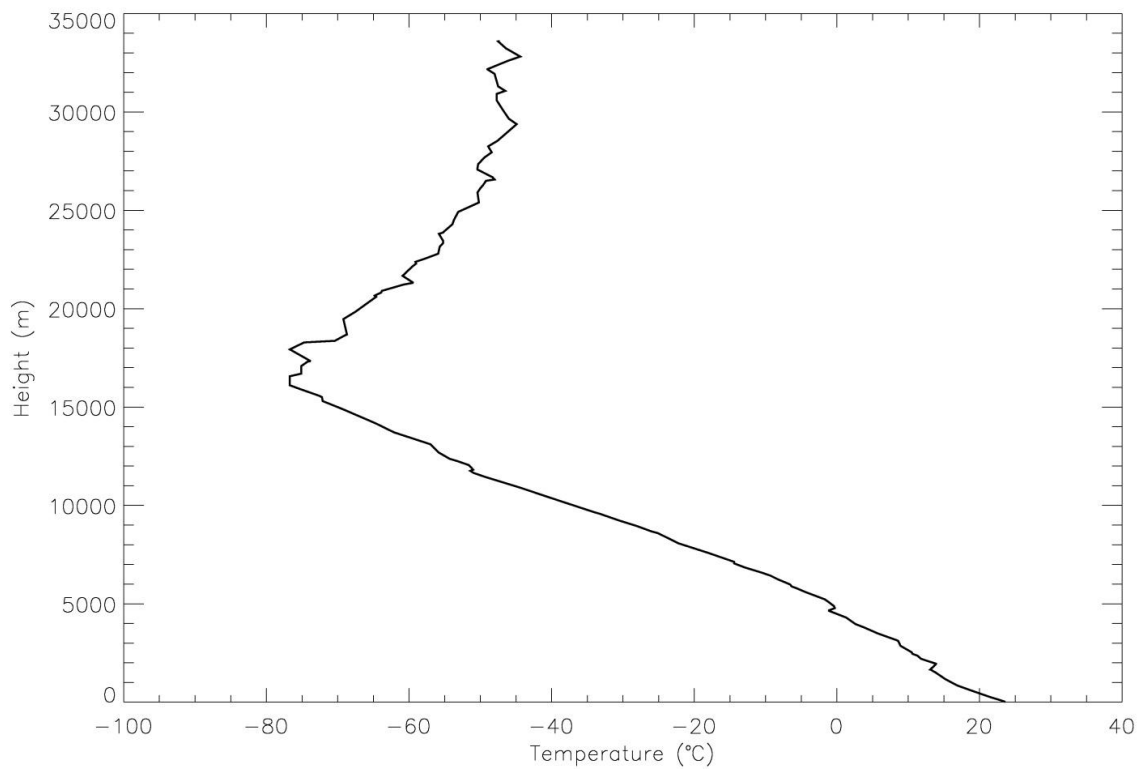
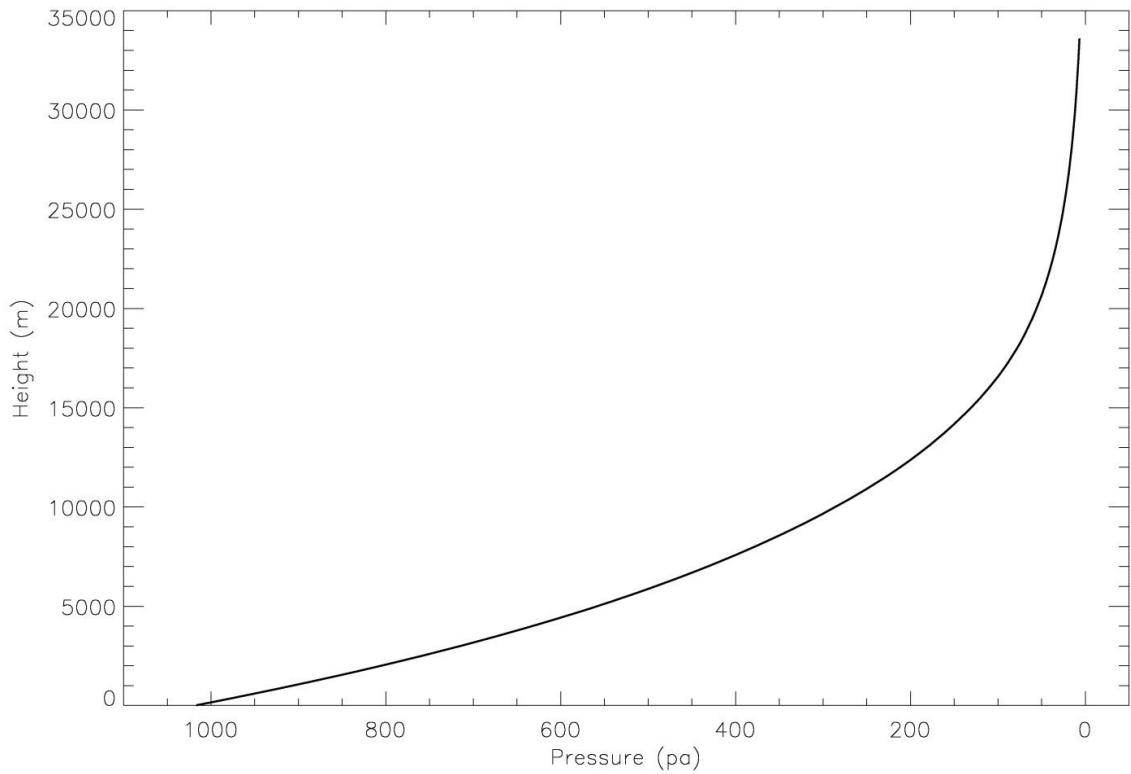


Fig 4-4.2. The height to pressure fig (up) and the height to temperature fig (down) during observe at October 28, 2011 night, the data is from the CWB rawinsonde which launched at 12:00 UT October 28, 2011.

Table 4-1. This table shows the unrefracted incident angle, modeled refracted angle and the observed refracted angle on the different time during the observation on September 17, 2011 morning. The value means the altitude angle which is above the real horizon in degrees. The “Difference” means the difference between the modeled refraction angle and the observed angle in arcsec.

September 17, 2011 Sunrise

Time		Unrefracted altitude	Modeled refracted	Observed refracted	Astronomical refraction	Difference
21:48:10 UT	Upper limb	1°39' 2".85	1°56' 18".64	1°56' 12".88	17' 10".02	1' 31".19
	Center	1°23' 8".28	1°41' 32".70	1°41' 27".02	18' 18".74	2' 09".41
	Lower limb	1°07' 13".70	1°26' 54".11	1°26' 45".53	19' 34".83	1' 40".11
21:48:52 UT	Upper limb	1°48' 32".38	2°05' 01".57	2°05' 40".14	17' 07".76	0' 35".56
	Center	1°32' 37".80	1°50' 14".70	1°51' 06".08	18' 28".28	0' 51".38
	Lower limb	1°16' 43".23	1°35' 31".69	1°36' 11".90	19' 28".68	0' 40".22
21:49:19 UT	Upper limb	1°54' 38".49	2°10' 47".52	2°11' 08".63	16' 09".02	0' 21".11
	Center	1°38' 43".92	1°55' 55".28	1°56' 06".55	17' 11".36	0' 11".27
	Lower limb	1°22' 49".35	1°41' 09".51	1°41' 42".43	18' 20".16	0' 32".92
The mean of difference		0' 57".02				
The terrestrial refraction angle		2' 15.59"				

Table 4-2. This table shows the unrefracted incident angle, modeled refracted angle and the observed refracted angle on the different time during the observation on September 17, 2011 evening. The value means the altitude angle which is above the real horizon in degrees. The “Difference” means the difference between the modeled refraction angle and the observed angle in arcsec.

September 17, 2011 Sunset

Time		Unrefracted altitude	Modeled refracted	Observed refracted	Astronomical refraction	Difference
09:50:44 UT	Upper limb	1°33' 10".31	1°50' 44".73	1°50' 30".95	17' 20".64	0' 02.86"
	Center	1°17' 15".86	1°36' 0".33	1°35' 46".17	18' 30".60	0' 16.31"
	Lower limb	1°01' 21".42	1°21' 23".31	1°21' 08".69	19' 47".27	0' 11.23"
09:49:18 UT	Upper limb	1°11' 07".61	1°30' 51".71	1°31' 06".18	18' 55".21	0' 14.47"
	Center	0°56' 02".05	1°16' 16".87	1°16' 28".09	20' 14".81	0' 11.22"
	Lower limb	0°40' 56".50	1°01' 50".38	1°01' 49".99	21' 42".78	0' 00.37"
09:47:44 UT	Upper limb	0°52' 29".20	1°13' 02".87	1°13' 13".16	20' 33".67	0' 10.26"
	Center	0°36' 34".75	0°58' 38".39	0°58' 55".14	22' 03".64	0' 16.75"
	Lower limb	0°20' 40".31	0°44' 23".25	0°44' 43".84	23' 42".95	0' 20.59"
The mean of difference		0' 11".57				
The terrestrial refraction angle		2' 10".45				

Table 4-3. This table shows the unrefracted incident angle, modeled refracted angle and the observed refracted angle on the different time during the observation on October 17, 2011 evening. The value means the altitude angle which is above the real horizon in degrees. The “Difference” means the difference between the modeled refraction angle and the observed angle in arcsec.

October 17, 2011 Sunset

Time		Unrefracted altitude	Modeled refracted	Observed refracted	Astronomical refraction	Difference
09:16:57 UT	Upper limb	1°29'09".21	1°46'32".87	1°47'28".10	17'23".67	0'55".22
	Center	1°13'06".36	1°31'44".78	1°33'6".26	18'38".43	1'21".47
	Lower limb	0°57'03".51	1°17'04".37	1°17'39".33	20'00".86	0'34".96
09:18:52 UT	Upper limb	1°02'37".10	1°22'56".32	1°23'45".98	20'19".21	0'49".66
	Center	0°46'34".25	1°08'20".78	1°9'25".66	21'46".53	1'04".87
	Lower limb	0°30'31".41	0°53'53".96	0°54'22".99	23'22".56	0'29".02
09:20:44 UT	Upper limb	0°37'38".36	1°00'17".25	1°1'14".61	22'38".89	0'57".37
	Center	0°21'35".51	0°45'55".41	0°47'15".92	24'19".91	1'20".50
	Lower limb	0°5'32".66	0°31'42".59	0°32'48".14	26'09".92	1'05".56
The mean of difference		0'57".63				
The terrestrial refraction angle		2'23".89				

Table 4-4. This table shows the unrefracted incident angle, modeled refracted angle and the observed refracted angle on the different time during the observation on October 28, 2011 evening. The value means the altitude angle which is above the real horizon in degrees. The “Difference” means the difference between the modeled refraction angle and the observed angle in arcsec.

October 28, 2011 Sunset

Time		Unrefracted altitude	Modeled refracted	Observed refracted	Astronomical refraction	Difference
09:08:35 UT	Upper limb	1° 17' 20".14	1° 34' 54".70	1° 34' 26".99	17' 34".56	0' 27".71
	Center	1° 01' 17".29	1° 20' 09".77	1° 19' 41".74	18' 52".48	0' 28".04
	Lower limb	0° 45' 14".44	1° 05' 33".17	1° 04' 58".71	20' 18".72	0' 34".45
09:10:59 UT	Upper limb	0° 44' 55".93	1° 06' 12".36	1° 06' 23".84	21' 16".43	0' 11".48
	Center	0° 28' 53".08	0° 51' 44".19	0° 52' 06".80	22' 51".11	0' 22".61
	Lower limb	0° 12' 50".23	0° 37' 25".09	0° 37' 38".55	24' 34".85	0' 13".47
09:13:17 UT	Upper limb	0° 13' 56".06	0° 39' 07".40	0° 39' 06".34	25' 16".43	0' 01".06
	Center	-0° 02' 06".78	0° 24' 55".53	0° 25' 33".37	27' 51".11	0' 37".84
	Lower limb	-0° 18' 09".63	0° 10' 46".57	0° 10' 53".50	28' 34".85	0' 06".93
The mean of difference		0' 20".40				
The terrestrial refraction angle		1' 08".55				

The difference between the modeled and the observed sun with the measured real horizon, the maximum is 2' 09".41, and the minimum is 0' 01".06. The mean of difference is 0' 11".57 on September 17 evening, is 0' 57".63 on October 17, 2011 evening, is 0' 20".40 on October 28, 2011 evening, and is 57".02 on September 17 morning. The terrestrial refraction is 2' 15.59" on September 17, 2011 morning, is 2' 10".45 on September 17, 2011 evening, is 2' 23".89 on October 17, 2011 evening, and is 1' 08".55 on October 28, 2011 evening.

The difference between the observed and the modeled sun may cause by:

- (a) The time interval between the observation and the rawinsonde launch.
- (b) The uncertainty of the composition of the real atmosphere.
- (c) The accuracy of the time.
- (d) The accuracy of the measured real horizon.
- (e) The inappropriate operator during the observation

The time between the observation and the rawinsonde launch is 2 to 3 hours delay after the sunset or sunrise, the temperature of the atmosphere might be changed after the sunset or sunrise, especially the atmosphere near the ground which influence the refraction most and also changed temperature most significant during this time.

The composition of the atmosphere we use the rawinsonde to detect, but it is only detect the pressure, temperature, and the relativity humidity, we know nothing about the amount of the ice, water and the cloud during the light path go through the atmosphere. When the period of sunset, we notice that when the sun has been covered by an obvious cloud, the

position of the Sun would be changed significantly. It is reasonable supposed that the refraction may be influence by the unobvious cloud that can be detected by the rawinsonde.

The accuracy of the time in this work is less than 1 second, about 15". If we could improve the record time to 0.1 second, it could significant reduce the error of the difference of position of the setting sun between the model and observation.

The accuracy of the measured real horizon in this work is more than 12", if we could use the electric total station which accuracy is 2" to measure the altitude angle between the landscape to the sun in the same image, we could make the measured real horizon more accuracy.

For the observations before year 2011, it is not take into account the shaking of the reflex mirror in the DSLR, and it is also caused about 60" uncertainty of the field. For the obaervations during the year 2011, the method of the mirror lockup and remote control the camera by a computer is used, and the shaking of the camera with lens is reduced a lot.

Conclusion

We used the Canon DSLR camera with 400mm lens to observed the setting sun at Tamshui and observed of the rising sun near the Gouliiao, then compared with the astronomical refraction model which established by the CWB rawinsonde data.

In our work, the difference between the observed sun and the modeled sun with the measured real horizon, is about from 0' 01".06 to 2' 09".41. The mean of difference is 0' 11".57 on September 17 evening, is 0' 57".63 on October 17, 2011 evening, is 0' 20".40 on October 28, 2011 evening, and is 57".02 on September 17 morning. Total in mean is 0' 36".65.

The terrestrial refraction is 2' 15.59" on September 17, 2011 morning, is 2' 10".45 on September 17, 2011 evening, is 2' 23".89 on October 17, 2011 evening, and is 1' 08".55 on October 28, 2011 evening. Total in mean is 1' 59".62.

The CWB rawinsonde data is used to construct the vertical atmosphere structure, but in fact, the structure of the atmosphere in different places will be different. The rawinsonde is also not stay up of the same place, when the rawinsonde is increasing its height, it is also pushed by the wind to the different direction, so that the atmosphere structure of the rawinsonde detected may be not responded the real structure of the atmosphere above the observation place, especially to the west direction from the west coast of Taiwan, because the rawinsonde in the stratosphere would pushed by the wind to the east direction of the observe location. In order to construct a better vertical atmosphere

structure, the other rawinsonde data launched at locations nearby the direction of setting sun should be used to improve the model of atmosphere at different height, especially the upper atmosphere like the stratosphere.

The rawinsonde is also launched at different time of observe the setting sun, late about 3 hours from the sun setting, and the structure of the atmosphere would change during this period. The structure of the atmosphere at the right time could be calculated with numerical weather model.

The terrestrial refraction in this work could be measured, but it could not simulated because the pressure and the temperature near the ground changed complex, and the pressure and temperature changed in small scale could influence the result of the refraction. The Lidar technology could be used to find the density and temperature along the light path (W.N. Chen, 2002), and the atmosphere structure along the light path may be constructed, and position of setting sun in the model may be improved .

Reference

- Auer L. H., "Astronomical Refraction: Computational Method for All Zenith Angles," **AJ**, **119:2472-2474 (2000)**.
- Attas M. and McMurry J., "Nailing the Equinox Sunrise," **JRASC**, **93, 163A (1993)**.
- Bruton D., "Optical Determination of Atmospheric Temperature Profiles," **Ph.D. thesis (Department of Physics and Astronomy, University of Texas A&M University, 1996)**.
- Chen W. N., "The measurements and scattering properties of aerosol, cirrus, and temperature between 10-30 km above Chung-li," **Ph.D. (Department of Physics, National Central University, 2002)**.
- Chen C. L., "The Derivations of the Four-Part Formulae and Its Inference in Spherical Trigonometry," **Maritime Quarterly**, **Vol. 16 No. 2, June 2007, pp. 67~84 (2007)**.
- Ciddor P. E., "Refractive index of air: new equations for the visible and infrared," **APPLIED OPTICS**, **Vol. 35, No. 9 (1996)**.
- Garfinkel B., "Astronomical Refraction in a Polytopic Atmosphere," **AJ**, **72, 235G (1967)**.
- Gubler J. and Tytler D., "Differential Atmospheric Refraction and Limitations on the Relative Astrometric Accuracy of Large Telescope," **PASP**, **110:738-746 (1998)**.
- Kireev S. V. and Sokolovskiy S. V., "Variations of refraction angles from observations of the Moon from space," **Applied Optics**, **Vol. 33, No. 36 (1994)**.
- Mahan A. I., "Astronomical Refraction-Some History and Theories," **Applied Optics**, **Vol 1, No. 4 (1962)**.

- Sampson R. D., "Astronomical Refraction And The Equinox Sunrise," **JRASC, 94:26 (2000).**
- Sampson R. D., "Astronomical Refraction and the Equinox Sunrise," **RASC, 94:26S (2000).**
- Sampson R. D., "Comparison of modelled and observed astronomical refraction," **Ph.D. thesis (Department of Earth and Atmospheric Sciences, University of Alberta, 2001).**
- Sampson R. D., "Variability in the Astronomical Refraction of the Rising and the setting sun," **PASP, 115:1256-1261 (2003).**
- Sampson R. D., "Comparison of modeled and observed astronomical refraction of the setting Sun," **Applied Optics, Vol. 42, No. 3 (2003).**
- Sampson R. D., "Variability of observed low-altitude astronomical refraction (LAAR) from different geographic locations: progress toward a global map of LAAR variability," **Applied Optics, Vol. 44, No. 27 (2005).**
- Sampson R. D., "Variability in low altitude astronomical refraction as a function of altitude," **Applied Optics, Vol.47, No.34 (2008).**
- Schaefer B. E., "Refraction Near The Horizon," **PASP, 102, 7968 (1990).**
- Schiebener P. and Straub J., "Refractive Index of Water and Steam as Function of Wavelength, Temperature and Density," **J. Phys. Chem. Ref. Data, Vol. 19, No. 3 (1990).**
- Smith, M. A., "Ptolemy's Theory of Visual Perception: an English Translation of the Optics," **Transaction of the American Philosophical Society, Vol, 86, Part 2, 300 pp (1996).**
- Thomas M. E., "Astronomical Refraction," **Johns Hopkins APL Technical Digest, Volume 17, Number 3 (1996).**
- Wei M., Lei Y. and Tie Q. X., "On Astronomical Atmospheric Refraction,"

j-chinastron, 2008.10.011 (2008).

Astronomical Almanac 2010, Central Weather Bureau, Ministry of Transportation and Communications, R.O.C. (2010)

Astronomical Almanac 2011, Central Weather Bureau, Ministry of Transportation and Communications, R.O.C. (2011)

Department of Defense World Geodetic System 1984 Its Definition and Relationships with Local Geodetic Systems, NIMA STOCK NO. DMATR83502WGS84, NSN 7643-01-402-0347 (2000).

Appendix

A. The CWB rawinsonde data

Table App-A-1. The CWB rawinsonde data at 00:00 UT September 17, 2011.

中央氣象局 探空站氣象資料

測站:466920 臺北

TAIPEI

時間: 2011.09.17 00Z

Levels: 141

經度: 121°30' 24" E

緯度: 25°02' 23" N

[NLHMCWWAPP]=2550102305

NO	Si	P(hPa)	H(gpm)	T(°C)	U(%)	Td(°C)	WD(360°)	WS(m/s)
1	1	1004.6	11	25.3	74	20.3	185	0.9
2	2	1003.1	24	24.9	75	20.1	0	0
3	10	1000	51	24.8	75	20.1	0	0
4	2	970	319	23.4	83	20.3	211	1.8
5	2	958.5	423	23.2	75	18.6	17	1.8
6	2	936.1	630	23.5	59	15.1	28	3.7
7	10	925	734	22.6	61	14.6	19	3.1
8	6	887	1098	20	73	15	18	3.7
9	2	884.4	1124	19.8	74	15.1	18	4.1
10	2	870.6	1260	20.2	45	7.8	25	7.9
11	2	866.2	1304	20	42	6.8	23	9.4
12	4	859.3	1373	18.9	64	11.9	21	11.5
13	2	854.2	1424	18.2	77	14.2	30	10.7
14	10	850	1466	18.3	75	13.8	38	9.5
15	2	839	1577	19.3	30	1.5	47	7.7
16	6	835.5	1613	19.2	25	-1.3	40	7.1
17	6	821	1764	18.6	18	-6.1	11	6.5
18	4	788.8	2105	17	26	-2.7	23	5.3
19	2	783.1	2167	16.7	27	-2.5	20	5.3
20	6	771.3	2296	16.8	18	-7.4	29	6.5
21	2	762.9	2389	17.1	11	-13.4	22	7.4
22	6	754.3	2486	16.9	9	-16.2	9	5.3
23	6	707.6	3026	13.7	8	-19.8	27	5.3
24	10	700	3117	13.1	8	-19.8	27	4.9
25	2	555.3	5019	0.9	20	-19.9	283	4
26	6	542.1	5210	-0.2	10	-28.4	282	5.3
27	2	539.2	5254	0	4	-37	288	6.3
28	2	534.6	5321	-0.6	28	-16.7	294	6.8
29	6	524.2	5478	-1.5	17	-23.4	318	5.1
30	2	520.8	5531	-2	26	-18.7	342	4.9
31	2	509.2	5710	-1.7	4	-40	297	1.9
32	10	500	5854	-2.5	3	-43	280	2.7
33	6	478	6210	-4.2	3	-42.8	215	5.2
34	6	456	6580	-6.3	1	-51.4	194	5.4
35	6	447.7	6723	-7.3	2	-51.1	165	5.9
36	10	400	7589	-13.1	1	-58.8	133	4
37	6	391.9	7744	-13.9	1	-59.4	166	5.4
38	6	385.5	7870	-14.7	1	-59.9	153	5.1
39	2	380.6	7966	-14.7	1	-59	143	3
40	4	376.1	8056	-15.5	6	-44.6	143	0.9
41	6	336.1	8891	-22.5	26	-37	191	5.4
42	2	335.1	8914	-22.7	25	-37.3	190	5.5
43	2	326.4	9108	-24.5	63	-29.6	164	6.8
44	6	325.7	9122	-24.6	57	-30.7	163	6.7
45	2	323.6	9170	-24.9	31	-37.3	166	6.3

46	6	315.4	9355	-26.1	44	-34.9	205	5.7
47	2	314.2	9382	-26.3	45	-34.9	207	6
48	2	309.9	9483	-27	27	-40.4	206	7.4
49	10	300	9716	-28.9	41	-38.2	212	9.8
50	6	297.9	9767	-29.4	39	-39.1	214	10.3
51	6	289.9	9960	-31	51	-37.9	190	10.5
52	2	284.2	10101	-32.2	72	-35.6	201	9.5
53	6	282.2	10151	-32.4	72	-35.8	205	9.2
54	6	257.1	10799	-37.6	59	-42.8	201	7.5
55	2	255.2	10850	-38.1	57	-43.4	203	8
56	10	250	10993	-38.9	43	-47	218	8.5
57	6	247.3	11067	-39.3	35	-49.1	228	9.1
58	2	220.4	11845	-44.6	16	-60.2	234	8.2
59	6	202.1	12420	-49.6	12	-67	227	9.6
60	2	200.3	12479	-50.1	11	-68	230	9.4
61	10	200	12488	-50.1	11	-68.1	230	9.4
62	6	185.1	12989	-54.1	14	-69.5	257	8.1
63	6	160.1	13905	-61.7	7	-80.8	202	7.5
64	2	155.4	14087	-63.3	6	-82.4	204	7.1
65	10	150	14304	-65.4	9	-82.2	194	7
66	6	130.7	15126	-72.5	15	-84.9	162	8.1
67	2	130.5	15138	-72.7	15	-84.9	162	8.3
68	6	117.8	15731	-76.6	18	-87.4	203	6.8
69	3	115.2	15860	-77.4	18	-88	190	5.8
70	6	112.3	16007	-76.9	18	-87.6	165	7.6
71	6	108.2	16222	-76.3	19	-86.8	186	5.6
72	6	102.4	16538	-76.8	19	-87.4	141	5.1
73	2	100.1	16666	-77.2	19	-87.8	142	7.1
74	10	100	16674	-77.3	19	-87.8	141	7.1
75	6	95.7	16925	-76.8	19	-87.2	137	7.6
76	6	90.2	17268	-77.4	19	-87.9	64	5.3
77	6	86.6	17499	-76.7	18	-87.5	84	8.6
78	6	83.4	17714	-76.3	17	-87.5	64	7.2
79	2	81.8	17831	-74.9	16	-86.6	73	8.4
80	6	81.1	17877	-75.1	16	-86.8	74	8.4
81	6	78.9	18035	-75.1	15	-87.4	54	9.3
82	2	74.9	18342	-76.8	13	-89.6	62	13.2
83	6	73	18485	-75.9	12	-89.2	63	9.9
84	6	70.9	18653	-74	11	-88.1	89	10.2
85	10	70	18732	-74.3	10	-88.6	88	11.7
86	6	68.7	18837	-74.1	10	-88.8	88	12.4
87	4	67.2	18968	-73.1	9	-88.7	102	13.7
88	6	66	19076	-71.4	8	-88	113	11.9
89	6	61.7	19471	-69.4	4	-89.5	101	9.1
90	6	57	19955	-65.5	2	-92.3	131	5.8
91	6	54.7	20203	-64.2	1	-93.8	80	5.7
92	4	53.9	20294	-63.1	1	-93.1	74	4.7
93	6	51.6	20568	-61.8	1	-92.2	49	9.3
94	10	50	20757	-61.8	1	-92.1	63	12.8
95	2	48.9	20897	-61.4	1	-91.9	73	13.8
96	6	47.3	21098	-62.5	1	-92.7	96	10.4
97	2	47	21142	-62.7	1	-92.8	96	9.5
98	6	43.4	21639	-60.3	1	-91.1	87	12.7
99	4	40.2	22106	-58.4	1	-89.7	98	20.2
100	6	37.4	22566	-57.8	1	-89.3	116	17.3
101	6	32.7	23429	-55.3	1	-87.6	110	16.5
102	2	31.3	23698	-54	1	-86.6	97	10.2
103	4	30.8	23807	-54.1	1	-86.7	91	9.5
104	10	30	23972	-54.3	1	-86.8	78	9.9
105	6	29.9	23986	-54.2	1	-86.7	77	10
106	2	29	24188	-54.6	1	-87	83	13.2

107	4	26.9	24679	-50.9	1	-84.4	100	16.8
108	6	26	24888	-50	1	-83.8	110	12.6
109	2	25.4	25053	-49.3	1	-83.3	95	11.7
110	6	24	25425	-50	1	-83.8	73	9.9
111	6	23.3	25609	-49.4	1	-83.4	82	9
112	6	22	25982	-50	1	-83.8	46	9.4
113	6	21.3	26194	-50.7	1	-84.3	53	7.8
114	4	21.1	26259	-51.3	1	-84.7	62	7.2
115	6	20.5	26439	-51.9	1	-85.1	90	9.2
116	10	20	26609	-51.5	1	-84.9	82	9
117	2	18.8	27002	-52.6	1	-85.6	72	10.7
118	6	18.6	27064	-52.6	1	-85.7	72	10.4
119	6	17	27645	-49	1	-83.1	108	10
120	2	16.3	27940	-47.4	1	-82	104	8.6
121	6	14.4	28748	-46.2	1	-81.2	94	12.2
122	6	13.6	29158	-45.1	1	-80.3	128	11.3
123	2	12.9	29478	-44.7	1	-80.1	110	7.2
124	6	12.4	29784	-45.3	1	-80.5	148	6
125	2	12	29961	-46	1	-81	147	6.5
126	6	11.8	30067	-45.9	1	-81	153	5.3
127	4	11	30587	-44.3	1	-79.8	80	2.4
128	6	10.3	31001	-44.8	1	-80.2	6	6.9
129	6	10.2	31084	-45.2	1	-80.4	9	6.5
130	6	10.1	31139	-45.2	1	-80.5	20	5.3
131	10	10	31196	-45.5	1	-80.7	42	4.2
132	6	9.8	31299	-45.5	1	-80.6	95	5.4
133	6	9.5	31518	-45.3	1	-80.5	105	5.6
134	6	9.3	31681	-44.7	1	-80.1	57	5.2
135	2	9.2	31754	-44.8	1	-80.1	46	5.9
136	6	9.1	31836	-44.2	1	-79.8	38	6.4
137	6	8.9	31986	-41.7	1	-78	53	5.3
138	2	8.6	32224	-38.2	1	-75.6	52	3.9
139	6	8.1	32610	-37.8	1	-75.4	55	8.3
140	6	7.8	32913	-38.7	1	-75.9	56	5.2
141	20	6.9	33720	-37.3	1	-75	21	3.7

Table App-A-2. The CWB rawinsonde data at 12:00 UT September 17, 2011.

中央氣象局 探空站氣象資料

測站:466920 臺北

TAIPEI

時間:2011.09.17 12Z

Levels : 72

經度:121°30' 24" E

緯度:25°02' 23" N

[NLHMCWWAPP]=2550102315

NO	Si	P(hPa)	H(gpm)	T(°C)	U(%)	Td(°C)	WD(360°)	WS(m/s)
1	1	1003.9	11	27.8	65	20.6	83	3.5
2	2	1002.4	25	27.8	69	21.5	95	3.4
3	10	1000	46	27.6	70	21.6	95	4.2
4	6	990.9	127	26.8	72	21.3	97	7
5	6	971.1	305	25.3	74	20.4	91	6.3
6	6	954.6	456	24.7	69	18.7	66	5.1
7	10	925	733	23.4	68	17.3	83	2.2
8	2	901	962	22	73	16.9	124	2.1
9	2	891.2	1058	23.2	42	9.4	85	1.6
10	4	870.1	1267	22.6	24	1.3	342	1
11	10	850	1469	21.5	20	-2.3	4	3.2
12	6	834.5	1627	20.9	18	-4.6	16	5.1
13	2	808.5	1900	19.9	10	-12.1	12	7.8
14	4	795.3	2041	18.9	16	-7.6	18	9.2
15	2	776.3	2248	17.4	30	-0.5	12	7.1
16	6	752.7	2510	16	24	-4.4	8	7
17	6	728.1	2791	14.6	16	-11.1	26	8.2
18	2	722.3	2859	14.4	12	-14.4	26	8.5
19	10	700	3122	12.4	15	-13.9	26	6.6
20	2	613.6	4209	4.5	15	-20.2	9	3.1
21	2	590.5	4521	2.8	10	-25.5	1	5.2
22	6	571.7	4781	1.3	17	-21.2	353	6.9
23	2	540.4	5235	-0.1	48	-9.8	359	7.5
24	6	539.5	5247	-0.1	45	-10.5	359	7.3
25	2	528.8	5407	-0.6	40	-12.6	336	6.2
26	6	526.9	5437	-0.4	33	-14.8	331	6
27	2	523	5496	-0.3	18	-21.9	328	5.3
28	10	500	5854	-2.8	14	-26.4	346	4.6
29	2	428.8	7056	-9	1	-56.2	172	1.3
30	4	421.5	7190	-10	1	-56.6	0	0
31	10	400	7590	-13.2	29	-27.8	214	2.5
32	2	367.2	8237	-17.2	39	-27.9	229	5.3
33	6	365.4	8274	-17.5	36	-29	228	5.3
34	2	353.9	8512	-19.3	19	-37.1	191	3.5
35	6	346.7	8665	-20.5	27	-34.7	187	5.2
36	2	343.1	8743	-21.1	19	-38.9	195	5.4
37	2	338	8853	-22.1	58	-28.2	215	4.1
38	2	333.4	8954	-23	64	-28	228	3.5
39	6	328.5	9062	-23.8	63	-29	219	5.1
40	6	310	9483	-26.8	47	-34.7	214	6.5
41	2	305.4	9590	-27.5	36	-38.1	228	6.7
42	2	303.7	9630	-27.2	14	-46.6	233	7.3
43	6	301.8	9676	-27.6	13	-47.7	236	7.7
44	10	300	9719	-28	17	-45.6	234	7.9
45	6	279.8	10214	-32	6	-58.4	232	7.4
46	6	264.1	10621	-35.1	4	-63.5	253	7.4
47	2	260	10729	-36.1	4	-63.5	249	6.8
48	6	250.3	10992	-37.7	2	-70	232	8.6
49	10	250	11000	-37.7	2	-70.1	232	8.6
50	2	242.5	11209	-38.9	4	-66.4	242	10
51	6	236.3	11388	-40.5	7	-63.7	240	8.8

52	6	231.2	11534	-41.9	9	-62.7	222	8.1
53	6	218.3	11921	-45.2	10	-64.4	241	8.9
54	6	202.6	12415	-48.9	5	-72.3	201	7.7
55	10	200	12500	-49.6	5	-72.8	201	8
56	2	187.4	12924	-52.7	4	-76.3	195	9.1
57	6	179.4	13201	-55.4	9	-73.6	193	9.1
58	6	161.4	13867	-61	13	-76.1	208	11
59	10	150	14318	-65.1	14	-78.9	200	9.4
60	2	147.9	14403	-65.9	14	-79.4	200	9.6
61	6	140	14736	-68.1	14	-81.3	179	5.7
62	6	134.9	14959	-69.7	14	-82.8	197	5.4
63	6	127.9	15272	-72.6	15	-85.2	171	5.1
64	6	124.1	15449	-74.2	15	-86.3	177	7
65	6	110.3	16129	-78.5	19	-88.7	154	7.1
66	2	109.5	16167	-78.8	20	-88.8	151	6.7
67	6	107.5	16272	-78	21	-87.8	131	7.5
68	6	104.2	16452	-78.6	23	-87.8	131	7.8
69	12	100	16686	-78.9	25	-87.6	107	6.9
70	6	95.2	16965	-79.7	27	-88	135	5.7
71	6	90.7	17237	-79.1	27	-87.3	84	5.3
72	20	87.8	17422	-78.3	27	-86.5	85	10.9

Table App-A-3. The CWB rawinsonde data at 12:00 UT October 17, 2011.

中央氣象局 探空站氣象資料

測站:466920 臺北

TAIPEI

時間:2011.10.17 12Z

Levels : 125

經度 : 121°30' 24" E

緯度 : 25°02' 23" N

[NLHMCWWAPP]=4550003214

NO	Si	P(hPa)	H(gpm)	T(°C)	U(%)	Td(°C)	WD(360°)	WS(m/s)
1	1	1016.7	11	23.6	63	16.1	74	3.8
2	2	1015.1	25	23.6	60	15.6	74	3.2
3	10	1000	156	22.6	62	14.9	76	6.1
4	6	947.9	619	18.1	76	13.8	62	10.1
5	10	925	828	16.3	79	12.8	66	10.8
6	4	916.6	905	15.6	82	12.5	70	11.1
7	2	906.8	997	14.8	84	12.1	74	10.5
8	6	877.4	1275	13.3	81	10.2	90	8.5
9	10	850	1542	11.7	99	11.5	85	6.7
10	2	849	1552	11.6	99	11.4	84	6.7
11	2	837.2	1669	13.1	43	0.9	74	6.7
12	2	832.5	1717	12.9	43	0.5	75	6.2
13	2	830.2	1740	13.2	70	7.9	76	5.8
14	6	827	1773	13.4	82	10.3	76	5.1
15	2	824.6	1797	13.4	85	10.9	74	4.6
16	2	812.8	1919	14.5	62	7.4	39	1.9
17	4	801.1	2041	13.5	63	6.5	348	1.4
18	2	770.8	2365	11	89	9.3	242	5
19	6	769.6	2378	11	89	9.3	241	5.1
20	2	742.7	2675	10	30	-6.6	283	4.1
21	2	732.4	2791	9.3	58	1.4	306	4.2
22	2	708.2	3068	7.7	70	2.5	299	4.7
23	6	704.2	3115	7.5	69	2.3	294	5.1
24	10	700	3165	7.3	69	2.1	288	5.5
25	2	675.6	3456	5.3	81	2.3	263	7.3
26	6	673.5	3482	5.2	80	2.1	261	7.5
27	2	634.2	3971	2.1	66	-3.5	276	8.6
28	6	623.2	4112	1.4	62	-5	278	9.4
29	2	592.2	4522	0.2	48	-9.4	276	13.2
30	2	580.6	4680	0.4	27	-16.3	275	15.4
31	2	506.8	5758	-6.7	40	-18.1	280	15.4
32	2	501.9	5834	-5.9	22	-24.2	278	16
33	10	500	5864	-6	21	-24.8	278	16.2
34	2	491.6	5996	-6.6	11	-31.9	276	17
35	6	469.5	6354	-8.5	9	-35.5	268	18.3
36	2	449.9	6683	-10.5	7	-39.5	264	18.2
37	6	408.6	7417	-15.4	8	-43	273	17.6
38	10	400	7577	-16.6	7	-44.5	270	17.8
39	6	374	8079	-19.4	3	-55.4	250	16.1
40	2	370.3	8153	-19.8	3	-54.4	250	16.7
41	6	328.3	9033	-26.6	9	-50.5	257	15.7
42	6	309.5	9456	-30	33	-41.1	273	19.4
43	10	300	9678	-31.9	33	-43	267	19.8
44	10	250	10936	-42.8	45	-50.1	266	23.3
45	2	248.8	10968	-43.1	46	-50.3	266	22.9
46	2	219.4	11804	-48.8	7	-69.6	268	22.9
47	10	200	12406	-53.6	9	-72.4	270	23.5
48	6	187.5	12817	-56.6	8	-75.5	278	22.2
49	4	174.6	13268	-59.9	9	-77.8	272	25.6
50	6	158.5	13866	-64.5	16	-77.7	261	24.7

51	2	151.9	14122	-66.9	19	-78.5	268	24.1
52	10	150	14198	-67.1	19	-78.6	269	24.3
53	4	132.8	14927	-72.1	20	-83	276	21.1
54	6	119.6	15537	-75.5	22	-85.2	281	14
55	4	115.1	15760	-75.8	23	-85.2	248	7.3
56	6	114.1	15807	-76.1	23	-85.5	241	7.4
57	2	111.6	15934	-77	23	-86.2	241	10.1
58	6	107.6	16148	-76.5	24	-85.7	251	13.2
59	6	103.7	16356	-77.9	24	-87	238	14
60	12	100	16565	-78.8	24	-87.7	257	12.5
61	3	99.2	16610	-79.1	24	-87.9	262	11
62	6	97.7	16699	-78.7	25	-87.4	263	8
63	4	95.6	16822	-78.2	25	-87	240	5.7
64	6	93.6	16939	-78.3	25	-87.1	219	6.3
65	6	89.8	17178	-79.5	25	-88.1	221	9.5
66	4	88.4	17269	-80	25	-88.6	231	11.2
67	2	87.6	17318	-80.2	25	-88.7	239	11.1
68	6	84.1	17546	-76.7	25	-85.5	277	8.3
69	6	81.3	17747	-75.1	24	-84.3	273	6.1
70	2	79.9	17847	-73.1	23	-82.9	299	6.9
71	6	79.1	17907	-72.9	22	-82.8	311	6.9
72	4	70.9	18546	-71.5	12	-85.4	0	0
73	10	70	18625	-71.7	11	-85.9	208	1.5
74	2	62.5	19299	-68.6	5	-87.7	265	4.4
75	6	60.9	19453	-66.2	4	-87.3	305	5.2
76	2	58.7	19681	-63.5	3	-88	4	3.8
77	6	56.9	19876	-64	2	-91.2	63	5.3
78	6	53.1	20302	-63.2	1	-93.2	106	7.4
79	6	51.6	20478	-62.8	1	-92.9	89	7
80	2	51.4	20499	-62.6	1	-92.8	89	6.8
81	6	50.2	20641	-62.7	1	-92.8	108	6.5
82	10	50	20667	-62.8	1	-92.8	108	6.6
83	6	47.4	20991	-61	1	-91.6	73	7.2
84	6	45.3	21272	-60.5	1	-91.3	107	8.1
85	6	43.6	21521	-60	1	-90.8	104	7.1
86	6	42.1	21737	-59.5	1	-90.5	139	5.2
87	6	40.8	21935	-59.3	1	-90.3	116	8
88	4	39.9	22080	-58.6	1	-89.9	123	10.3
89	6	37.5	22455	-58.6	1	-89.8	115	7.2
90	2	37.3	22505	-58	1	-89.5	111	5.9
91	4	36.3	22662	-58.8	1	-90	63	3.6
92	6	35.3	22840	-59.8	1	-90.7	31	5.3
93	2	35.1	22875	-59.8	1	-90.7	35	6.2
94	6	33.9	23091	-57.8	1	-89.3	82	9.6
95	6	31.5	23568	-56.7	1	-88.5	91	11
96	6	30.7	23725	-56.3	1	-88.2	80	12.4
97	10	30	23871	-55.3	1	-87.5	96	13.3
98	6	29.4	24005	-55	1	-87.3	102	14
99	6	27.9	24332	-53.6	1	-86.3	88	14.5
100	2	27.5	24431	-52.7	1	-85.7	86	14.1
101	6	25.3	24965	-52.8	1	-85.8	89	13.6
102	6	23.1	25548	-52.1	1	-85.3	64	13.1
103	6	20.8	26249	-50.6	1	-84.2	73	13.9
104	10	20	26492	-50.2	1	-83.9	69	12.6
105	6	18.8	26904	-49.3	1	-83.3	71	11.2
106	6	17.8	27243	-48.7	1	-82.9	46	15
107	2	17.5	27376	-49.5	1	-83.4	47	15.4
108	6	16.9	27584	-48.6	1	-82.8	61	11.9
109	6	16.5	27774	-47.4	1	-82	42	12
110	2	15.9	27982	-45.8	1	-80.8	48	12.6
111	4	15.3	28261	-47	1	-81.7	49	16.2

112	2	15	28386	-47	1	-81.7	57	15.2
113	6	14.7	28539	-46.4	1	-81.3	67	12.8
114	2	13.4	29140	-43.5	1	-79.3	33	9.9
115	6	13.2	29264	-43.7	1	-79.4	26	11.2
116	6	12.3	29723	-45.6	1	-80.8	26	8.7
117	6	11.8	29972	-45.2	1	-80.5	44	6
118	10	10	31086	-48.5	1	-82.7	31	3.4
119	6	9.5	31418	-49	1	-83.1	21	6.4
120	2	9.4	31525	-49.2	1	-83.2	23	6.4
121	2	8.8	31960	-45.5	1	-80.7	22	2.6
122	4	8.5	32143	-47	1	-81.7	53	1.6
123	2	7.7	32794	-48.8	1	-82.9	138	4
124	6	6.9	33514	-46.4	1	-81.3	29	9
125	20	6.5	33908	-45.4	1	-80.6	63	11.8

Table App-A-4. The CWB rawinsonde data at 12:00 UT October 28, 2011.

中央氣象局 探空站氣象資料
 測站:466920 臺北 TAIPEI
 時間:2011.10.28 12Z Levels:137
 經度:121°30'24" E 緯度:25°02'23" N
 [NLHMCWWAPP]=2560002210

NO	Si	P(hPa)	H(gpm)	T(°C)	U(%)	Td(°C)	WD(360°)	WS(m/s)
1	1	1016.7	11	23.6	78	19.5	81	4.2
2	2	1014.8	27	23.5	74	18.7	76	3.6
3	6	1005.3	110	22.8	75	18.2	73	5.6
4	10	1000	156	22.4	76	18.1	81	6
5	6	989.9	244	21.6	79	17.9	94	7.5
6	6	952	582	18.9	84	16.2	72	12.9
7	10	925	829	17	86	14.8	86	10.1
8	2	921.8	858	16.8	87	14.7	85	10
9	2	888.9	1168	15.2	89	13.4	98	9.9
10	6	853.3	1515	13.8	85	11.4	108	8.4
11	10	850	1548	13.6	88	11.7	112	7.7
12	6	840.4	1644	13.2	89	11.4	132	5.2
13	2	839.3	1654	13.1	89	11.3	134	4.8
14	2	811.6	1938	13.9	61	6.5	27	1
15	4	810.3	1951	13.9	59	6.1	11	0.9
16	2	786.7	2200	11.8	73	7.1	257	2.6
17	2	772	2358	11.3	52	1.9	259	4
18	2	763.2	2453	10.6	67	4.7	238	5.8
19	6	756.1	2531	10.5	47	-0.2	256	6.7
20	6	744.8	2657	9.9	37	-4.1	250	5.1
21	2	728.4	2842	9	22	-11.4	270	4.9
22	6	725.6	2873	8.9	27	-9.1	269	5.2
23	2	704.9	3112	8.6	37	-5.4	249	4.8
24	6	700.9	3159	8.3	36	-5.8	248	5.1
25	10	700	3170	8.2	37	-5.6	248	5.2
26	2	672.8	3496	5.7	69	0.4	287	5
27	6	648.4	3798	3.8	65	-2.2	330	5.7
28	6	635	3967	2.6	70	-2.4	302	7.3
29	6	609.6	4297	1.3	54	-7	276	5.1
30	2	583.2	4652	-1.2	55	-9	281	6.5
31	2	574.2	4775	-0.3	44	-11.1	286	5.5
32	6	567	4876	-0.4	44	-11.1	293	6
33	6	551.6	5097	-1.2	39	-13.3	272	6.3
34	2	542.9	5223	-1.7	35	-15.1	271	6.8
35	6	518.1	5594	-4.4	35	-17.7	283	10.1
36	2	504.9	5796	-5.7	27	-21.9	268	8.6
37	2	501.7	5847	-6.1	39	-18	264	9.6
38	10	500	5873	-6.3	37	-18.7	262	9.9
39	2	492.7	5987	-6.6	20	-25.7	250	8.8
40	2	476.7	6245	-8.3	36	-20.7	239	9.4
41	2	465.6	6426	-9.3	17	-29.7	236	9.4
42	6	456.6	6577	-10.5	22	-28	222	10.8
43	6	441	6844	-12.9	35	-25.3	241	11.4
44	6	434.7	6952	-13.7	37	-25.4	225	11.6
45	2	429.1	7051	-14.4	37	-25.9	231	11.5
46	2	424.7	7129	-14.4	15	-35.2	233	12.2
47	10	400	7581	-18	29	-31.8	240	14.6
48	2	374.5	8070	-22.2	33	-34	240	13.7
49	2	348.8	8589	-25.1	20	-41.7	255	18.3
50	6	344.6	8677	-26	22	-41.6	259	18.4
51	2	331.5	8956	-28.1	26	-41.9	256	17.3

52	2	319.6	9217	-30.4	60	-35.8	262	19.1
53	2	303.6	9580	-33.3	63	-38.1	265	19.7
54	10	300	9664	-34.1	60	-39.2	265	19.7
55	4	269.6	10403	-40.3	49	-46.9	266	21.6
56	10	250	10911	-44.5	42	-52.4	263	16.6
57	6	230.6	11446	-49.3	29	-59.6	269	17.7
58	2	223.7	11644	-50.9	31	-60.7	264	15
59	2	220	11755	-51.4	25	-62.9	262	14
60	4	217.9	11815	-51	18	-64.9	261	13.6
61	2	210.3	12046	-51.6	5	-74.1	250	14.2
62	6	203.8	12248	-53.2	8	-72.6	244	16.6
63	10	200	12370	-54.3	12	-70.9	245	16.1
64	6	190.5	12682	-55.8	13	-71.7	258	17.6
65	2	178.1	13109	-57	4	-79.7	255	16.3
66	6	161.7	13711	-62.1	5	-82.5	253	20.2
67	10	150	14174	-64.7	6	-83.7	253	15.2
68	6	133.1	14895	-69.3	7	-86.5	251	12.5
69	6	124.2	15303	-72.1	7	-89	243	12.7
70	4	120.1	15501	-72.2	7	-88.9	225	11.1
71	6	118.7	15573	-72.6	7	-89.3	219	11.6
72	6	111.6	15932	-75.4	8	-91	236	13.3
73	3	108.3	16106	-76.7	9	-91.6	232	15.9
74	12	100	16564	-76.7	11	-90.3	238	13.5
75	6	97.7	16696	-75.1	12	-88.7	229	13.4
76	6	91.5	17081	-75.1	12	-88.4	273	5.7
77	4	87.9	17310	-74.2	12	-87.7	280	1.3
78	2	87.6	17333	-73.8	12	-87.3	278	1.3
79	2	79	17931	-76.7	12	-89.9	232	7.1
80	6	78.3	17985	-76.4	12	-89.7	236	7.7
81	2	74.3	18284	-74.7	12	-88.2	260	2.7
82	2	73.3	18364	-70.4	11	-84.9	283	3.8
83	10	70	18640	-69	8	-85.4	238	1.2
84	2	69.5	18684	-68.7	8	-85.5	201	1.5
85	2	61	19468	-69.2	3	-91.1	139	1.9
86	4	57.3	19843	-67.5	2	-92.1	0	0
87	6	50.5	20605	-64.6	1	-94.1	48	5.1
88	10	50	20665	-64.8	1	-94.3	58	5.7
89	6	48.7	20822	-63.9	1	-93.7	99	8
90	2	48.1	20904	-63.8	1	-93.6	105	7.2
91	6	45.7	21222	-60.8	1	-91.4	27	5.2
92	2	45	21318	-59.4	1	-90.5	36	8.6
93	6	42.5	21670	-60.9	1	-91.5	69	10.9
94	6	40.7	21944	-60.1	1	-90.9	71	6.7
95	6	39.3	22152	-59.5	1	-90.5	104	12
96	2	38.5	22291	-59	1	-90.2	109	9.6
97	6	37.9	22378	-59.1	1	-90.2	108	6.7
98	6	37	22538	-57.8	1	-89.3	84	6
99	6	35.5	22793	-55.9	1	-87.9	100	5.9
100	4	33.6	23143	-55.7	1	-87.8	81	4
101	6	32.6	23342	-55.2	1	-87.5	80	5.1
102	6	32.1	23435	-55.2	1	-87.5	97	6.2
103	6	30.3	23802	-55.8	1	-87.9	92	6.4
104	10	30	23871	-55.2	1	-87.5	80	5.1
105	6	29.9	23887	-55.2	1	-87.5	77	5.1
106	6	28.1	24293	-53.9	1	-86.5	116	6.6
107	6	27.1	24513	-53.7	1	-86.4	76	6.8
108	4	25.5	24919	-53.1	1	-86	72	4.2
109	6	23.7	25397	-50.2	1	-84	47	11.9
110	6	21.9	25904	-50.4	1	-84.1	71	9.6
111	6	21.2	26118	-50	1	-83.8	58	8.8
112	6	20.7	26286	-49.6	1	-83.5	79	6.2

113	10	20	26498	-49.2	1	-83.2	64	9.9
114	2	19.8	26564	-48	1	-82.4	59	10.7
115	6	19.4	26685	-48.3	1	-82.6	53	11.1
116	2	18.3	27069	-50.4	1	-84.1	51	9.7
117	6	18.1	27142	-50.4	1	-84.1	51	9.7
118	6	17.6	27349	-50.3	1	-84	35	9.4
119	6	16.7	27690	-49.4	1	-83.4	50	8.4
120	6	16	27949	-48.4	1	-82.7	14	8.7
121	6	15.3	28249	-48.9	1	-83.1	21	5.2
122	4	14.7	28530	-47.6	1	-82.1	0	0
123	2	12.9	29379	-44.9	1	-80.2	344	7.4
124	6	12.4	29652	-46	1	-81	327	5.2
125	6	11.5	30135	-46.9	1	-81.6	335	6
126	6	10.8	30590	-47.7	1	-82.2	309	7
127	6	10.2	30917	-47.7	1	-82.2	308	9.8
128	10	10	31071	-46.5	1	-81.4	324	13.2
129	6	9.7	31298	-47.5	1	-82	329	12.3
130	6	8.8	31936	-48	1	-82.4	308	16.2
131	2	8.5	32165	-49	1	-83.1	321	13.4
132	6	8.5	32175	-49	1	-83.1	321	13.2
133	6	7.9	32605	-46.1	1	-81.1	297	12.5
134	2	7.7	32816	-44.4	1	-79.9	308	15.3
135	6	7.2	33231	-46.4	1	-81.3	318	12.3
136	6	6.8	33587	-47.5	1	-82.1	296	6
137	20	6.8	33599	-47.3	1	-81.9	999	999.9

B. The IDL source code

Program 1. Use linear interpolation to separate each layer of the atmosphere into 200 layers.

```
pro divide_20111028
close,/all

aaa=' '
openr, 1,'G:\WORK\All_Observed_Datas\20111028\20111028.txt'
openw, 3,'G:\WORK\All_Observed_Datas\20111028\20111028_divide.txt'

divide=200.0d0
Po=0.0d0 ;pressure in minibar
phpao=0.0d0 ; pressure in hPa
Ho=0.0d0 ;Height in meters
RHo=0.0d0 ;Relative humidity in %

nn=137 ; the number of the dblarr
P=dblarr(nn)
Phpa=dblarr(nn)
H=dblarr(nn)
Tc=dblarr(nn)
RH=dblarr(nn)

dH=dblarr(nn-1)
dPhpa=dblarr(nn-1)
dTc=dblarr(nn-1)
dRH=dblarr(nn-1)

readf,1,aaa
readf,1,aaa
readf,1,aaa
readf,1,aaa
readf,1,aaa
readf,1,aaa

i=0
while not eof(1) do begin
  readf,1,format='(18x, f6.1, 3x, f5.0, 3x, f5.1, 4x, f4.0)', phpao, Ho, Tco, RHo
  if RHo ge 100 then RHo=0.0d0
  H(i)=Ho
  PhPa(i)=phpao
  Tc(i)=Tco
  RH(i)=RHo
  i=i+1
endwhile

for j=0, nn-2,0 do begin
  dH(j)=H(j+1)-H(j)
  dPhPa(j)=PhPa(j+1)-PhPa(j)
  dTc(j)=Tc(j+1)-Tc(j)
  dRH(j)=RH(j+1)-RH(j)
  j=j+1
endfor

printf,3,' P (hPa)    H (m)    T (C)    RH (%)'
```

```

for kk=0, nn-2 ,0 do begin

  Hs1=H(kk)
  dHs1=dH(kk)
  PhPas1=PhPa(kk)
  dPhPas1=dPhPa(kk)
  Tcs1=Tc(kk)
  dTcs1=dTc(kk)
  RHs1=RH(kk)
  dRHs1=dRH(kk)

  nnn=divide
  HH1=dblarr(nnn)
  PP1=dblarr(nnn)
  TT1=dblarr(nnn)
  RHH1=dblarr(nnn)

  for jj=0.0d0, (divide-1.0d0),0 do begin
    HH1(jj)=Hs1+(jj*(dHs1/divide))
    PP1(jj)=PhPas1+(jj*((dPhPas1))/(divide))
    TT1(jj)=Tcs1+(jj*((dTcs1))/(divide))
    RHH1(jj)=RHs1+(jj*((dRHs1))/(divide))
    printf,3,format='(f9.4, 2x, f10.4, 2x, f8.4, 2x, f8.4)', PP1(jj), HH1(jj), TT1(jj), RHH1(jj)
    jj=jj+1
  endfor

  kk=kk+1
endfor

  printf,3,format='(f9.4, 2x, f10.4, 2x, f8.4, 2x, f8.4)', PhPa(nn-1), H(nn-1), Tc(nn-1),
RH(nn-1)

  print, 'ok'
  close, /all
end

```

Program 2. Use the result from program 1 to calibrate the refraction index of each layer.

pro refraction_index_20111028

; This program is used to calculate the index of refraction n from the observed Temperature, Pressure, and Height Data. reference is from "Refractive index of air: new equations for the visible and near infrared, Philip E. Ciddor, 1996"
close,/all

aaa=' '

phpa=double(0.0d0);observed pressure in hPa

P=double(0.0d0) ;observed pressure in pa

H=double(0.0d0) ;Height in meters

Tc=double(0.0d0) ;Temperature in centigrade

Tk=double(0.0d0) ;Temperature in Kelvin

RH=double(0.0d0) ;relative humidity in %

rho=double(0.0d0)

; density of atmosphere

rhoaxs=double(0.0d0)

; The density of dry air under standared condition. (Tc=15, P=101325, 0% RH, 450ppm of CO2)

rhoa=double(0.0d0)

; The density of dry air (0% RH) under the observed conditions.

rhows=double(0.0d0)

; The density of pure water vapor under standared condition. (Tc=15, P=101325, 100% RH, 450ppm of CO2)

rhow=double(0.0d0)

; The density of water vapor under observed condition.

nprop=double(0.0d0)

; The index of refraction

nas=double(0.0d0) ;

naxs=double(0.0d0)

; The index of refraction of dry air for a particular wavelength under standard condition

nws=double(0.0d0)

; The index of refraction of pure water vapor for a particular wavelength under standared conditions.

f=double(0.0d0) ;f is the enhancement factor of water vapor in air

svp=double(0.0d0) ;

Xw=double(0.0d0) ; Xw is the molar fraction of water vapor in moist air

Z=double(0.0d0) ; Z is the compressibility of the moist air

;The density of dry air under standared condition. (Tc=15, P=101325, 0% RH, 450ppm of CO2)

faxs=double(0.0d0) ;f is the enhancement factor of water vapor in air

svpaxs=double(0.0d0) ;

Xwaxs=double(0.0d0) ; Xw is the molar fraction of water vapor in moist air

Zaxs=double(0.0d0) ; Z is the compressibility of the moist air

;The density of dry air (0% RH) under the observed conditions.

fa=double(0.0d0) ;f is the enhancement factor of water vapor in air

svpa=double(0.0d0) ;

Xwa=double(0.0d0) ; Xw is the molar fraction of water vapor in moist air

Za=double(0.0d0) ; Z is the compressibility of the moist air

```

; The density of pure water vapor under standard condition. (Tc=15, P=101325, 100% RH,
    450ppm of CO2)
    fws=double(0.0d0) ;f is the enhancement factor of water vapor in air
    svpws=double(0.0d0) ;
    Xwws=double(0.0d0) ; Xw is the molar fraction of water vapor in moist air
    Zws=double(0.0d0) ; Z is the compressibility of the moist air

; The density of water vapor under observed condition.
    fw=double(0.0d0) ;f is the enhancement factor of water vapor in air
    svpw=double(0.0d0) ;
    Xww=double(0.0d0) ; Xw is the molar fraction of water vapor in moist air
    Zw=double(0.0d0) ; Z is the compressibility of the moist air

Tcs=double(15.0d0) ; Temperature at standard condition (Tc=15) in Centigrade
Tks=double(Tcs+(273.15d0)) ; Temperature at standard condition in Kelvin
Ps=double(101325d0) ; Pressure in Standard condition
RH0=double(0.0d0) ; Humidity of Dry air
RH100=double(100.0d0); Humidity of 100% air

    AA=double(1.2378847d-5)
    BB=double(-1.9121316d-2)
    CC=double(3.393711047d1)
    DD=double(-6.3431645d3)
    a0=double(1.58123d-6)
    a1=double(-2.9331d-8)
    a2=double(1.1043d-10)
    b0=double(5.707d-6)
    b1=double(-2.051d-8)
    c0=double(1.9898d-4)
    c1=double(-2.376d-6)
    d=double(1.83d-11)
    e=double(-0.765d-8)

    k0=double(238.0185d0)
    k1=double(5792105d0)
    k2=double(57.362d0)
    k3=double(167917d0)

    cf=double(1.022d0)
    w0=double(295.235d0)
    w1=double(2.6422d0)
    w2=double(-0.032380d0)
    w3=double(0.004028d0)

    Ma=double((1d-3)*(28.9635d0+((12.011d-6)*(450.0d0-400.0d0))))
        ; The molar mass of dry air containing 450 ppm of CO2
    Mw=double(0.018015d0) ; The molar mass of water vapor
    R=double(8.314510d0) ; The gas constant

    sigma=double(1.0d0/0.551d0)
        ; The wave number (reciprocal of the vacuum wavelength) in inverse micrometers (if
        Lamda=550 nm)

openr,1,'G:\WORK\All_Observed_Datas\20111028\20111028_divide.txt'
openw,2,'G:\WORK\All_Observed_Datas\20111028\20111028_out_b.txt'
readf,1,aaa

    printf,2,' Press Height Temperature(C) Temperature(K) RH% n'
while not eof(1) do begin

```

```

readf,1,format='(f9.4, 2x, f10.4, 2x, f8.4, 2x, f8.4)', phpa, H, Tc, RH
P=double(phpa*100d0)
Tk=double(Tc+273.15d0)

if RH ge 101 then begin
  RH=0.0d0
endif

f=double((1.00062d0)+((3.14d-8)*(P))+((5.6d-7)*((Tc)^2.0d0)))
svp=double(exp(((AA)*((Tk)^2))+((BB)*(Tk))+((CC))+((DD)/(Tk))))
;svp=svpx
Xw=double((f*(RH/100.0d0)*svp)/(P))

Z=double(1.0d0-((P/Tk)*((a0)+(a1*Tc)+(a2*(Tc)^2.0d0))+((b0)+((b1)*(Tc))*(Xw))
+((c0)+((c1)*(Tc))*(Xw)^2.0d0))))+((P/Tk)^2.0d0)*((d)+((e)*(Xw)^2.0d0))))
rho=double(((P*Ma)/(Z*R*Tk))*(1.0d0-(Xw*(1.0d0-(Mw/Ma))))))

faxes=double((1.00062d0)+((3.14d-8)*(Ps))+((5.6d-7)*((Tcs)^2.0d0)))
svpaxs=double(exp(((AA)*((Tks)^2.0d0))+((BB)*(Tks))+((CC))+((DD)/(Tks))))
Xwaxs=double((f*(RH0/100.0d0)*svpaxs)/(Ps))

Zaxs=double(1.0d0-((101325d0/288.15d0)*((a0)+(a1*Tcs)+(a2*(Tcs)^2.0d0))+((b0)
+((b1)*(Tcs))*(0.0d0))+((c0)+((c1)*(Tcs))*(0.0d0)^2.0d0))))+((101325d0/288.15d
0)^2)*((d)+((e)*(0.0d0)^2.0d0))))
rhoaxs=double(((Ps*Ma)/(Zaxs*R*Tks))*(1.0d0-(Xwaxs*(1.0d0-(Mw/Ma))))))

fa=double((1.00062d0)+((3.14d-8)*(P))+((5.6d-7)*((Tc)^2.0d0)))
svpa=double(exp(((AA)*((Tk)^2.0d0))+((BB)*(Tk))+((CC))+((DD)/(Tk))))
;svpa=svpx
Xwa=double((f*(RH0/100.0d0)*svpa)/(P))

Za=double(1.0d0-((P/Tk)*((a0)+(a1*Tc)+(a2*(Tc)^2.0d0))+((b0)+((b1)*(Tc))*(Xw)
)+((c0)+((c1)*(Tc))*(Xw)^2.0d0))))+((P/Tk)^2.0d0)*((d)+((e)*(Xw)^2.0d0))))
rhoa=double(((P*Ma)/(Z*R*Tk))*(1.0d0-(Xw*(1.0d0-(Mw/Ma))))))

fws=double((1.00062d0)+((3.14d-8)*(Ps))+((5.6d-7)*((Tcs)^2.0d0)))
svpws=double(exp(((AA)*((Tks)^2.0d0))+((BB)*(Tks))+((CC))+((DD)/(Tks))))

Zws=double(1.0d0-((1333d0/293.15d0)*((a0)+(a1*Tcs)+(a2*(Tcs)^2.0d0))+((b0)+((b
1)*(Tcs))*(1.0d0))+((c0)+((c1)*(Tcs))*(1.0d0)^2.0d0))))+((1333d0/293.15d0)^2.0
d0)*((d)+((e)*(1.0d0)^2.0d0))))
rhow=double(((Ps*Ma)/(Zws*R*Tks))*(1.0d0-(Xwws*(1.0d0-(Mw/Ma))))))

fwp=double((1.00062d0)+((3.14d-8)*(P))+((5.6d-7)*((Tc)^2.0d0)))
svpw=double(exp((AA*(Tk^2.0d0))+((BB)*Tk)+((CC))+((DD)/Tk)))
;svpw=svpx
Xww=double((f*(RH/100.0d0)*svpw)/(P))

Zw=double(1.0d0-((P/Tk)*((a0)+(a1*Tc)+(a2*(Tc)^2.0d0))+((b0)+((b1)*(Tc))*(Xw)
)+((c0)+((c1)*(Tc))*(Xw)^2.0d0))))+((P/Tk)^2.0d0)*((d)+((e)*(Xw)^2.0d0))))
rhow=double(((P*Ma)/(Z*R*Tk))*(1.0d0-(Xw*(1.0d0-(Mw/Ma))))))

nas=double((((k1/(k0-((sigma)^2.0d0)))+(k3/(k2-((sigma)^2.0d0)))/1d8)+1.0d0)
naxs=double(((nas-1.0d0)*(1.0d0+(0.534d-6)*(450.0d0-450.0d0)))+1.0d0)

nws=double((((cf*(w0)+(w1*((sigma)^2.0d0)))+(w2*((sigma)^4.0d0)))+(w3*((sigma)^6.
0d0)))/1d8)+1.0d0)

nprop=double((((rhoa/rhoaxs)*(naxs-1.0d0))+((rhow/rhow=)*(nws-1.0d0)))+1.0d0)

```



```
        printf,2,format=(f9.4, 2x , f10.4, 2x, f8.4, 2x ,f8.4, 2x, f8.4, 2x, d15.5)', Phpa, H, Tc, Tk, RH,  
            nprop*1.0d8  
endwhile  
  
close,/all  
print,'ok'  
end
```

Program 3. Calibrate the altitude angle of the real sun.

```

pro dii_20111028_4817
; This program is to calbrate the altitude angle (from the real horizon) of the real sun.
close,/all

openw,1,'G:\WORK\All_Observed_DatasX\20111028\dii_4817.txt'
;Rs=(1913.807d0/2.720353d0)/2.0d0 ;the solar angular diameter from JPL Horizon
Re=6374248.3d0; Earth's r in meters
h=5.0d0 ; Height of the observe location in meters
diphtheta=0.0d0 ; When h>o, the angle between "Horizon" to "real horizon"
phy=25.1851093d0 ; The longituge of the observation location.

; ===== The sun's RA and Dec during transit =====
RAAt=210.140491d0 ; Transit RA in degree
Dect=-12.976758d0 ; Transit Dec in degree

; ===== The sun's RA and Dec during take photo =====
RA=210.155095d0 ; Photoed RA in degree
Dec=-13.053414d0 ; Photoed Dec in degree
;Dec=23+(8.12/60)

; ===== The time in hours =====
Tt=3.637015d0 ; Sun Transit time in hours
T=9.143056d0 ; Take photo time

dT=0.0d0 ; Delta T
dRA=0.0d0 ;Delta RA
dDec=0.0d0 ; Delta Dec
dDegree=0.0d0 ; From Transit time to Photoed time, the angle to the zenith
dT=T-Tt
RAp=RA-RAAt
dDec=Dec-Dect
diphtheta=double((acos(Re/(Re+h)))/!dtor) ; dip angle of height in degree
L=double(asin(((sin((90.0d0)*!dtor))*sin((Dec)*!dtor))/(sin((90.0d0-phy)*!dtor))))
LL=L/!dtor
X=double(asin((sin(phy*!dtor))*sin((L)))/(cos((Dec)*!dtor)))/!dtor
Ltr=0.0d0
Xt=0.0d0
dX=0.0d0
Ltr=double(((sin((90.0d0)*!dtor))*sin((Dect)*!dtor))/(sin((90.0d0-phy)*!dtor))))
Xt=double(asin((sin(phy*!dtor))*sin((Ltr)))/(cos((Dect)*!dtor)))/!dtor
dX=X-Xt
theta=0.0d0
theta=Xt

angle=((90.0d0+(Xt)+dX-RAp)-((15.0d0*dT))) ;The theta c
anglex=0.0d0
thetaa=0.0d0
alpha=0.0d0
L=0.0d0
P=0.0d0
Beta=0.0d0
LL=0.0d0
Lx=0.0d0
N=0.0d0
ThetaX=0.0d0
ThetaAa=0.0d0
ThetaAaa=0.0d0

```

```

thtt=0.0d0
aaaaa=0.0d0
ThetaZ=0.0d0

alpha=double((asin((sin(phy*!dttor)) / (cos(dec*!dttor))))/!dttor)
L=double((asin((sin(dec*!dttor)) / (cos(phy*!dttor))))/!dttor)
thetaa=double((asin((sin(L*!dttor))*sin(alpha*!dttor))))/!dttor)
aaaaa=double(angle-thetaa)
thetaz=((asin(((sin(alpha*!dttor))*cos(L*!dttor))/sin(phy*!dttor))))/!dttor)
Beta=acos((sin((thetaz+angle)*!dttor))*cos(phy*!dttor))/!dttor)
Ll=double((asin((sin(aaaaa*!dttor)) / (sin(Beta*!dttor))))/!dttor)
Lx= (acos((1/(tan((thetaz+angle)*!dttor))) * (1/(tan((beta)*!dttor)))))/!dttor)
N=double(Lx+Dec-90.0d0)
ThetaX=double((asin((sin(N*!dttor))*sin(Beta*!dttor))))/!dttor)
ThetaAa=double((asin(((cos(Beta*!dttor))*sin(N*!dttor))/cos(ThetaX*!dttor))))/!dttor)
ThetaAaa=double(360.0d0-(90.0d0+Ll-ThetaAa))

printf,1,format='(f11.7, 2x, f11.7)',ThetaX, ThetaAaa

print, 'ok'
close,/all
end

```

Program 4. Calibrate the modeled refracted sun

```
pro n2n_20111028_4817
; This program is to calibrate the modeled refracted sun
close,/all

Re=6374248.3d0; Earth's R in meters without height
rsun=((1931.493d0/3600.d0)/2.0d0) ; the diameter of the sun, in degree
h=5.0d0 ; the height of the observer
Reh=0.0d0
Reh=Re+h
aaa= ' '
dii=0.0d0 ; the altitude (from the real horizon) of the real sun

openr, 6,'G:\WORK\All_Observed_DatasX\20111028\dii_4817.txt'
  readf, 6,format='(2x, f9.7)', dii
close, 6

dip=0.0d0
des=0.0d0 ; the distance between the earth to the sun (From USNO)
des=0.993681736d0*1.4959787066d0*((10.0d0)^(11.0d0))

openr,5,'G:\WORK\All_Observed_DatasX\20111028\20111028_out_b.txt'
  Ri=0.0d0
  Phi=0.0d0
  Deltai=0.0d0
  Taoi=0.0d0
  Thetai=0.0d0
  allthetai=0.0d0

  zo1=1.0d0
  no1=1.0d0
  zo2=1.0d0
  no2=1.0d0

ja=0.0d0
readf,5,aaa
  while not eof(5) do begin
    readf,5,format='(11x , f10.4, 31x, d16.6)', Zo1, No1
    ja=double(ja+1.0d0)
  endwhile
close, 5

openr,1,'G:\WORK\All_Observed_DatasX\20111028\20111028_out_b.txt'
openw,2,'G:\WORK\All_Observed_DatasX\20111028\20111028_allsun_4817z.txt'
openw,3,'G:\WORK\All_Observed_DatasX\20111028\20111028_allint_4817z.txt'
openr,4,'G:\WORK\All_Observed_DatasX\20111028\20111028_allint_4817z.txt'

na=ja
Z1=dblarr(na)
N1=dblarr(na)
R1=dblarr(na-1.0d0)

Z=dblarr(na)
N=dblarr(na)
R=dblarr(na-1.0d0)
taoin=dblarr(na)
```

```

deltain=dblarr(na-1.0d0)
phyin=dblarr(na)
thetain=dblarr(na-1.0d0)
  XX=dblarr(na+1.0d0)
  YY=dblarr(na+1.0d0)

Zoo=double(0.0d0)
Noo=double(0.0d0)
axx=0.0d0

  readf,1,aaa
j=1.0d0
  readf,1,format='(11x , f10.4, 31x, d16.6)', Zo1, No1
  Z(0)=Zo1
  N(0)=No1/1.0d8
while not eof(1) do begin
  readf,1,format='(11x , f10.4, 31x, d16.6)', Zo1, No1
  Z(j)=Zo1
  N(j)=No1/1.0d8
  j=double(j+1.0d0)
endwhile

  R(0)=Z(0)
for m=1, na-2 ,0 do begin
  R(m)=(Z(m)-z(m-1))+R(m-1)
  m=m+1
endfor
n(na-1)=1.0d0
Ri=R(na-2)

close,1
close,5

;---- The point of the real sun ----
nnn=512.0d0 ;The point number of the real sun
xs=dblarr(nnn+1)
ys=dblarr(nnn+1)

bx=0.0d0
ax=0.0d0
for i=0.0d0, nnn do begin
  tt=(i*2.0d0*!dpi/nnn)/!dtor
  ys(i)=(asin((sin((tt)*!dtor))*(sin((rsun)*!dtor)))/!dtor
  xs(i)=(asin((sin((90.0d0-tt)*!dtor))*(sin((rsun)*!dtor)))/!dtor
  dip=dii+ys(i)
  bb=90.0d0+dip
  alphas=(asin(((Reh)*(sin((bb)*!dtor)))/(Re+Ri)))/!dtor
  acc=180.0d0-alphas-bb
  bx=(asin(((Re+Ri)*(sin((bb)*!dtor)))/(des)))/!dtor
  ax=180.0d0-bb-bx
  printf,3,format='(f11.8, 2x, f11.8, 2x, f10.6, 2x, f10.6)',alphaa, acc, Xs(i), Ys(i)
endfor
close,3

printf,2,' X          Y          dip      deltain'
uu=0.0d0
Deltaa=0.d0
aax=0.0d0
dxx=0.0d0
dyy=0.0d0

```

```

rxx=0.0d0
upinr=0.0d0

;-----
uuu=0.0d0
while not eof(4) do begin
  readf,4, format='(f11.8, 2x, f11.8)', alpha, ac
  uuu=uuu+1
  parameter=0.01d0
  parameter2=0.0d0
  parameter2=parameter/100.0d0
  parameter3=0.0d0
  parameter3=parameter2/100.0d0
nin=double(reverse(N))
Rin=double(reverse(r))
upin=alpha
upinr=alpha
  jump1:

  taoin(0)=upinr

deltain(0)=double(((acos(((Re+Rin(0))*(nin(0))*(sin(upinr*!dtonr)))/((Re+Rin(1))*(nin(1)))))/!dtonr))
  phyin(0)=double((asin(nin(0))*((sin(upinr*!dtonr)))/nin(1)))/!dtonr
  thetain(0)=90.d0-deltain(0)-phyin(0)
  taoin(1)=double((90.0d0)-(deltain(0)))
  for k=1,na-3,0 do begin
    rrein=Re+Rin(k)
    rrin=Re+Rin(k+1)

deltain(k)=double(((acos(((rrein*(nin(k))*(sin((taoin(k))*!dtonr)))/((rrin*(nin(k+1)))))/!dtonr))
  phyin(k)=double((asin(nin(k))*((sin((taoin(k))*!dtonr)))/nin(k+1)))/!dtonr
  thetain(k)=90.d0-deltain(k)-phyin(k)
  taoin(k+1)=double(90.0d0-(deltain(k)))
  k=k+1
endfor

deltain(na-2)=double(((acos(((Re+Rin(na-2))*(nin(na-2))*(sin((taoin(na-2))*!dtonr)))/((Re)*(nin(na-1)))))/!dtonr))
  phyin(na-2)=double((asin(nin(na-2))*((sin((taoin(na-2))*!dtonr)))/nin(na-1)))/!dtonr
  thetain(na-2)=90.d0-deltain(na-2)-phyin(na-2)
  taoin(na-1)=double((90.d0)-(deltain(na-2)))
  allthetain=total(thetain)
  YY=( (Re^2.0d0)/(((tan((ac-allthetain)*!dtonr))^2.0d0)+1) )^(0.5d0)
  XX=YY*(tan((ac-allthetain)*!dtonr))
  axx=ac-allthetain

  err=0.000005d0
;
  if axx le 0.1 then parameter=parameter2
  if axx le 0.0001 then parameter=parameter3
  if axx ge err then upin=upin +(parameter)
  if axx ge err then ac=ac-parameter
  if aXX le -err then parameter=parameter/2.0d0
  if aXX le -err then upin=upin-(parameter)
  if axx le -err then ac=ac+parameter
  aax=ax+parameter
  dxx=(Re+Ri)*(cos(aax*!dtonr))
  dyy=(Re+Ri)*(sin(aax*!dtonr))
  rxx=(atan(dyy/(des-dxx)))/!dtonr
  upinr=upin+rxx

```

```

uu=uu+1
  if uu eq 10000 then goto, jump2
  if abs(aXX) le err then goto, jump2
goto, jump1
  jump2:

printf,2,format='(f14.7, 2x, f10.2, 2x, f10.7, 2x, f10.7, 2x, f13.10)', XX, YY, dip, deltain(na-2),
rxx
  endwhile
;-----

print, 'ok'
close,/all
end

```

Program 5. Plot the real sun, modeled sun on the image of the observed sun.

```

pro RealSunLocation_20111028
; This program is used to plot the real sun, modeled sun on the image of the observed sun.
close,/all

file = 'G:\WORK\All_Observed_DatasX\20111028\images\_MG_4817_4836_4853X.jpg'
image=read_image(file)
scale=2.232932d0; Image scale arcsec/pixel
Rs=(1931.493d0/scale)/2.0d0
Re=6374248.3d0; Earth's r in meters
h=5.0d0 ; Height of the observe location in meters
diphtheta=0.0d0 ; When h>o, the angle between "Horizon" to "real horizon"
phy=25.1851093d0 ; the longitude of the observation location
RS=2652.0d0 ; The apparent sea level in the image (in pixel)
RH=2567.0d0; The real horizon in the image (in pixel)
anglex=0.0d0 ; the altitude (fram the real horizon) of the real sun
openr,4,'G:\WORK\All_Observed_DatasX\20111028\dii_4817.txt'
readf,4,format='(f11.7, 2x, f11.7)', anglex, diphtheta
close,4

;-----draw the real horizon-----
xfit=fltarr(2)
yfit=fltarr(2)
  xfit(0)=0
  xfit(1)=3615
  yfit(0)=RH
  yfit(1)=RH
;-----draw the apparent sea level-----
xfit2=fltarr(2)
yfit2=fltarr(2)
  xfit2(0)=0
  xfit2(1)=3615
  yfit2(0)=RS
  yfit2(1)=RS
;-----draw the real sea level-----
xfit3=fltarr(2)
yfit3=fltarr(2)
  xfit3(0)=0
  xfit3(1)=3615
  yfit3(0)=RH+(diphtheta*3600/scale)
  yfit3(1)=RH+(diphtheta*3600/scale)
;-----draw the scale-----
xfit4=fltarr(2)
yfit4=fltarr(2)
  xfit4(0)=50
  xfit4(1)=50
  yfit4(0)=50
  yfit4(1)=50+5*60/scale

;-----
set_plot,'ps'
device,filename="G:\WORK\All_Observed_DatasX\20111028\20111028_4817_4836_4853.ps",
/color, bits=8
device, /inches, xsize=6, yoffset=0.0
TVLCT, [0,255,0,100, 255,150, 200, 255, 0], [0,200,255,255, 255,250, 150, 0, 100],
[0,220,255,100, 255,255,0, 255, 50]

```



```

plot, xfit, yfit, linestyle=0, xrange=[0,3480], yrange=[5200,0], /isotropic , xtitle='pixel',
ytitle='pixel', thick=2, xstyle=1, ystyle=1
TV,image , 2225 , 1415 , xsize=7075 , /true

oplot, xfit, yfit,color=1, linestyle=2 ; draw the real horizon
oplot, xfit2, yfit2,color=3 ; draw the apparent sea level
oplot, xfit3, yfit3,color=3,linestyle=1 ; draw the real sea level
oplot, xfit4, yfit4,color=3 ;draw the scale
xyouts, 50, 2960,'Real sea level at altitude=5 m',color=3,CHARTHICK=2,CHARSIZE =0.5
xyouts, 50, 2800,'Real horizon',color=1,CHARTHICK=2,CHARSIZE =0.5
xyouts, 50, 2880,'Apparent sea level at altitude=5 m',color=3,CHARTHICK=2,CHARSIZE =0.5
xyouts, 80, 50+5*60/scale,'5 arcmin',color=3,CHARTHICK=2,CHARSIZE =0.5

;---- The first sun ----
X=1787
Y=RH-(angleX*3600/scale)
print,y, anglex
openr,1,'G:\WORK\All_Observed_DatasX\20111028\20111028_allint_4817.txt'

XXs0=X
YYs0=RH-(angleX*3600/scale)
xs=dblarr(513)
ys=dblarr(513)
xxS=0.0D0
yys=0.0D0
aa=0.0d0
while not eof(1) do begin
  readf,1,format='(27x, f9.6, 3x, f9.6)', XXs, YYs
  xs(aa)=(XXs*3600.0d0/scale)+x
  ys(aa)=-(YYs*3600.0d0/scale)+y
  aa=aa+1
endwhile

XX=fltarr(1)
YY=fltarr(1)
XX(0)=X
YY(0)=Y

oplot, xs, ys, color=1, thick=1 , psym=1, symsize=0.05, linestyle=0
xxc=fltarr(1)
yyc=fltarr(1)
xxc(0)=X
yyc(0)=Y
close, 1

xxu=fltarr(1)
yyu=fltarr(1)
xxu(0)=X
yyu(0)=Y+Rs
XYouts, X-1200, 900, 'Unrefracted sun',color=1,CHARTHICK=2,CHARSIZE =0.5
XYouts, X-1200, 980, '09:08:35 UT',color=1,CHARTHICK=2,CHARSIZE =0.5
XYouts, X-1200, 300, 'Refracted sun',color=5,CHARTHICK=2,CHARSIZE =0.5
XYouts, X-1200, 380, '09:08:35 UT',color=5,CHARTHICK=2,CHARSIZE =0.5

Xxxx=X
openr,2,'G:\WORK\All_Observed_DatasX\20111028\20111028_allsun_4817.txt'
openr,3,'G:\WORK\All_Observed_DatasX\20111028\20111028_allint_4817.txt'
XXsr=0.0d0
YYsr=0.0d0
xsr=fltarr(513)

```

```

ysr=fltarr(513)
ac=0.0d0
while not eof(3) do begin
  readf,3,format='(27x, f9.6)', XXsr
  xsr(ac)=(XXsr*3600.0d0/scale)+Xxxx
  ac=ac+1
endwhile
aaa= ' '
readf,2,aaa
ab=0.0d0
while not eof(2) do begin
  readf,2,format='(40x, f10.7)', YYsr
  ysr(ab)=-(YYsr*3600.0d0/scale)+RH
  ab=ab+1
endwhile

oplot, xsr,ysr, color=5, thick=1 , psym=1 , symsize=0.05 ,linestyle=0
close,/all

; ---- The second sun ----
anglex=0.0d0
openr,4,'G:\WORK\All_Observed_DatasX\20111028\dii_4836.txt'
readf,4,format='(f11.7)', anglex
close,4

X=2190.5d0
Y=RH-(angleX*3600/scale)
openr,1,'G:\WORK\All_Observed_DatasX\20111028\20111028_allint_4836.txt'
XXs0=X
YYs0=RH+(angleX*3600/scale)
xs=dblarr(513)
ys=dblarr(513)
xxS=0.0D0
yys=0.0D0
aa=0.0d0
while not eof(1) do begin
  readf,1,format='(27x, f9.6, 3x, f9.6)', XXs, YYs
  xs(aa)=(XXs*3600.0d0/scale)+x
  ys(aa)=-(YYs*3600.0d0/scale)+y
  aa=aa+1
endwhile

XX=fltarr(1)
YY=fltarr(1)
XX(0)=X
YY(0)=Y

oplot, xs, ys, color=1, thick=1 , psym=1, symsize=0.05, linestyle=0
xxc=fltarr(1)
yyc=fltarr(1)
xxc(0)=X
yyc(0)=Y
close, 1

xxu=fltarr(1)
yyu=fltarr(1)
xxu(0)=X
yyu(0)=Y+Rs
XYouts, X-1200, 1800, 'Unrefracted sun',color=1,CHARTHICK=2,CHARSIZE =0.5
XYouts, X-1200, 1880, '09:10:59 UT',color=1,CHARTHICK=2,CHARSIZE =0.5

```

```
XYouts, X-1200, 1200, 'Refracted sun',color=5,CHARTHICK=2,CHARSIZE =0.5
XYouts, X-1200, 1280, '09:10:59 UT',color=5,CHARTHICK=2,CHARSIZE =0.5
```

```
Xxxx=X
openr,2,'G:\WORK\All_Observed_DatasX\20111028\20111028_allsun_4836.txt'
openr,3,'G:\WORK\All_Observed_DatasX\20111028\20111028_allint_4836.txt'
XXsr=0.0d0
YYsr=0.0d0
xsr=fltarr(513)
ysr=fltarr(513)
ac=0.0d0
while not eof(3) do begin
  readf,3,format='(27x, f9.6)', XXsr
  xsr(ac)=(XXsr*3600.0d0/scale)+Xxxx
  ac=ac+1
endwhile
aaa=' '
readf,2,aaa
ab=0.0d0
while not eof(2) do begin
  readf,2,format='(40x, f10.7)', YYsr
  ysr(ab)=- (YYsr*3600.0d0/scale)+RH
  ab=ab+1
endwhile
oplot, xsr,ysr, color=5, thick=1 , psym=1 , symsize=0.05 ,linestyle=0
close,/all
```

```
; ---- The third sun ----
anglex=0.0d0
openr,4,'G:\WORK\All_Observed_DatasX\20111028\dii_4853.txt'
readf,4,format='(f11.7)', anglex
close,4
```

```
X=2586.0d0
Y=RH-(angleX*3600/scale)
print,y
openr,1,'G:\WORK\All_Observed_DatasX\20111028\20111028_allint_4853.txt'
XXs0=X
YYs0=RH+(angleX*3600/scale)
xs=dblarr(513)
ys=dblarr(513)
xxS=0.0D0
yys=0.0D0
aa=0.0d0
while not eof(1) do begin
  readf,1,format='(27x, f9.6, 3x, f9.6)', XXs, YYs
  xs(aa)=(XXs*3600.0d0/scale)+x
  ys(aa)=- (YYs*3600.0d0/scale)+y
  aa=aa+1
endwhile
```

```
XX=fltarr(1)
YY=fltarr(1)
XX(0)=X
YY(0)=Y
```

```
oplot, xs, ys, color=1, thick=1 , psym=1, symsize=0.05, linestyle=0
xxc=fltarr(1)
yyc=fltarr(1)
xxc(0)=X
```

```

yyc(0)=Y
close, 1

xxu=fltarr(1)
yyu=fltarr(1)
xxu(0)=X
yyu(0)=Y+Rs
XYouts, X-1200, 2450, 'Unrefracted sun',color=1,CHARTHICK=2,CHARSIZE =0.5
XYouts, X-1200, 2530, '09:13:17 UT',color=1,CHARTHICK=2,CHARSIZE =0.5
XYouts, X-1200, 2000, 'Refracted sun',color=5,CHARTHICK=2,CHARSIZE =0.5
XYouts, X-1200, 2080, '09:13:17 UT',color=5,CHARTHICK=2,CHARSIZE =0.5

Xxxx=X
openr,2,'G:\WORK\All_Observed_DatasX\20111028\20111028_allsun_4853.txt'
openr,3,'G:\WORK\All_Observed_DatasX\20111028\20111028_allint_4853.txt'
XXsr=0.0d0
YYsr=0.0d0
xsr=fltarr(513)
ysr=fltarr(513)
ac=0.0d0
while not eof(3) do begin
  readf,3,format='(27x, f9.6)', XXsr
  xsr(ac)=(XXsr*3600.0d0/scale)+Xxxx
  ac=ac+1
endwhile
aaa= ' '
readf,2,aaa
ab=0.0d0
while not eof(2) do begin
  readf,2,format='(40x, f10.7)', YYsr
  ysr(ab)=- (YYsr*3600.0d0/scale)+RH
  ab=ab+1
endwhile
oplot, xsr,ysr, color=5, thick=1 , psym=1 , symsize=0.05 ,linestyle=0

device,/close
close,/all
print, 'ok'
end

```

Appendix

C. The observation without measured the real horizon.

The observation before year 2011 was not measure where the real horizon is so that the result needs to shift an angle which is from $-49.22''$ to $296.10''$ to keep the modeled sun closer to the observed sun. This is only shift the modeled sun on to the approximate observed sun's altitude, this is not real response the terrestrial refraction and only used to refer.

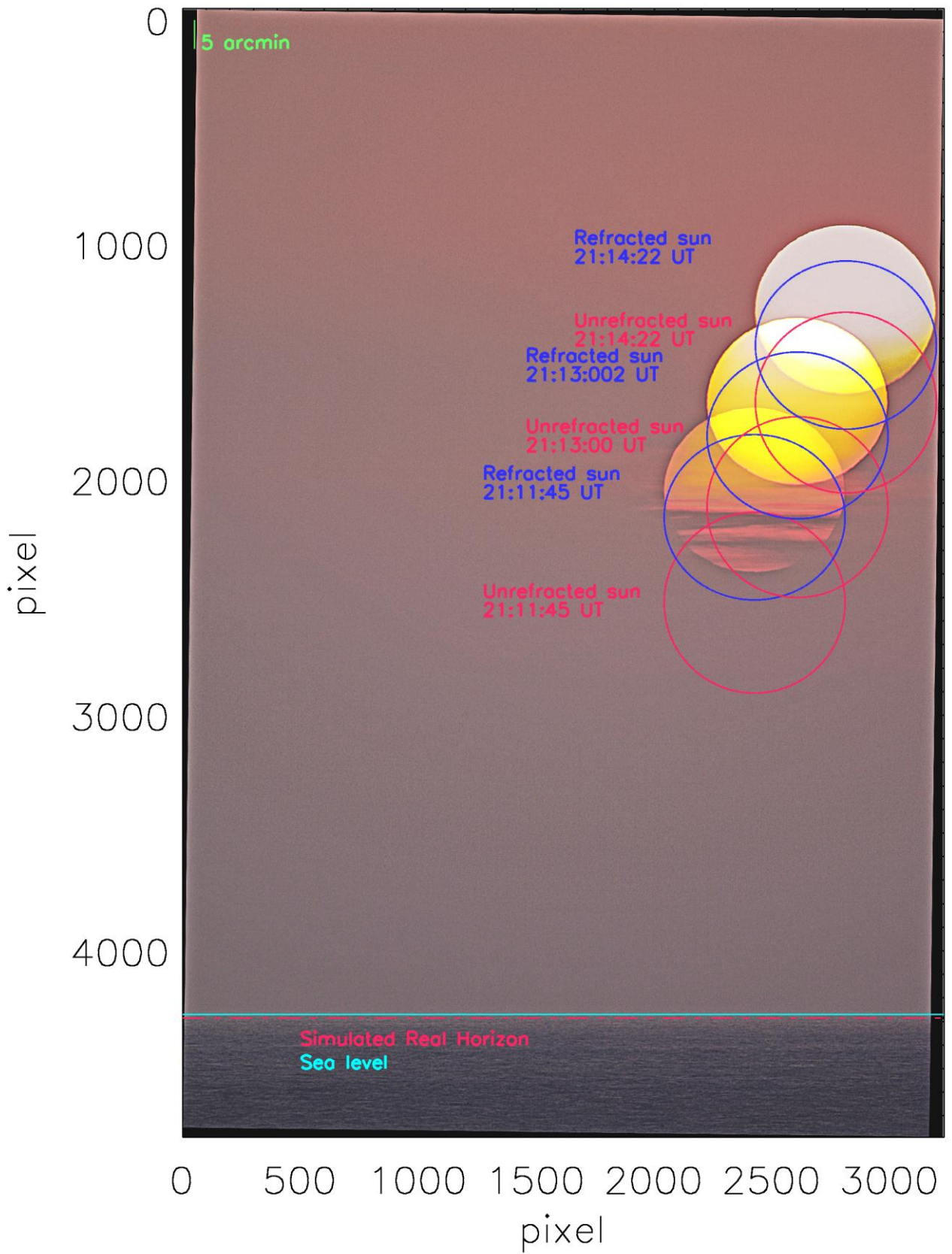


Fig App-C.1-1. The refracted sun (blue) and the unrefracted sun (pink), compared with the observed sun during the sunrise in June 1, 2010 without measured the real horizon.

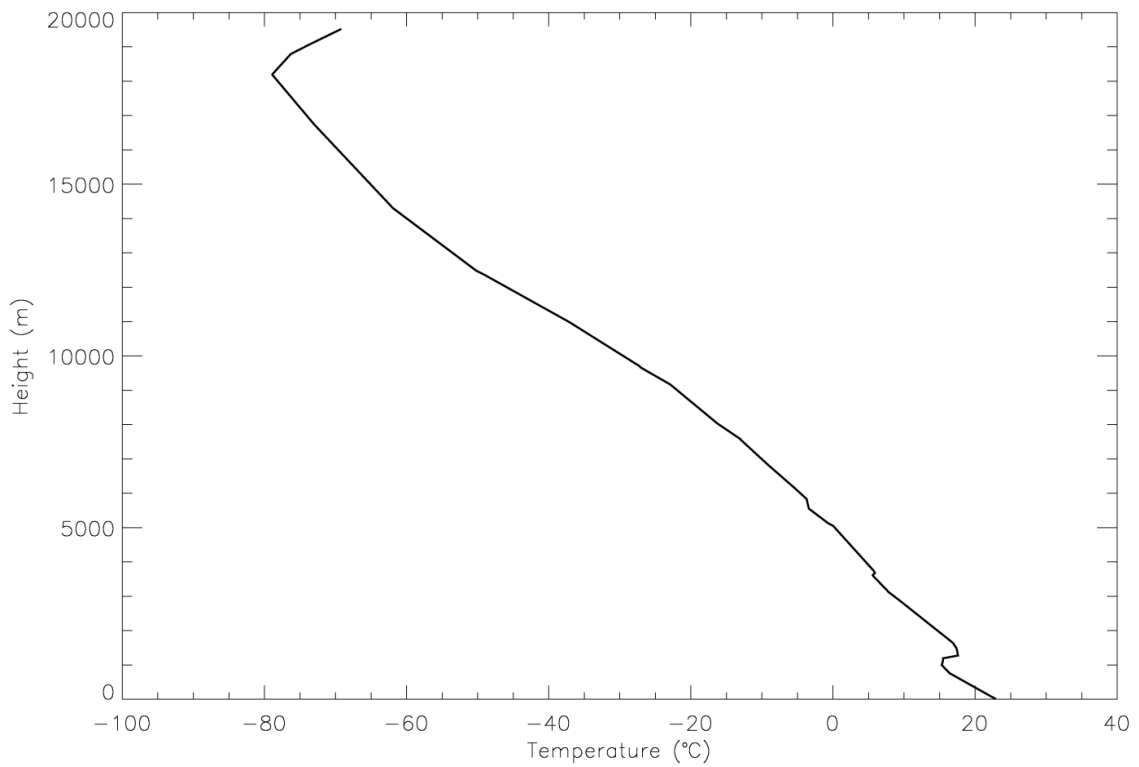
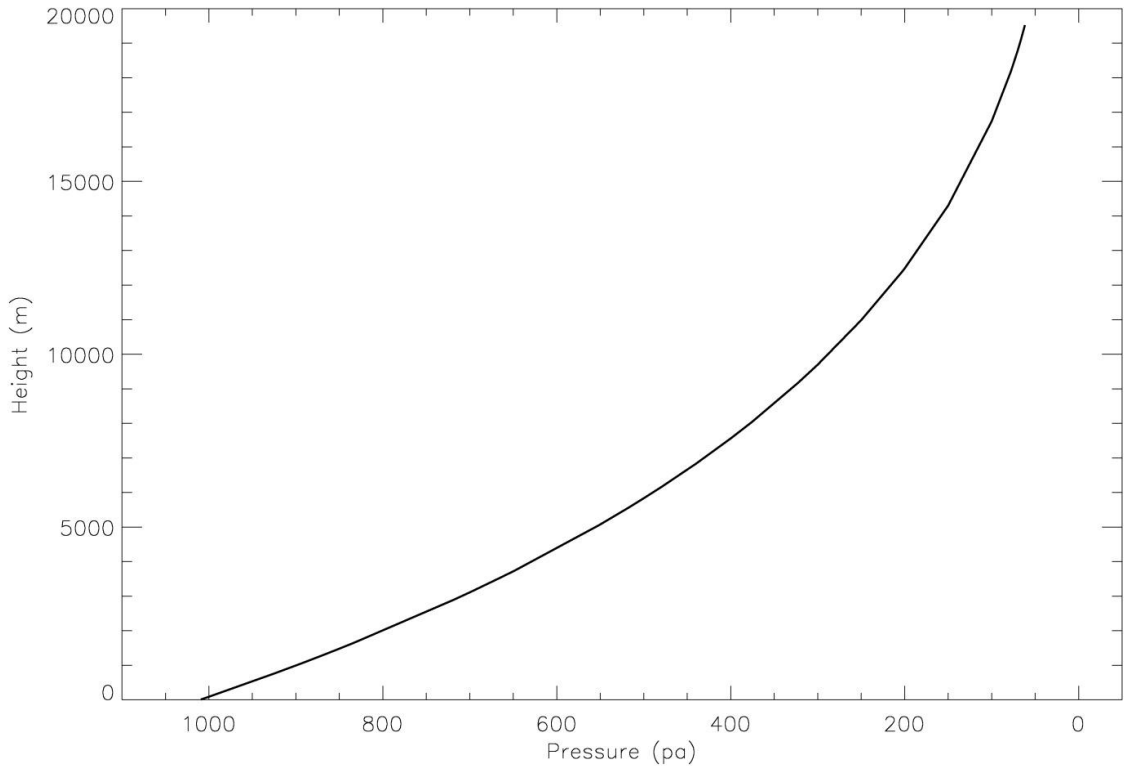


Fig App-C.1-2. The height to pressure fig (up) and the height to temperature fig (down) during observe at June 1, 2010 morning, the data is from the CWB rawinsonde which launched at 00:00 UT June 1, 2010.

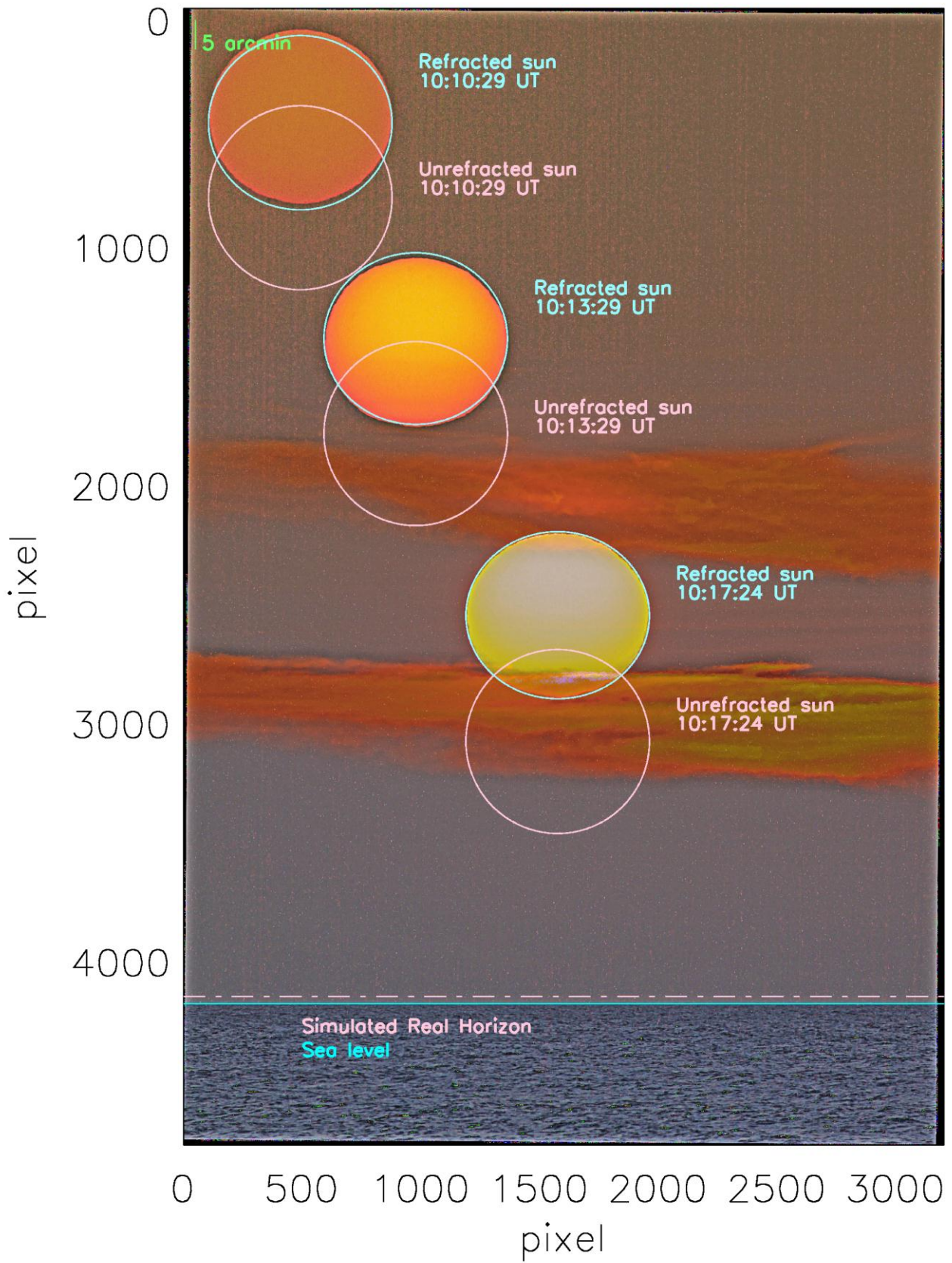


Fig App-C.2-1. The refracted sun (blue) and the unrefracted sun (pink), compared with the observed sun during the sunset in August 21, 2010 without measured the real horizon.

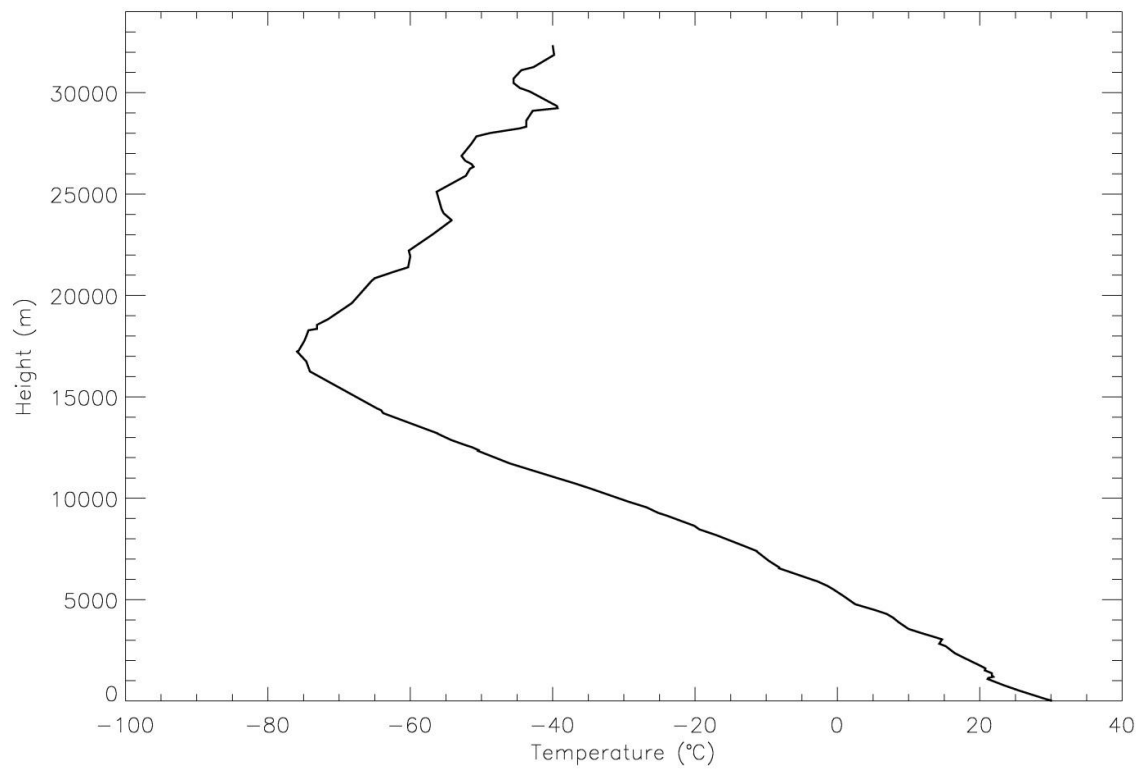
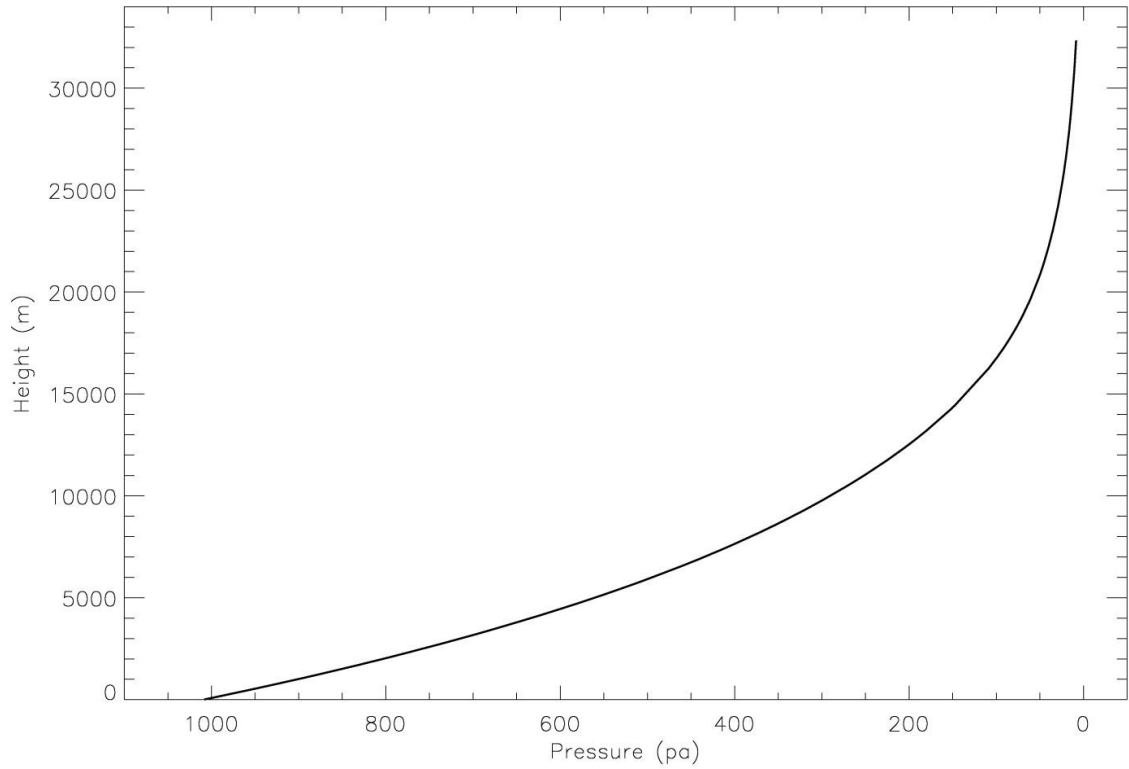


Fig App-C.2-2. The height to pressure fig (up) and the height to temperature fig (down) during observe at August 21, 2010 night, the data is from the CWB rawinsonde which launched at 12:00 UT August 21, 2010.

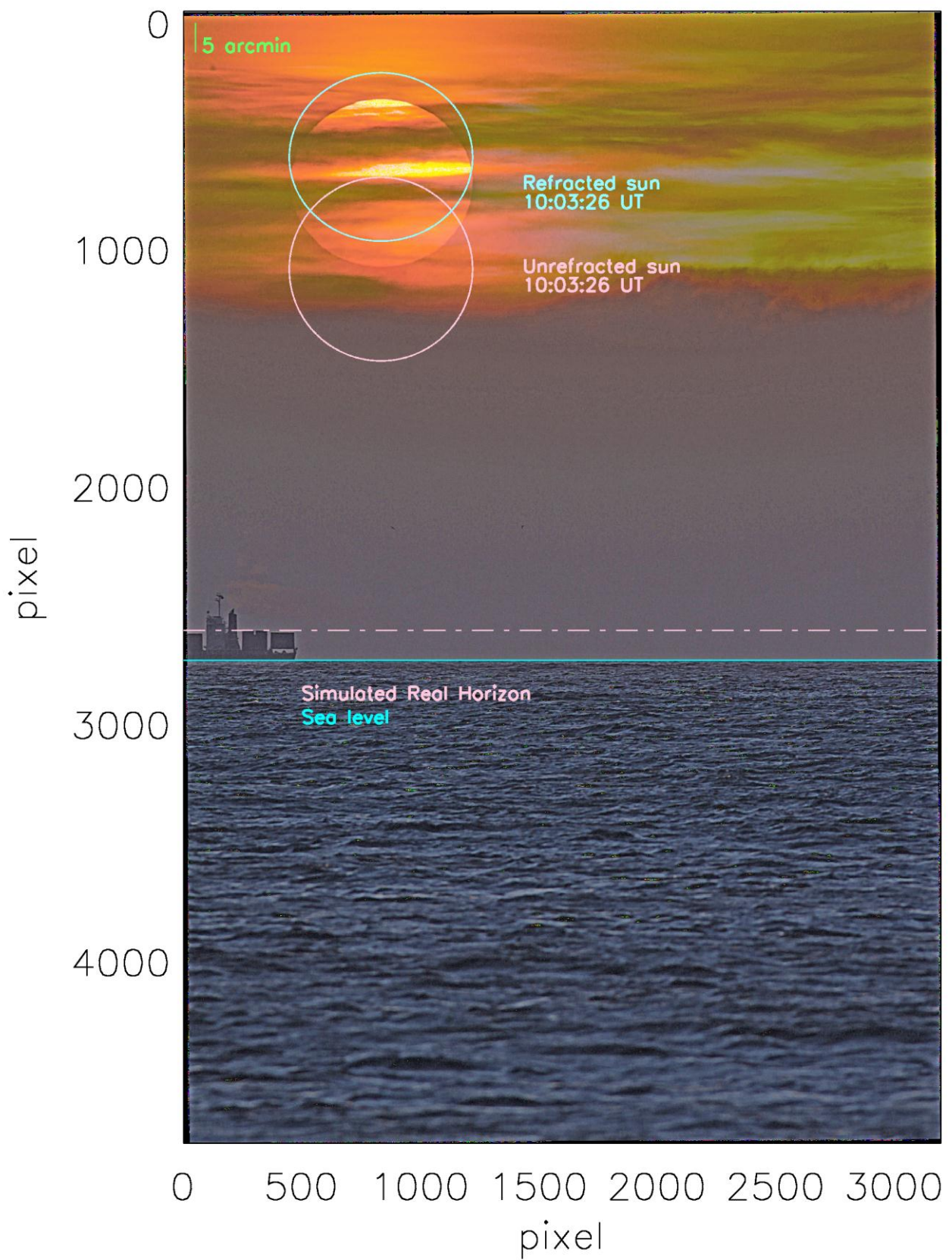


Fig App-C 3-1. The refracted sun (blue) and the unrefracted sun (pink), compared with the observed sun during the sunset in September 3, 2010 without measured the real horizon.

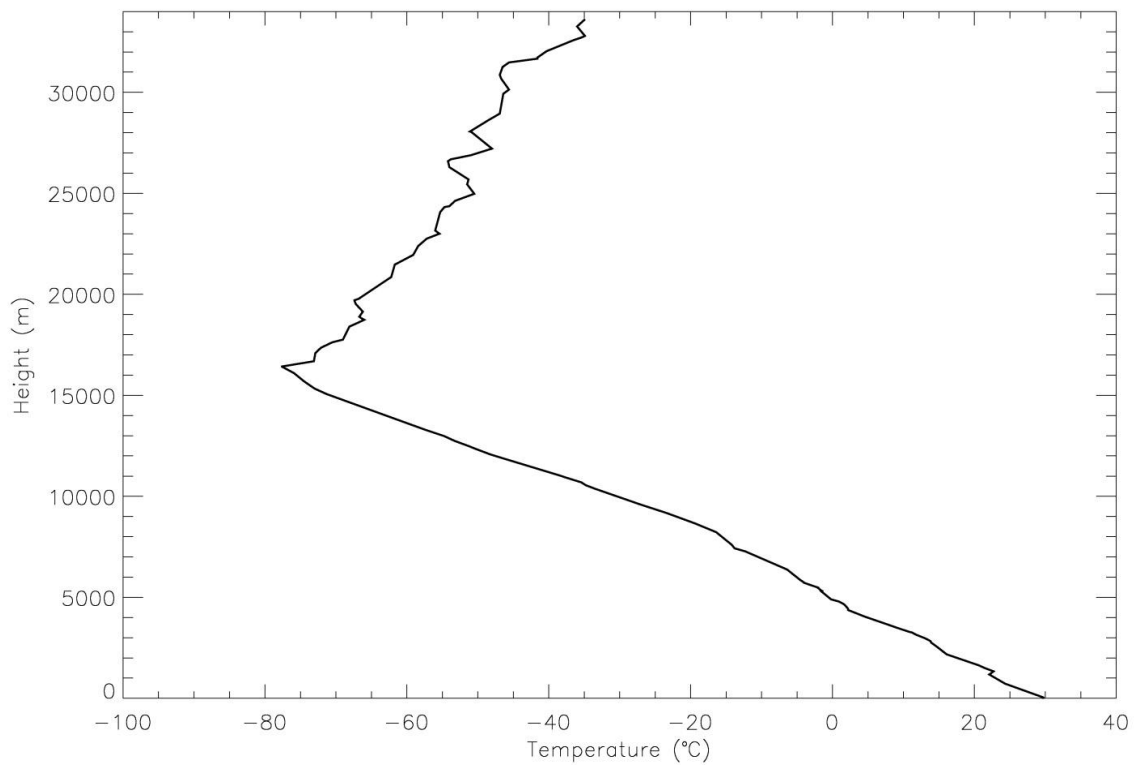
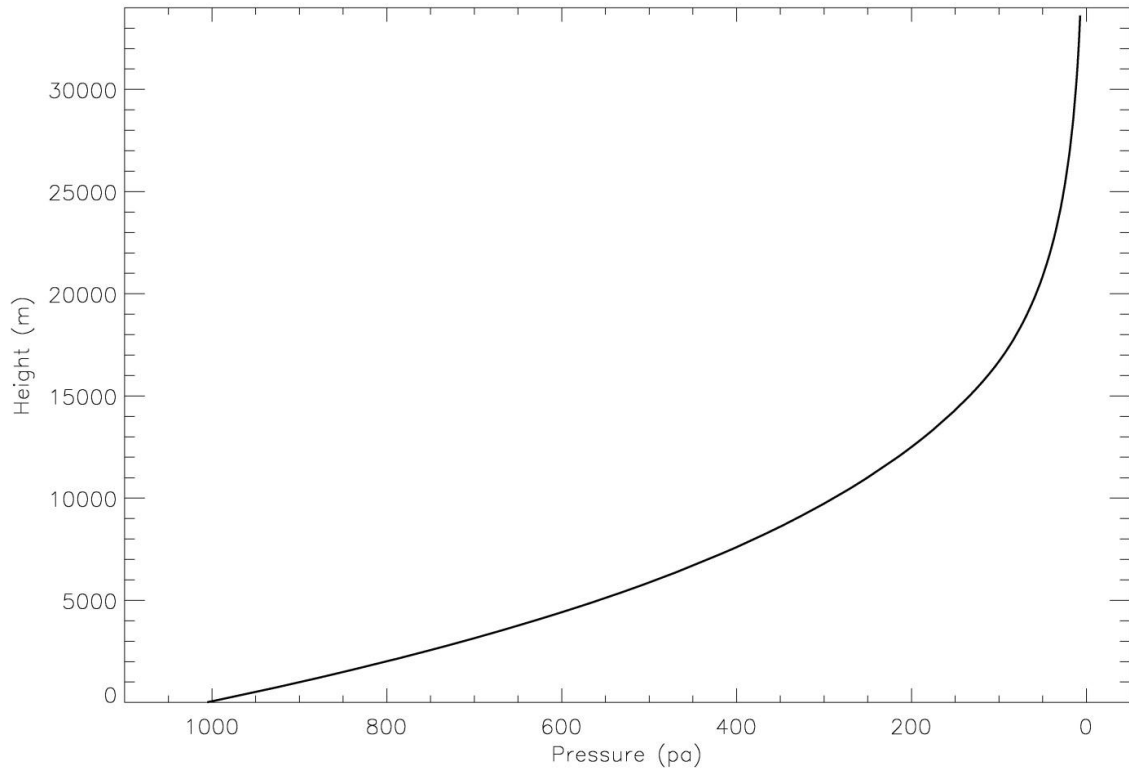


Fig App-C 3-2. The height to pressure fig (up) and the height to temperature fig (down) during observe at September 3, 2010 night, the data is from the CWB rawinsonde which launched at 12:00 UT September 3, 2010.

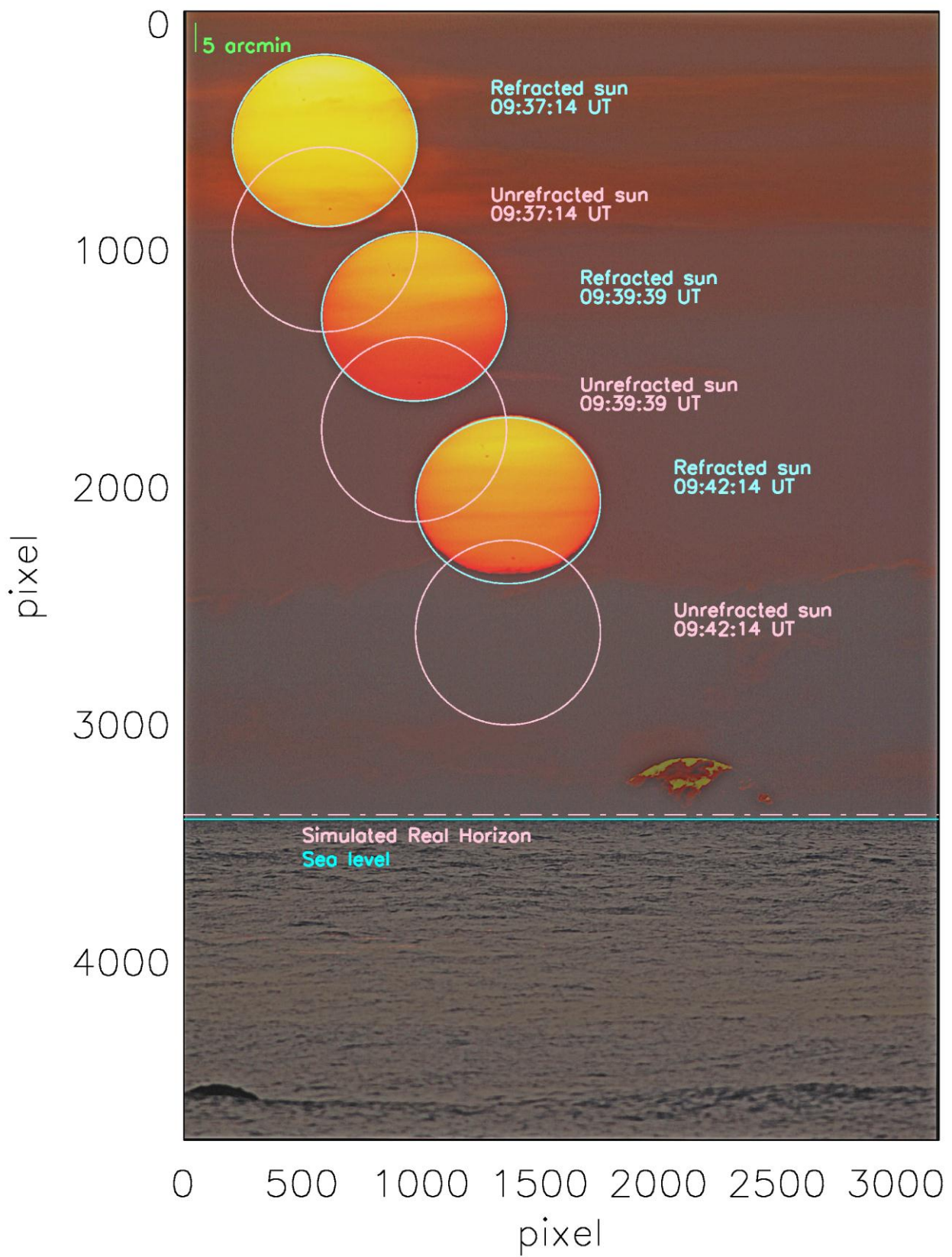


Fig App-C. 4-1. The refracted sun (blue) and the unrefracted sun (pink), compared with the observed sun during the sunset in September 25, 2010 without measured the real horizon.

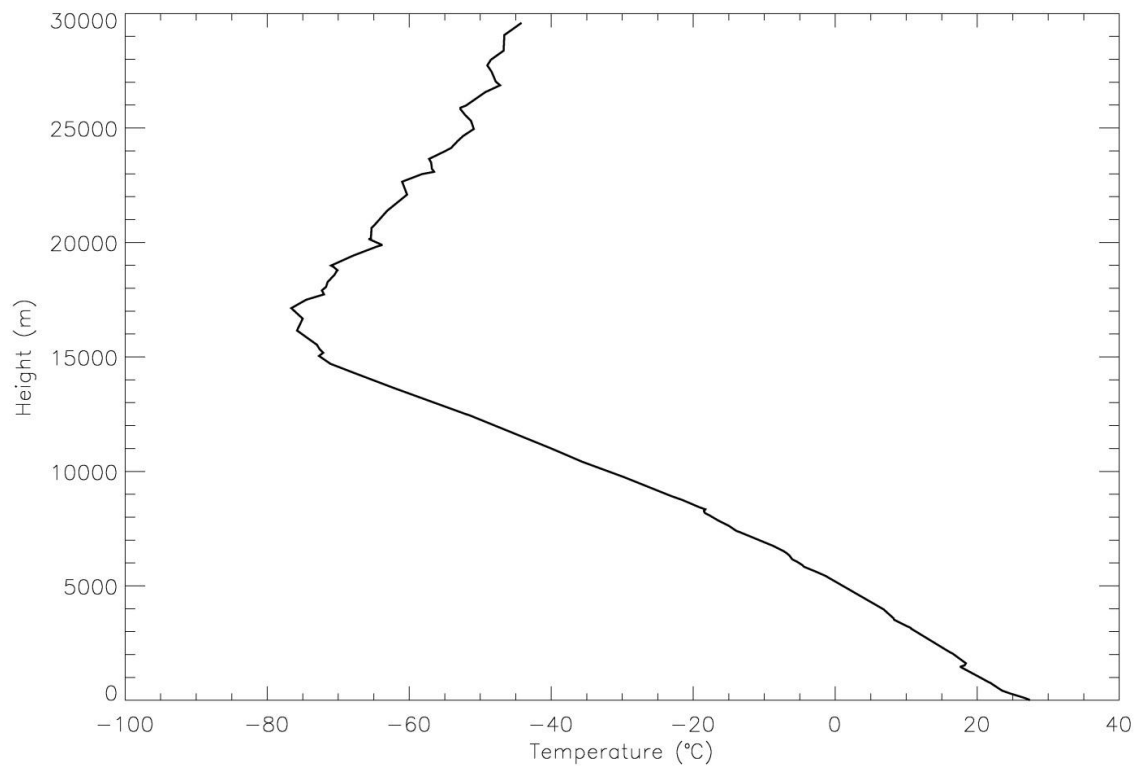
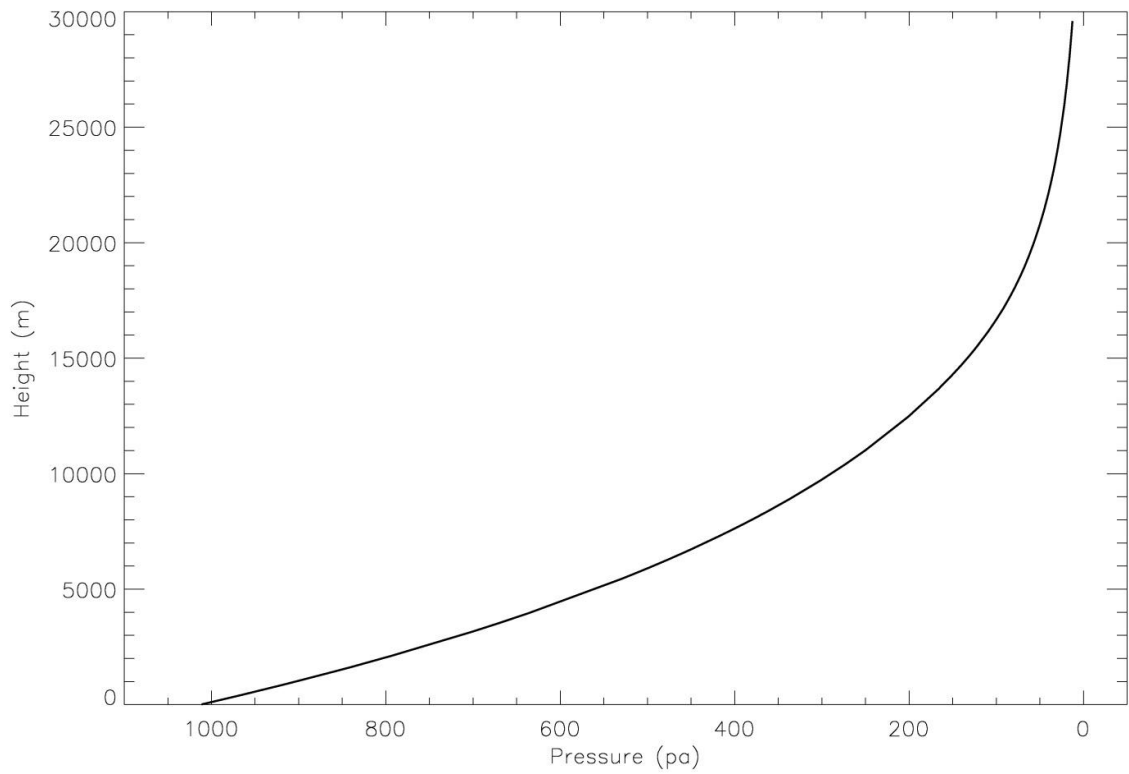


Fig App-C. 4-2. The height to pressure fig (up) and the height to temperature fig (down) during observe at September 25, 2010 night, the data is from the CWB rawinsonde which launched at 12:00 UT September 25, 2010.

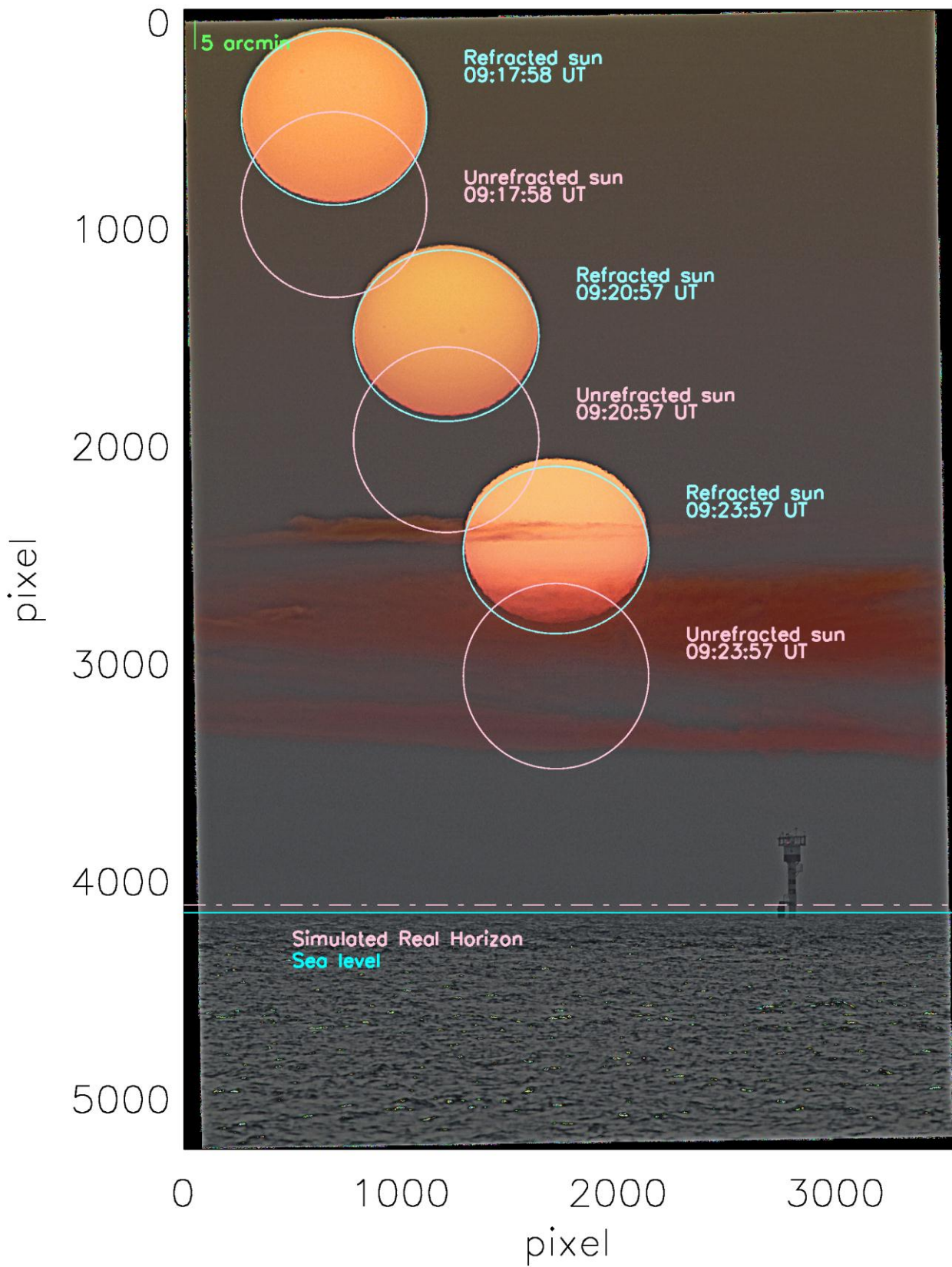


Fig App-C. 5-1. The refracted sun (blue) and the unrefracted sun (pink), compared with the observed sun during the sunset in October 12, 2010 without measured the real horizon.

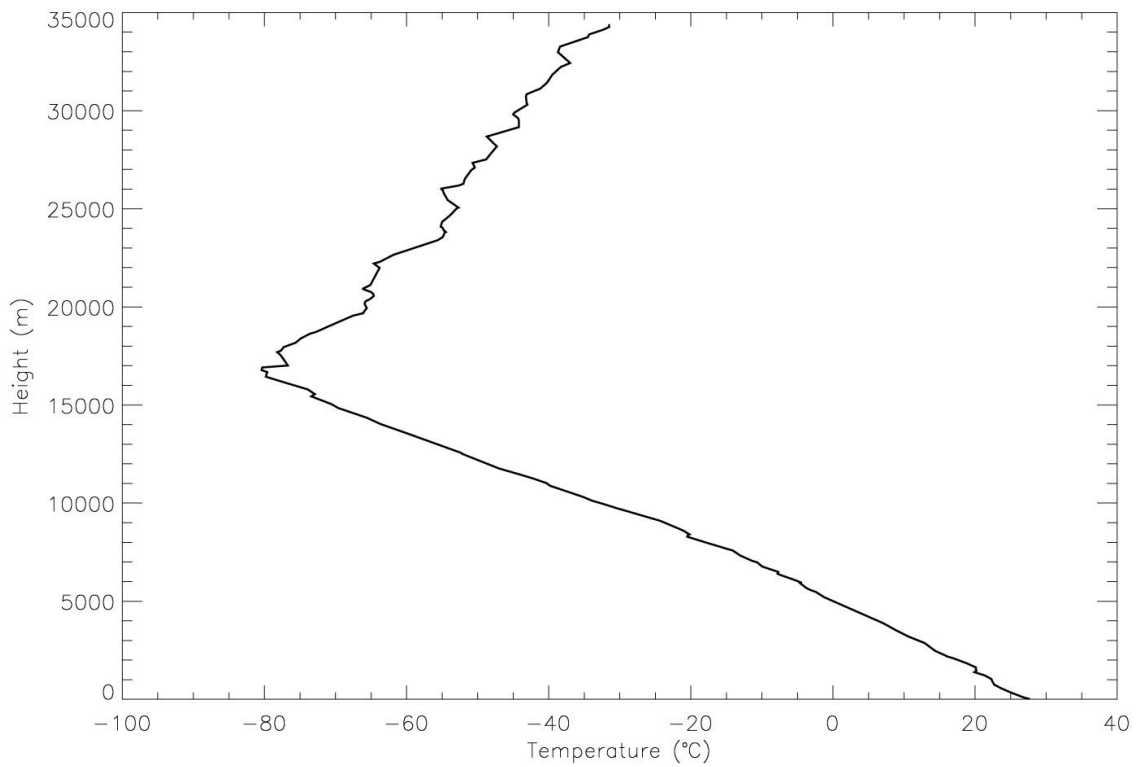
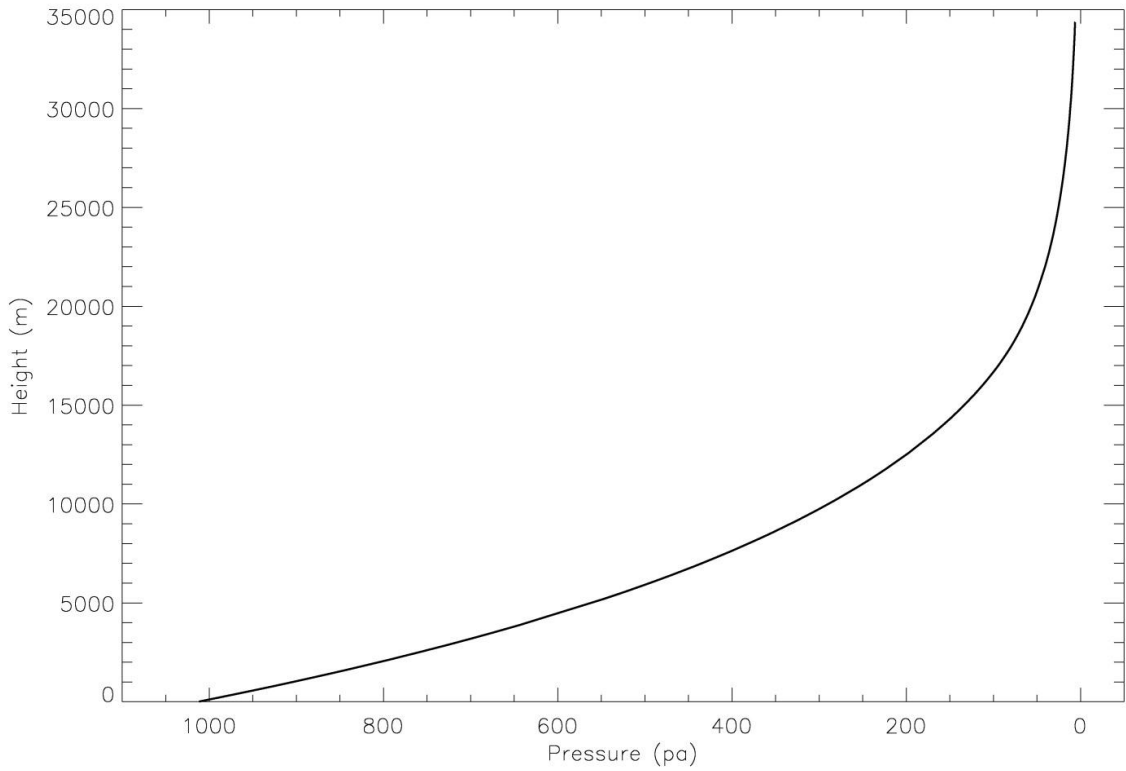


Fig App-C. 5-2. The height to pressure fig (up) and the height to temperature fig (down) during observe at October 12, 2010 night, the data is from the CWB rawinsonde which launched at 12:00 UT October 12, 2010